การตรวจสอบแรงดันอิมพัลส์เบรกดาวน์ของแกปอากาศมาตรฐาน

นายฉอม วัฒณา ฉม

วิทยานิพนธ์นี้เป็นส่วนหนึ่งของการศึกษาตามหลักสูตรปริญญาวิศวกรรมศาสตรมหาบัณฑิต
สาขาวิชาวิศวกรรมไฟฟ้า ภาควิชาวิศวกรรมไฟฟ้า
คณะวิศวกรรมศาสตร์ จุฬาลงกรณ์มหาวิทยาลัย
ปีการศึกษา 2560

A revisit to impulse breakdown voltage of standard air gaps

Mr. Chhoum Vathana Chhom

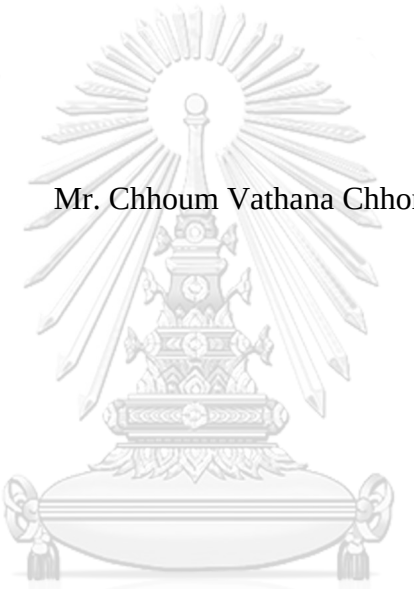

A Thesis Submitted in Partial Fulfillment of the Requirements
for the Degree of Master of Engineering Program in Electrical Engineering
Department of Electrical Engineering
Faculty of Engineering
Chulalongkorn University
Academic Year 2017

Thesis Title	A revisit to impulse breakdown voltage of standard air gaps
By	Mr. Chhoum Vathana Chhom
Field of Study	Electrical Engineering
Thesis Advisor	Assistant Professor Komson Petcharaks

Accepted by the Faculty of Engineering, Chulalongkorn University in Partial Fulfillment of the Requirements for the Master's Degree

.....Dean of the Faculty of Engineering
(Associate Professor Supot Teachavorasinskun)

THESIS COMMITTEE

.....Chairman
(Professor Boonchai Techaumnat)

.....Thesis Advisor
(Assistant Professor Komson Petcharaks)

.....External Examiner
(Assistant Professor Nutthaphong Tanthanuch)

ฉอม วัฒณา ฉม : การตรวจสอบแรงดันอิมพัลส์เบรกดาวน์ของแกปอากาศมาตรฐาน (A revisit to impulse breakdown voltage of standard air gaps) อ.ที่ปรึกษาวิทยานิพนธ์หลัก: ผศ. ดร. คมสัน เพ็ชรรักษ์, หน้า.

แกปทรงกลมมักใช้เป็นอุปกรณ์วัดอ้างอิงในการตรวจสมรรถนะของระบบวัดแรงดันอื่นๆ เนื่องจากมีการใช้งานที่ง่าย ความไม่แน่นอนในการวัดแรงดันของแกปทรงกลมขึ้นกับระยะช่องว่างอากาศ S และขนาดเส้นผ่านศูนย์กลางทรงกลม D สำหรับการวัดค่ายอดแรงดันแรงดันกระแสสลับและแรงดันอิมพัลส์ ความไม่แน่นอนในการวัดมีค่า ±3% เมื่อ $S \leq 0.5D$ อย่างไรก็ตามแรงดันเบรกดาวน์ของแกปทรงกลมบางขนาดที่ระยะช่องว่างอากาศเท่ากัน มีแนวโน้มที่ต่างไปจากแรงดันเบรกดาวน์ของแกปทรงกลมขนาดอื่น เช่น เมื่อใช้ทรงกลมขนาด 5 cm และ 10 cm วัดแรงดันอิมพัลส์ขั้วลบ

วิทยานิพนธ์นี้จึงศึกษาค่าแรงดันเบรกดาวน์ $U_{50\%}$ ของทรงกลมขนาด 5 cm และ 10 cm ที่ขนาดช่องว่างอากาศ S = 0.5, 1.0, 1.5, 2.0 และ 2.4cm ด้วยแรงดันอิมพัลส์รูปคลื่นมาตรฐาน T_1/T_2 = 1.2/50 µs ทั้งขั้วบวกและลบ ที่ความชื้นค่าต่างๆ เมื่อทำการฉายรังสีให้ช่องว่างอากาศ แกปทรงกลมในการศึกษานี้ได้ติดตั้งในภาชนะควบคุมบรรยากาศที่ออกแบบด้วยวิธีไฟไนต์อิลิเมต์ เพื่อให้มั่นใจว่าสนามไฟฟ้าในช่องว่างอากาศที่อยู่ในภาชนะนี้เหมือนกับสนามไฟฟ้าในช่องว่างอากาศปกติ นอกจากนั้นยังใช้ระบบวัดแรงดันอิมพัลส์ที่เหมาะกับขนาดของแรงดันเบรกดาวน์ที่ต้องการวัด

ผลการศึกษาพบว่าแรงดัน $U_{50\%}$ จากการศึกษาแตกต่างไปจากค่าที่ระบุในมาตรฐาน เมื่อ $S \leq 1.0$cm แต่ความแตกต่างจะน้อยลงเมื่อช่องว่างอากาศกว้างขึ้น และแรงดันเบรกดาวน์ของทรงกลม 5 cm และ 10 cm ที่ขนาดช่องว่างอากาศเดียวกัน มีค่าใกล้เคียงกัน

ภาควิชา วิศวกรรมไฟฟ้า ลายมือชื่อนิสิต .....

สาขาวิชา วิศวกรรมไฟฟ้า ลายมือชื่อ อ.ที่ปรึกษาหลัก .....

ปีการศึกษา 2560

5970364121 : MAJOR ELECTRICAL ENGINEERING
KEYWORDS: SPHERE-GAP / BREAKDOWN VOLTAGE / IRRADIATION / TEST CHAMBER

CHHOUM VATHANA CHHOM: A revisit to impulse breakdown voltage of standard air gaps. ADVISOR: ASST. PROF. KOMSON PETCHARAKS, pp.

By its simplicity, sphere gaps method for the measuring of peak voltage is preferred to be used as standard for calibration purposes. The limits of accuracy of the standard sphere-gaps depends on the ratio of the gap spacing S to the sphere diameter D, as follows. For AC, switching and lightning impulse voltage, $S \leq 0.5D$, uncertainty is ±3%, but for gap spacing $0.75D > S > 0.5D$, the uncertainty is larger than ±3%. However, the $U_{50\%}$ disruptive discharge of some standard spheres at the same gap spacing showed the different value from each other. The significant case occurred between 5cm and 10cm sphere-gap for negative polarity.

Hence, the objective of this thesis is to study the characteristic of the curve of $U_{50\%}$ disruptive discharge voltage against the gap spacing S for 5cm and 10cm diameter sphere. The standard lightning impulse voltage (T_1=1.2 μs and T_2=50 μs) of negative and positive polarities for S= 0.5, 1.0, 1.5, 2.0 and 2.4cm, was taken for this study by taking account the influence of humidity and the application of external irradiation. In order to control the atmospheric condition around the sphere-gap during the breakdown phenomena, both sphere-gap was enclosed in a cylindrical shape test chamber. This chamber was designed by using the finite element method (FEM) to ensure that there is an acceptable influence on the electrical field distribution across the gap of spheres. Two different measuring devices were chosen according to the applied voltage level for the purpose of measuring accuracy. The experiment results showed that the difference between $U_{50\%}$ of this present study and the one of the standard decrease as the gap spacing increase, especially for $S \leq 1.0$cm. And the value of $U_{50\%}$ for D=5cm and D=10cm from this experiment tended to be close to each other.

Department:	Electrical Engineering	Student's Signature	.....
Field of Study:	Electrical Engineering	Advisor's Signature	.....
Academic Year:	2017		

ACKNOWLEDGEMENTS

This work would not have been possible without the help of the precious people during my research study. I would like express a deepest appreciation to my thesis advisor Assistance Professor Komson Petcharaks for his guidance help and insightful comment through learning process of this master thesis.

I would like to thank my thesis chairman Professor Boonchai Techaumnat and my thesis committee Assistance Professor Nutthaphong Tanthanuch for their valuable comments, helpful questions for improving the quality of this thesis.

My sincere thanks to high voltage laboratory in department of Electrical Engineering, Chulalongkorn University, and especially Mister Thavorn Auedee and Kriengkrai Odthanu for their help and collaboration during my experiment process.

I would like to gratefully thank to the ASEAN University Network/Southeast Asia Engineering Education Development Network (AUN/SEED-Net) for give an opportunity to pursue my master degree and the financial support for my research. I am also grateful to the staff in the Internal School of Engineering (ISE) for their assist and care during my study.

Last but not the least, I would like to thank my family for giving me an unconditional support and encouragement throughout my life time.

CONTENTS

Page

Page

List of Figures

List of Tables

Chapter 1
Introduction

1.1 General introduction

As the demand for electrical power supply, the transmission voltages of power system have been increasing to deliver the power energy as high as possible to feed the demand. The main benefit of delivering high voltage on the transmission line is the reduction of line loss. However, the power apparatus in the high voltage system must be ensured to withstand such high voltage stresses. Moreover, the electrical equipment also must have the capability of withstanding both external and internal overvoltage during the operation. Hence, the insulation and protective devices must be well designed not only for normal operating voltage but also for overvoltage case to guarantee a low probability of failure in the high-voltage power system. Accordingly, it is necessary to test high-voltage equipment during its development stage and prior to commissioning. The magnitude and type of test voltage vary with the rated voltage of a particular apparatus. The standard methods of measurement of high-voltage and the basic techniques for application to all types of apparatus for alternating voltages, direct voltages, switching impulse voltages and lightning impulse voltages are laid down in the relevant national and international standards.

Therefore, the high-voltage test and measuring techniques have to be able to properly test the apparatus which belong to the high-voltage power system. The basic principle of high-voltage testing expresses that test voltage stresses shall represent the characteristic stresses in service since not all these stresses were known [1]. Additionally, the type and amplitude of stresses depend on the system configuration, the used equipment, the environmental conditions and other influences.

In high voltage test technique, the measuring devices play an important role in the test of equipment. The measurements must provide an accuracy for measuring value during the test, according to IEEE standard for high-voltage testing techniques [2], the measuring system for DC voltage, AC voltage and impulse peak voltage peak require the basic uncertainty of ± 3%. However, after a long period of operation, the accuracy

of the measuring devices may be changed, so the satisfactory performance of a high voltage measurement device shall be shown by a calibration method.

As such, the breakdown voltage varies with the gap spacing; and for a nearly uniform field gap, a high consistency could be obtained, so that the sphere-gap is very useful as a measuring device as well as checking device [3, 4].

By precise experiments, the breakdown voltage variation with gap spacing, for different diameters and distances, have been obtained and represented in IEC60052-2002 [5]. In the measuring device, two metal spheres are used, separated by a gas-gap. The potential difference between the spheres is raised until a spark passes between them. The breakdown strength of a gas depends on the size of the spheres, their distance apart and a number of other factors. A spark gap may be used for the determination of the peak value of a voltage wave, for the checking and calibrating of voltmeters and other voltage measuring devices.

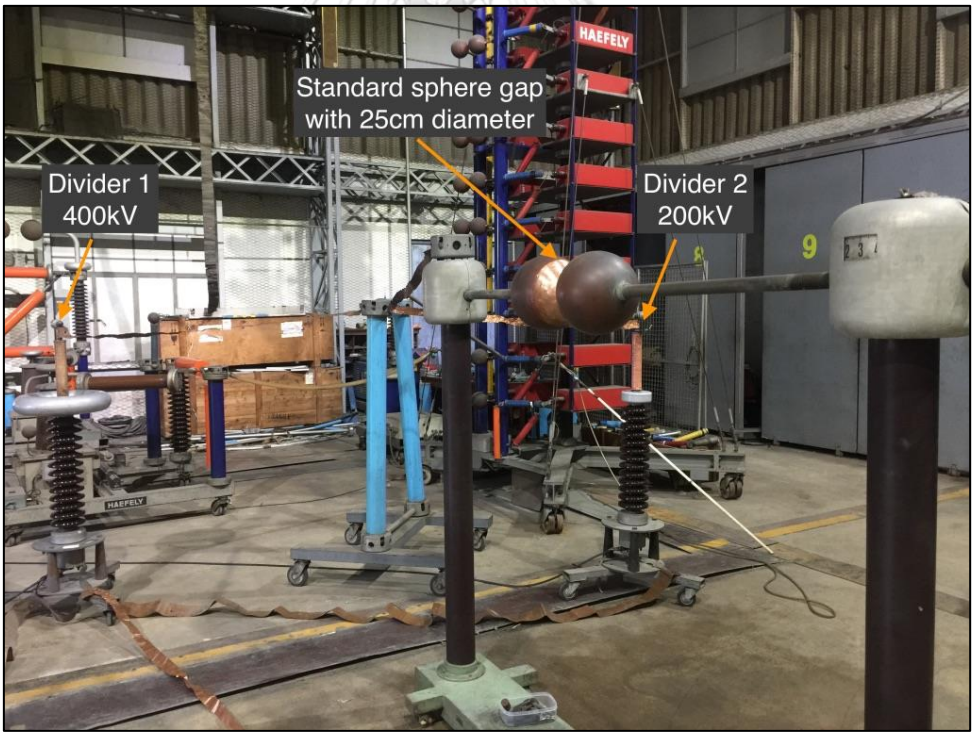

Figure 1-1 The standard sphere-gap with 25cm diameter is used for the performance check of voltage dividers ratio.

The limits of accuracy of the standard sphere-gaps are depended on the ratio of the gap spacing S to the sphere diameter D, as follows. For AC, switching and lightning impulse voltage, $S \leq 0.5D$, the uncertainty is ±3%, but for gap spacing $0.75D > S > 0.5D$, the

uncertainty are larger than ±3% [5]. However standard sphere-gap is not recommended to measure DC voltage since the erratic disruptive discharge may occur at low voltages. For this reason, a standard air gap is also used for the performance check of Approved Measuring System "AMS" to ensure that the most recent performance test is still valid (see Figure 1-1). According to IEC 60060-2 [6], the user of AMS is responsible for the performance checks and repeat them accordingly to ensure the stability of the AMS, at least once a year.

1.2 Literature review

By its simplicity, sphere gaps method of measuring the peak voltage is prefer to be used as the standard for calibration purposes. Actually, Sphere-to-sphere gaps are used to measure the peak voltage since 1913 base experimental and theoretical from Peek [7]. The relationship between the breakdown voltage and the humidity has been studied since that time. In an early 21st century, the measurement of high-voltage by means of sphere-gap has been led to the completed standard of HV testing represented by IEC 60052:2002. Furthermore, the IEC standard [5] simply states that, as the absolute humidity increases, the disruptive discharge voltage $U_{50\%}$ of sphere-gap increases at a rate of 0.2% per g/m^3.

1.2.1 The relationship between humidity and breakdown voltage of sphere-gap

Kuffel had done the experiment to study the effect of humidity on the breakdown voltage of sphere-gap and uniform-field gaps [8]. The sphere-gap of 2, 6.25, 12.5 and 25 cm-diameter spheres were used and the humidity was controlled artificially by enclosed in an air-tight chamber. According to his results, it showed that the effect of humidity of sphere-gap changed with the sphere diameter and also with the gap-spacing. The influence of humidity was greatest for largest sphere diameter and reduce for the smaller size of the sphere. The variation of voltage for a given change of humidity increased with gap spacing. The effect reached a maximum value at a well-defined gap length and descended to nearly half of the maximum value as the gap increased to a longer length. However, the author cannot find a numerical relation between voltage change and humidity.

Gourgoulis, Mikropoulos and Stassinopoulos [9] conducted the experiment to study the influence of impulse shape, gap spacing and of humidity on $U_{50\%}$ of 25 cm diameter spheres under standard lightning and switching impulse for both polarities. The authors simply stated that relationship between the $U_{50\%}$ and the humidity displays four characteristic features:

- The influence of humidity was higher for a large sphere than for small sphere
- The effect of humidity became lower with increasing of gap spacing
- For lightning impulse voltage, the influence of humidity on $U_{50\%}$ under negative polarity was stronger than under positive polarity
- The influence of humidity was more obvious under SI impulse than under LI

Later on, Gourgoulis and Stassinopoulos [10] investigated the breakdown mechanism of 75 cm diameter sphere-gap under standard lightning and switching impulse of both polarities by comparison with 25 cm sphere. The aim of this research was to study the effect of the applied impulse voltage on the breakdown mechanism of the gap, with emphasis on the waveshape, the gap spacing, the polarity, the diameter of the sphere and the absolute humidity. The results showed that the influence of humidity on $U_{50\%}$ depended on gaps spacing and the combination of waveshape and polarity. The effect reduced with increased gap length for positive polarity under lightning impulse. The authors explained that the relationship of humidity with the influence of polarity and waveshape is because the main mechanism of number free electron in critical volume is the detachment of electrons. Therefore, under negative polarity, the initial avalanche starts near the cathode, the electrons are driven with a reduction in their density in the critical volume which produces more chaos in primary electron than under positive polarity. With very short gaps length, the correlative abundance of the primary electrons is the main breakdown mechanism of air over the effect of humidity. Because the hindering action of increasing humidity on breakdown through the attachment of electrons to water vapour molecules leads to an increased rarity of primary electrons. However, the effect of humidity on the $U_{50\%}$ is inverse when humidity increases above 13 g/m^3, it can be attributed to an increased effect of augmenting of negative ion density that combined with the scarcity of electrons, which leads to a higher probability of electron detachment.

The influence of irradiation breakdown voltage of sphere-gap also has been investigating by Gourgoulis and Stassinopoulos [10]. An ultraviolet lamp was used to provide irradiation for 25 and 75cm diameter sphere under standard switching and lightning impulse voltage of both polarities. The experiment results showed that the influence of irradiation on $U_{50\%}$ acted relatively with impulse shape and polarity, gap spacing and sphere diameter and absolute humidity. It also showed that the application of external irradiation improved the reliability of standard sphere-gap (especially for small gap spacing) in the purpose of measurement and calibration.

1.2.2 Atmospheric correction method of IEC-60052:2002

IEC60052:2002 [5] provided an atmospheric correction method to regulate the breakdown voltage value of $U_{50\%}$ measured under actual conditions to the standard value. The breakdown voltage in the air at the actual condition can be corrected to the breakdown voltage at the standard condition by two factors, air density correction factor (δ) and humidity correction factor (k).

The standard atmospheric condition of IEC standard is described as follow:

Temperature $t_0 = 20$ °C

Pressure $b_0 = 760$ mmHg or 101.3 kPa

Absolute humidity $h_0 = 8.5$ g/m^3

The relative air density δ is defined as

$$\delta = \frac{b}{b_0} \times \frac{273 + t_0}{273 + t} \quad (1)$$

Where the atmospheric pressure b and b_0 are expressed in the same units;

t and t_0 are the temperatures in degree Celsius.

The values in this standard were obtained under conditions of absolute humidity in range between 5 g/m^3 and 12 g/m^3 with an average of 8.5 g/m^3 and the values of $U_{50\%}$ in the tables 2 and 3 of IEC standard could be corrected for humidity by multiplying

the values in those table by the humidity correction factor k given by the following equation:

$$k = 1 + (0.002 \times (h / \delta - 8.5)) \quad (2)$$

where the ambient absolute humidity h in g/m^3 and δ is the relative air density.

Breakdown voltage values U measured under actual conditions with the temperature t, the pressure b and the absolute humidity h are converted to standard reference atmosphere as follows:

$$U_0 = \frac{U}{\delta \times k} \quad (3)$$

1.2.3 The validity of IEC humidity correction factor in high humidity regions

Fujii, T. Hayakawa Student et al. discussed the usage of the humidity correction method in high absolute humidity regions[11]. The experiment of AC and lightning impulse voltage application had been conducted to study the effect of absolute humidity on disruptive discharge voltage of standard sphere-gap with diameter 50 cm. According to the experiment result, the validity of humidity correction factor by the IEC standard can be summarized as follow:

i. The usage of humidity correction method is acceptable for absolute humidity up to 12 g/m^3, and it also seems proper up to 22 g/m^3 under AC voltage. However, the percentage of the measured value within the range between 1± 3% of standard value, is relatively low for small gap spacing.

ii. For lightning impulse, the validity of humidity correction factor is acceptable for absolute humidity up 22 g/m^3 under both polarities. However, there is relatively low percentage of the measured value within 1 ± 3% of standard value for gap spacing of 4.0 cm under negative and for 16.0 cm under positive polarity.

Later on, Mizuno, Masuda et al. had done the experiment to investigate the validity of the humidity correction method from the IEC standard in case of high humidity region such as tropical countries [12]. The aim of their study was to evaluate the existing humidity correction method for absolute humidity up to 22 g/m^3. Since the data of this standard were only obtained under conditions of absolute humidity 5 g/m^3 and 12g/m^3.

Spheres of 12.5 cm and 50 cm in diameter were used in the test under both AC voltage and lightning impulse with positive and negative polarities. $U_{50\%}$ disruptive discharge voltage of 7.5 cm and 12.0 cm gap spacing for positive and negative lightning were shown in Figure 1-2 and 1-3, respectively.

In the below figures, the green line represents the value of $U_{50\%}$ disruptive discharge voltage of the standard, where the red lines represent the ±3% of the standard value. The blue dots represent the corrected $U_{50\%}$ disruptive discharge voltage from the experiment at the different range of absolute humidity.

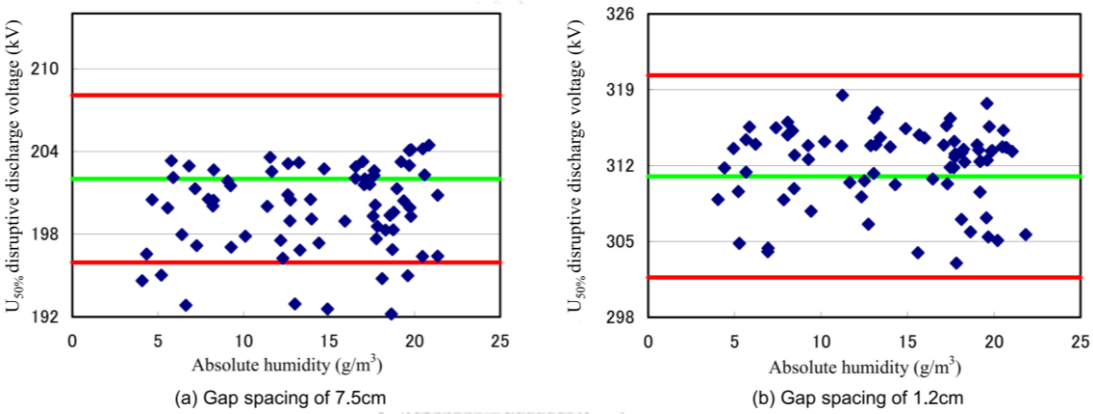

Figure 1-2 50% disruptive discharge voltage under positive lightning impulse of sphere diameter of 50cm [12].

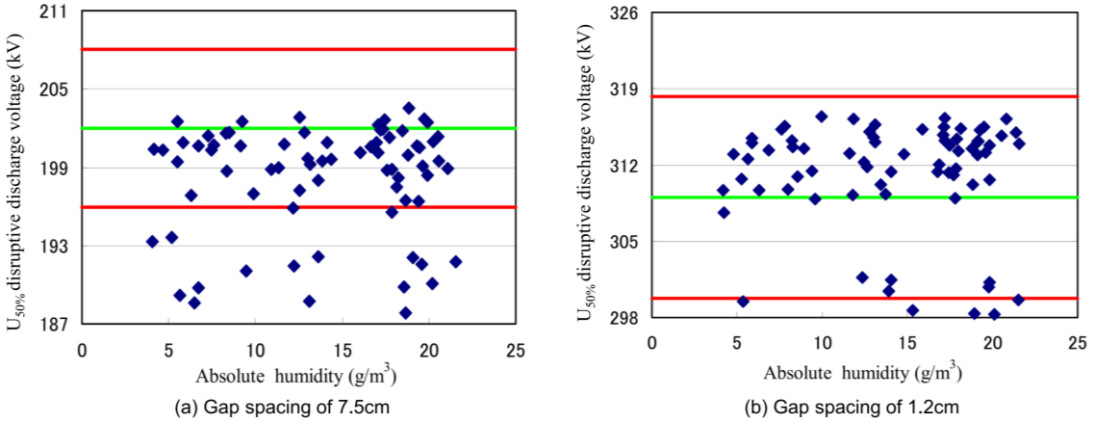

Figure 1-3 50% disruptive discharge voltage under negative lightning impulse of sphere diameter of 50cm [12].

Table 1-1 summarizes the results of experiments for AC disruptive discharge voltage. The evaluation of IEC humidity correction method for lighting impulse voltage with negative and positive polarity, are shown in Table 1-2 and 1-3, respectively.

Table 1-1 Evaluation of existing humidity correction method for breakdown voltage of AC voltage

Diameter (cm)	Spacing (mm)	Percentage within 1±3%		
		4-12g/m^3	12-23g/m^3	All range
2.0	3.0	11	54	43
	4.0	90	76	80
	5.0	100	88	91
	6.0	50	96	85
	7.0	43	92	82
12.5	1.0	78	38	50
	2.0	90	85	87
	3.0	100	60	73
	4.0	100	90	93
	5.0	40	25	30
50	2.6	87	62	72
	5.5	100	89	93
	11.0	97	98	97
	16.0	100	96	97

Table 1-2 Evaluation of existing humidity correction method for breakdown voltage of lighting impulse voltage with positive polarity

Diameter (cm)	Spacing (cm)	Percentage within 1±3%		
		4-12g/m^3	12-23g/m^3	All range
12.5	4.5	50	6	25
	5.0	27	6	14
	5.5	36	6	18
	6.0	64	33	43
50.0	4.0	75	74	76
	7.5	81	79	81
	12.0	100	100	100
	16.0	84	83	83

Table 1-3 Evaluation of existing humidity correction method for breakdown voltage of lighting impulse voltage with negative polarity

Diameter (cm)	Spacing (cm)	Percentage within 1±3%		
		4-12g/m^3	12-23g/m^3	All range
12.5	4.5	27	16	21
	5.0	6	11	8
	5.5	9	11	10
	6.0	9	16	14
50	4.0	70	50	60
	7.5	72	78	76
	12.0	90	89	89
	16.0	86	84	85

According to [12], it can be simply defined the validity of existing humidity correct method as follow:

i. Under AC voltage, the existing IEC humidity correction method is valid and it is possible to extend its validity up to 23 g/m^3 based on experimental results. Humidity correction method by IEC standard is usable for absolute humidity up to 23 g/m^3. However, the percentage $U_{50\%}$ of some gap spacing within the range between 1±3% of the standard voltage is too low, hence it is worth to make another investigation on some gap spacing.

ii. For lightning impulse with positive and negative polarities, the correction method seems proper for measurement with gap length larger than 7.5 cm. However, for smaller gap length the errors are unacceptable, so it is necessary to make another study the validity of the humidity correction method for small gaps spacing.

1.3 Problem statement

According to [11, 12], it can be seen that the existing humidity correction method seems not proper for small gap spacing under both AC and lightning impulse voltage. The most significant is the sphere of 12.5 cm diameter under lightning impulse with both polarities, the percentage of measured voltage within ±3% of the standard value is undesirably low. By comparing the result with ∅50cm sphere, it can be concluded that

the validity of IEC humidity correct method is not acceptable for standard sphere-gap of small diameter under lightning impulse voltage.

IEC60052:2002 [3] stated that to measure the voltage with spheres diameter of 12.5cm or less for all voltage and to measure peak voltage below 50 kV, it usually requires artificial irradiation from an external source. However, the authors of [11, 12] did not mention the application of external irradiation in the experiment. Therefore, it is worth to take an investigation on the validity of IEC humidity correction factor for small diameter sphere with aid of external irradiation source.

Peak values of disruptive discharge voltages ($U_{50\%}$ in impulse tests) of the standard sphere of 5cm and 10cm from Table 2 of IEC60052:2002 [3], shown in Figure 1-4.

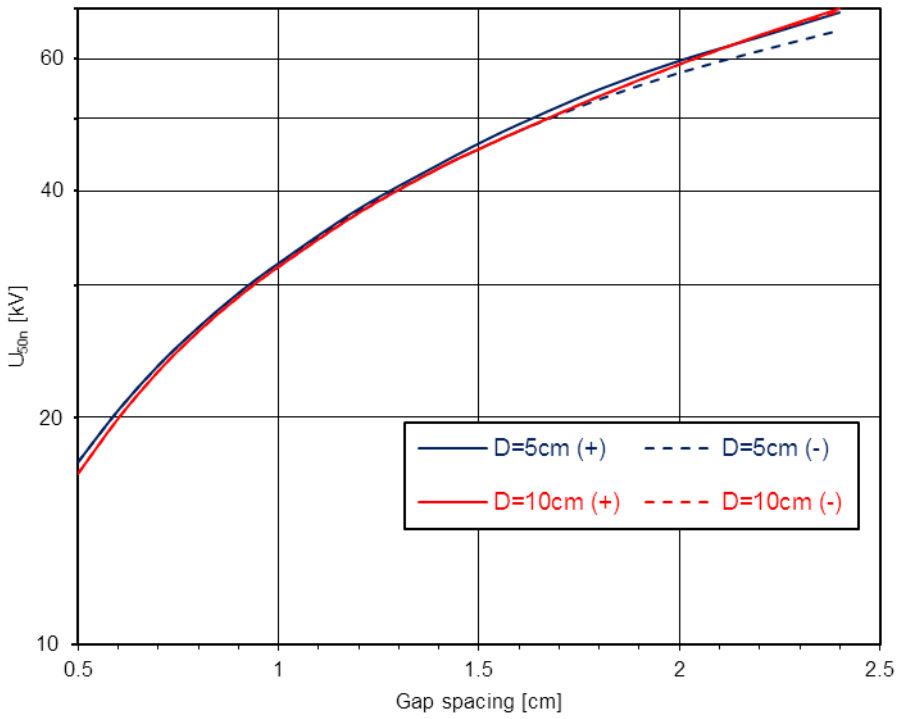

Figure 1-4 The plot of $U_{50\%}$ disruptive discharge voltage of 5cm and 10cm diameter sphere gap under negative and positive polarity against gap spacing.

From Figure 1-4, it can be seen that for negative polarity the breakdown voltage $U_{50\%}$ of the sphere of 5cm diameter is higher than 10cm diameter for the same gap spacing from 0.5 cm up to 1.2 cm. However, when gap spacing is higher than 1.2cm, the breakdown voltage $U_{50\%}$ of 5cm diameter sphere is smaller than the sphere of the 10cm diameter. The characteristic of the breakdown voltage between 5cm and 10cm spheres

is a doubt in comparison with the breakdown voltages of other spheres in the standard table.

With above matters, it is necessary to take an investigation to clarify the breakdown voltage of standard sphere-gap of 5cm and 10cm diameter. Moreover, the study should be taking into account the influence of humidity and the irradiation.

1.4 Objective and scope of work

The aim of this research is to clarify the breakdown voltage of standard sphere-gap by taking into account the validity of IEC humidity correction method for the following case:

- The standard sphere of 5 cm and 10 cm diameter with the gap spacing of 0.5, 1.0, 1.5, 2.0 and 2.4cm,
- The test was conducted to find disruptive discharge voltage $U_{50\%}$ under standard lightning impulse voltage (1.2/50μs) with both polarities,
- The artificial irradiation by the external source was used according to IEC60052:2002. In this present study, the UV Pen-Ray lamp was used to irradiate the sphere-gap.
- The absolute humidity was controlled by an artificial method in an enclosed test chamber. There are three range of humidity that were selected for this investigation: dry air, the absolute humidity of 10g/m^3 and 18 g/m^3.

1.5 Organization of this thesis

The organization of this thesis will be given as follows:

- Chapter 1: Reviews the general introduction, literature review, the research gap, the research objective and scope of work.
- Chapter 2: Presents the design of a cylindrical chamber that will be used to control the atmospheric condition around the spheres. The FEM software is used to study the effect of the chamber on the electric field distribution along the sphere-gap.

- Chapter 3: Presents the experimental setup for this present study including control and monitoring devices, impulse generators, measuring devices and the method that was used to treat the test results.
- Chapter 4: Presents the results and discussion.
- Chapter 5: Presents conclusion and recommendation.

1.6 Research outcome

The benefit of this research work is the revisit of the $U_{50\%}$ disruptive discharge voltage in Table 2 and Table 3 of standard IEC-60052, only for 5cm and 10cm diameter sphere-gap. Moreover, the humidity correction method provided by this standard is investigated to clarify that if it is valid or not for various humidity range and with artificial irradiation.

Chapter 2
The design of sphere-gap test chamber

2.1 Introduction

It is possible to carry out extensive modelling of the most complex geometries and use the experimental test to validate the accuracy of the Finite Element Method (FEM) results. In recent years, FEM has been widely used by the researchers who developed numerous FEM models of towers, insulators, conductors, switches, etc. to deal with the high-voltage engineering problems [13]. Gutiérrez, Sancho et al studied the influence of conductivity and electric field distribution caused protrusion and voids in DC cable. A 2D-FEM has been used to verify an agreement with analytical formulas [14]. Xie, Zheng et al. investigated the electric field analysis as well as the optimization design of grading ring configuration for a new Ultra High Voltage (UHV) equipotential shield capacitor voltage transformer, by using 3D-FEM simulation model [15]. Kumar & Kalaivani used 2D-FEM to analyze the electric field distribution of 110 kV composite insulator. Design of the 110 kV insulators with four different weather sheds is simulated under clean, uniformly polluted and dry band surface conditions to analyze the electric field and the factors affecting the electric field distribution along the 100 kV silicone rubber composite insulators [16]. With these numerous research, it indicates that the usage and the reliability of FEM for electric field analysis have been increasing.

In this chapter, a chamber of sphere-gap will be designed by using a modern FEM, the study is combining with two software: GID [17] and Elmer FEM solver[18]. The model geometry including material properties, boundary condition, and mesh generation will be created and simulated on the GID software. While Elmer will be used to simulate as well as calculate the electric field of preprocessing geometry model from GID software.

The purpose of this chapter is to study the effect of the enclosed chamber of cylinder shape on the electric field distribution across the gap of spheres. The chamber will be used to control the atmospheric condition of the sphere-gap. The aim of the design is to find the chamber size with the economic aspect as well as the size which is convenient for mechanical work. The configuration geometry of the simulation model will follow

the vertical sphere-gap of the standard IEC-60052, by taking into account with the clearance limits of the spheres [5]. The material that will be used to construct the chamber will be studied in this simulation process, to make sure that it will be valid for the actual experiment.

It necessary to mention that the geometry of the model will be designed in 2D. Hence, to simulate the real application of the sphere-gap chamber (3D), the axisymmetric coordination system will be used in Elmer to calculate the electric field.

2.2 The design of model geometry

According to IEC-60052, there are two arrangements of a sphere-gap for high voltage measurement: vertical gap and horizontal gap. For this study, the vertical sphere-gap arrangement will be transferred to a CAD design and this CAD will be simulated using GID and Elmer software. By having the IEC standard as a reference, it should be ensured that nothing in the vicinity of the model configuration, wall or ground object, can be influence the calculation of the results. Hence, the configuration geometry of both 5cm and 10cm diameter sphere-gap will follow Table 2-1 - clearance limit of the IEC standard [5].

Table 2-1 Clearance limits of the standard sphere-gap.

Sphere diameter D cm	Minimum of height A	Maximum value of height A	Minimum value of distance B
Up to 6.25	7D	9D	14S
10-15	6D	8D	12S
25	5D	7D	10S
50	4D	6D	8S
75	4D	6D	8S
100	3.5D	5D	7S
150	3D	4D	6S
200	3D	4D	6S

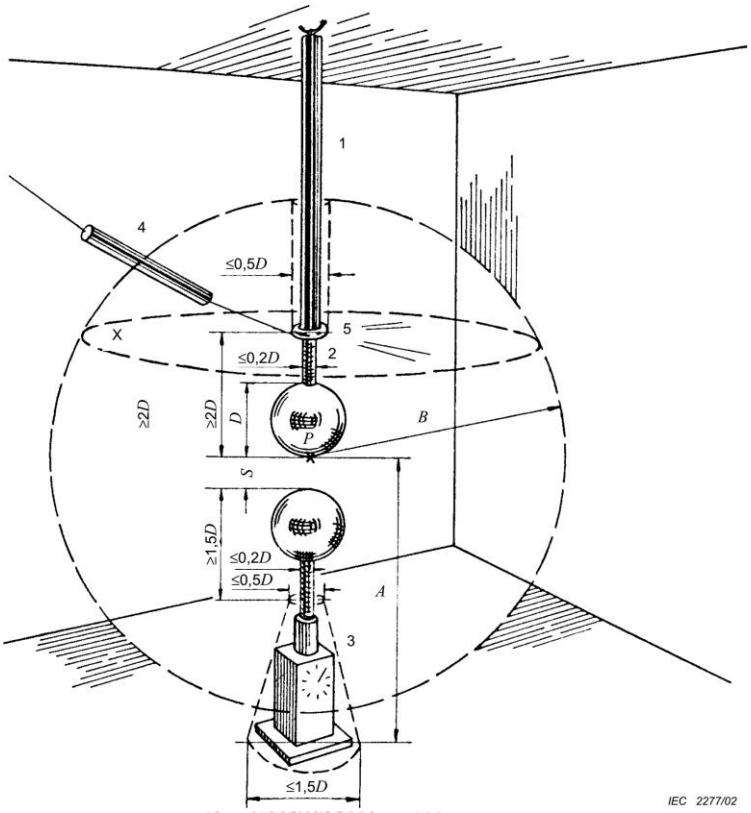

Figure 2-1 The real 3-dimensional geometry of vertical sphere-gap[5].

In this simulation study, the voltages of the high voltage sphere and earth sphere are set equal to 1 volt and 0 volts, respectively. The gap length is set equal to S=5cm and S=2.4cm for 10cm and 5cm sphere-gap, subsequently.

Before the study, the effect of the chamber on electric field distribution of sphere-gap, mesh size and boundary size of the simulation model must be chosen to ensure the precision of the simulation results [19]. The effects of mesh size and boundary size on electric field distribution of both 5cm and 10cm diameter sphere-gap are presented in section 2.4.

Design criteria of the cylindrical chamber for vertical sphere-gap:

- Influence on the electric field distribution of sphere-gap,
- Economical size,
- Ease of mechanical work and of the experiment process.

And, the flowchart for designing the chamber, is described in Figure 2-2.

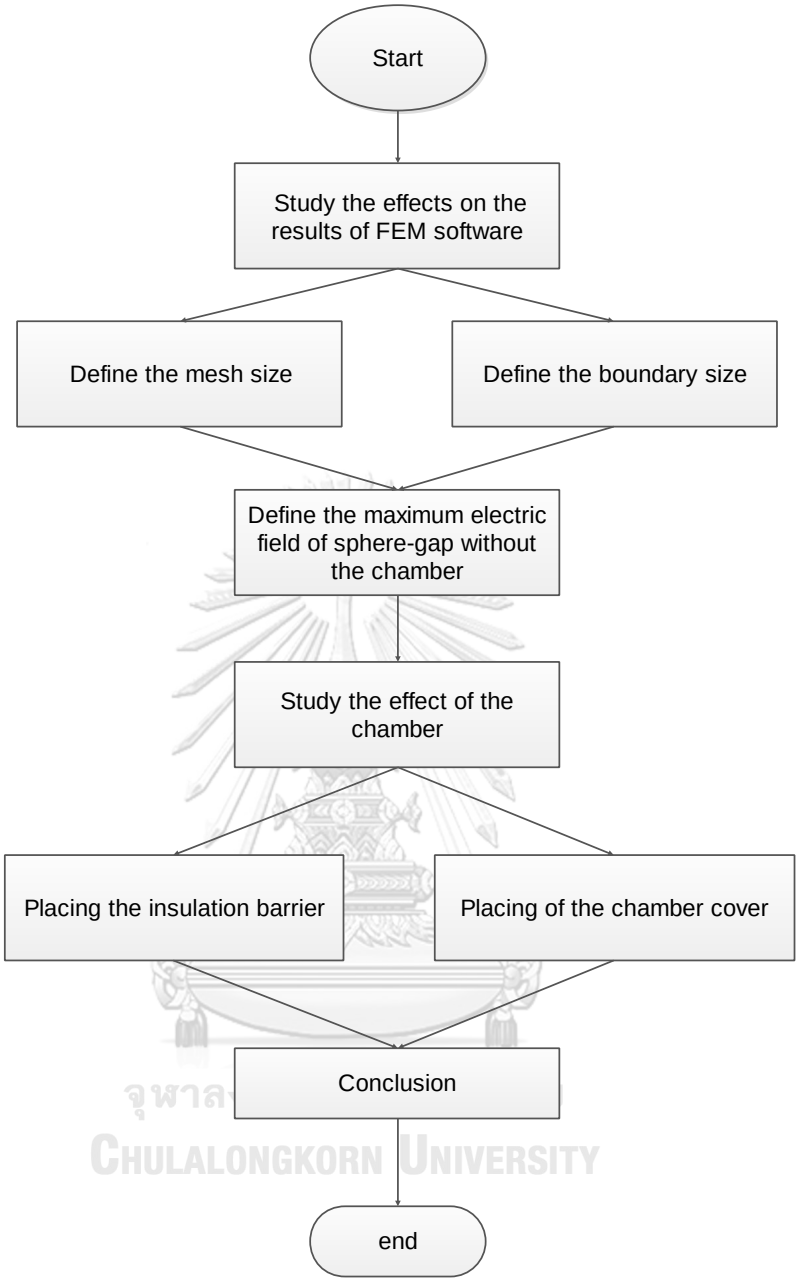

Figure 2-2 Design of the chamber's flowchart.

An initial version of the simulation model for both 10cm and 5cm diameter sphere-gap in GID software is presented in Figure 2-3.

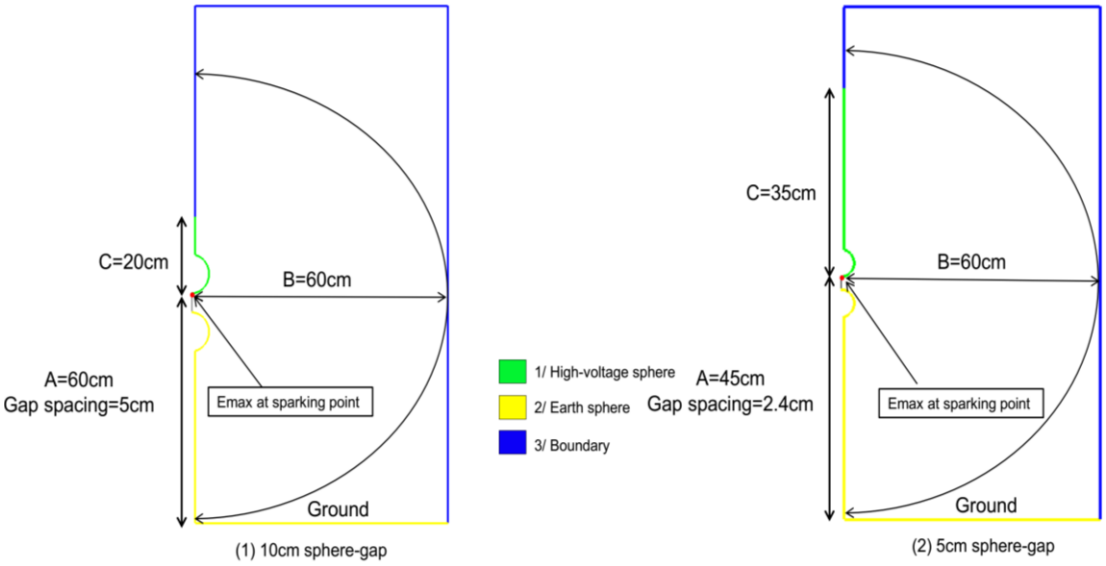

Figure 2-3 Sphere-gap configuration in GiD software.

Keyword:

C: High-voltage sphere shank

A: Height of sparking point above earth plane

B: Radius of space free from external structures

2.3 Simulation workflow

The workflow of the simulation process can be described by a simple and comprehensive flow-chart. The sequence of steps can be followed in order to design the configuration of the geometrical model using GiD software, while the result of preprocessing results of the GID will be used to simulate the electric field on Elmer software. The flowchart of the whole processes is shown in Figure 2-4.

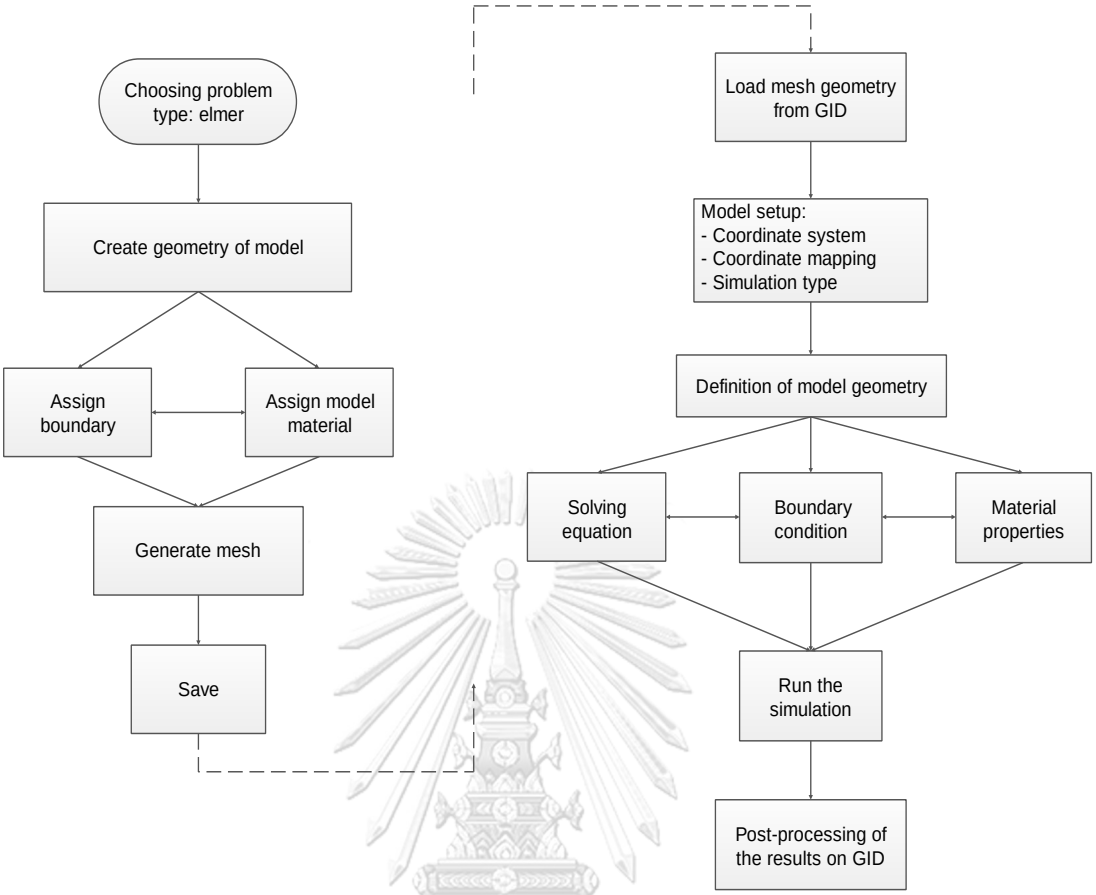

Figure 2-4 Flowchart of the simulation process.

2.4 The parameters affect the FEM simulation results

Because the stability of the results of the simulation model of FEM may be affected by two significant parameters such as mesh size, simulation space size [20]. Hence, the effects of these mentioned parameters will be studied to find the accuracy of the simulation results. As the sparking point is the point where the electric field is maximum "E_{max}" as well as the point where the breakdown is initiated. Hence, the accuracy of the simulation results will be studied on the value of E_{max}.

2.4.1 The effect of mesh size

The generation of the mesh is the most important part of designing the simulation model. In this process, the designed geometry is divided into small units of simple shapes, call mesh elements [21].

Generating a mesh is the process by which a mesh is calculated from the geometry definition of the domain. This mesh will be used for the numerical analysis at a later stage. Conditions and materials assigned to geometric entities will be transferred to the node and elements [17]. In 2D geometries, the continuous models are transferred into triangular or quadrilateral elements by process of discretization in GID. If the geometry shape consists of the curve, there will be a chance that the surrounding area, especially the boundaries is not well divided and the mesh size in the area may be larger. Hence, to get the high accuracy of calculation, it can be done by using the mesh structures which is able to smooth the size and resolution near these boundaries, where the solution is exposed to more steep changes and certainly is an area of higher interest (i.e The sparking point of sphere-gap) [21].

Depending on the numerical approach to be used for the calculation or the requirements of the numerical simulation, the different kind of meshes can be used to generate on GID. As the chordal error method is able to separately assign mesh size on the boundary of the model geometry, where is the area of interest. And by taking simulation time into account, assigning mesh size with chordal error will be used as a method to create a mesh of the model geometry.

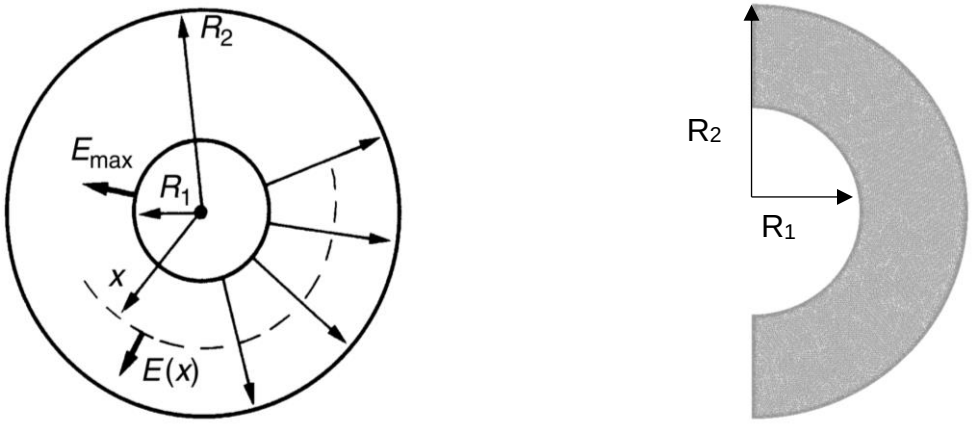

Figure 2-5 Coaxial sphere [22] and its configuration geometry (2D) on GID.

In this part, the suitable mesh size will be found for both ∅5cm and ∅10cm sphere. Since the electric field distribution of the coaxial sphere can be simply derived from the Equation (9) [22], and the model of the coaxial sphere is similar to the model of sphere-sphere. So, the model of a coaxial sphere, which has the inner sphere radius R_1 = 2.5

cm and 5cm and the outer sphere radius R_2 = 7.5 cm and 10cm, is used instead of sphere-gap of 5cm and 10 cm diameter, respectively, to define an acceptable mesh size.

$$E(x)=\frac{Q}{4\pi\xi}\frac{1}{x^2}=\frac{V}{(R_2-R_1)/R_1R_2}\frac{1}{x^2} \quad (4)$$

The E_{max} is reached when x equal to R_1, can be obtained by the following Equation:

$$E_{max}=\frac{V}{R_1\ 1-R_1/R_2} \quad (5)$$

The effect of mesh size on the electric field distribution of the coaxial sphere is studied by comparing the value of E_{max} from simulation with the $E_{max.analytical}$ from Equation (5). The %Error between E_{max} from $E_{max.analytical}$ can be derived from the following equation:

$$\%Error=\frac{E_{max.simulation}-E_{max.analytical}}{E_{max.analytical}}\times 100 \quad (6)$$

The study model: coaxial sphere 5cm 10cm (R_1=2.5, R_2=7.5) and coaxial sphere 10cm and 15cm (R_1=5, R_2=10) with a voltage equal to 1 volt for the inner sphere and 0 volts for the outer sphere.

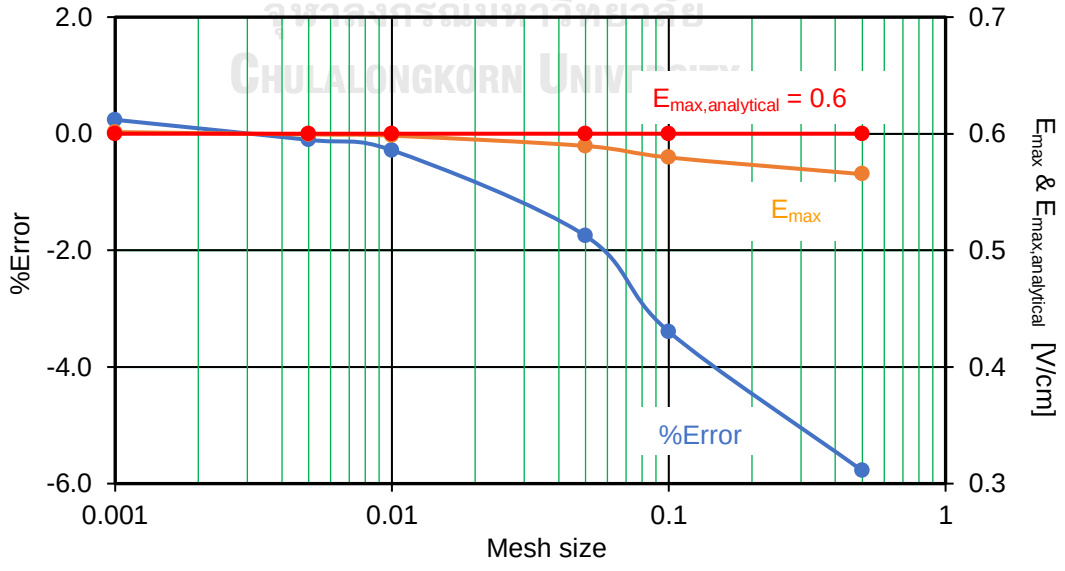

Figure 2-6 %Error of E_{max} for various mesh sizes (coaxial sphere 2.5cm 7.cm with difference mesh size).

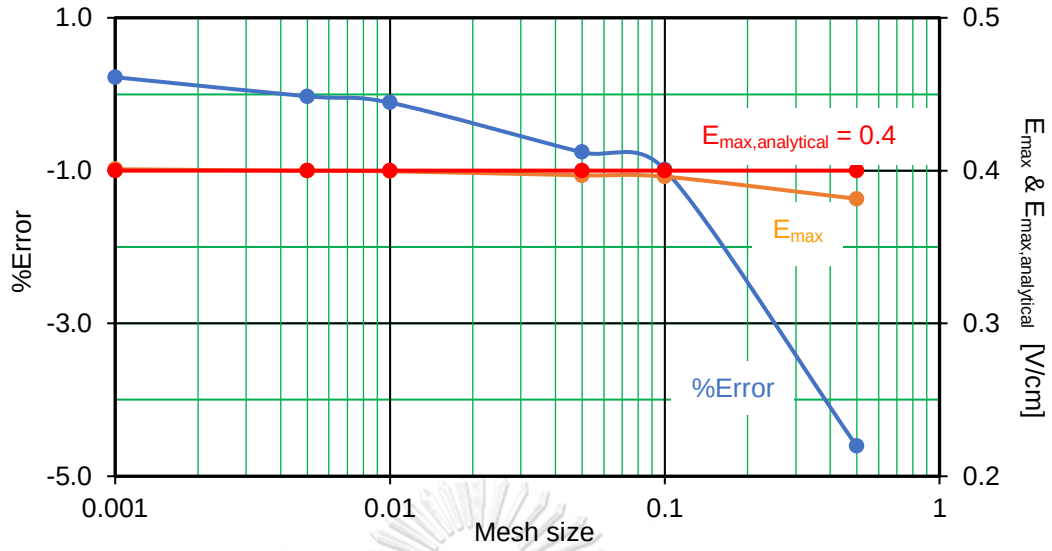

Figure 2-7 %Error of E_{max} for various mesh sizes (coaxial sphere 5cm 10cm with difference mesh size).

By considering for both calculation accuracy and simulation time, mesh size of 0.005 and 0.01 will be used for sphere diameter of 5cm and 10cm, respectively, with %Error of *-0.105* and *-0.11* for ∅5cm and ∅10cm sphere, respectively. (see Table 2-2).

Table 2-2 Desired simulation mesh size for each sphere-gap configuration model.

Sphere-gap diameter	Mesh size	%Error	$E_{max,\ without\ chamber}$ [V/cm]
∅5cm	0.005	-0.105	0.59937
∅10cm	0.01	-0.11	0.31520081

A free triangular mesh is created with an extra fine element size and the division of the domains seems quite uniform. However, there is a small change of the distribution of the elements in the vicinity of the sphere curve as well as on the boundary of the model. In the case of a fast and approximate solution, this mesh can be considered as sufficient (see Figure 2-8). But for a precise solution, an even finer mesh should be generated, at least on the boundaries of the model where is the major importance of electric field distribution (see Figure 2-9).

Assigning mesh size with chordal error, the mesh size is so tight around the boundary of the configuration geometry, especially the curve and the line that represents both spheres including the sparking point and electric field across the sphere-gap (see Figure

2-9). The mesh is so tight which means that the simulation results will be more precise in these areas of interest.

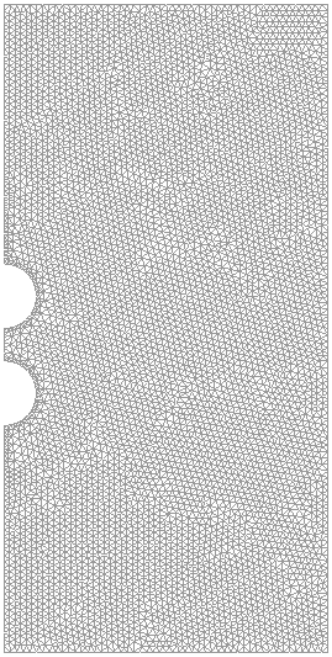

Figure 2-8 Mesh generation on GID by setting the size of the element (the mesh size of entire configuration geometry =1).

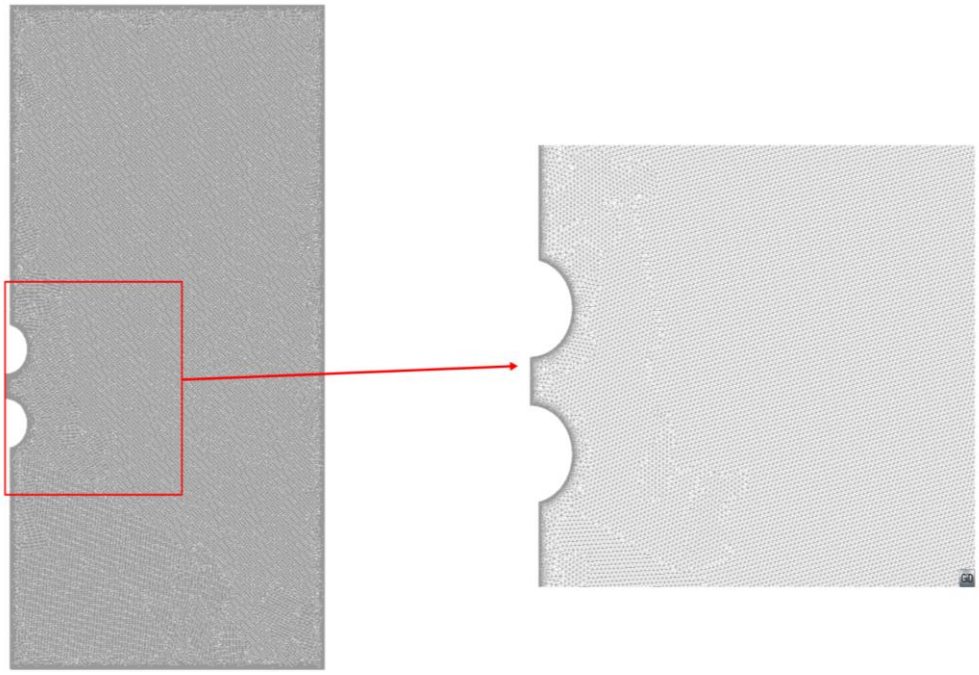

Figure 2-9 Mesh generation by using chordal error function (mesh size=0.01 on the boundary of configuration geometry).

2.4.2 The effect of boundary size

Unlike the charge simulation or surface charge simulation method, FEM needs boundary as it cannot simulate a model that has free space. This boundary may be defined as Dirichlet boundary condition, where it has a fixed potential, or Neumann boundary condition, where there is no change in the electric field in the direction normal to the boundary, e.g. $\frac{\partial E}{\partial n} = 0$.

Hence, in this part, the effect of boundary size will be studied on electric field distribution across the gaps between spheres. In order to eliminate errors, the boundary size has to set far enough from the model geometry [23]. However, as the mesh size is really small (0.005 for ∅5cm sphere and 0.01 for ∅10cm sphere), hence, the simulation will take time to complete if the boundary size is large. For this reason, the study will take into account both calculation accuracy and simulation time. The geometrical configuration of 10 cm diameter sphere-gap will be used to simulate for finding the acceptable boundary size. The acceptable boundary size will also use for geometrical configuration of 5cm diameter sphere.

"X" defined the size of the boundary size for both horizontal and vertical axis (Figure 2-10), will set initial value at 300cm. Then, the value "X" will be decreased to find acceptable error between E_{max} of each boundary size and of initial boundary size.

It is necessary to notify that the configuration geometry in Figure 2-10 is considered as the vertical arrangement of standard sphere-gap.

Simulation model:

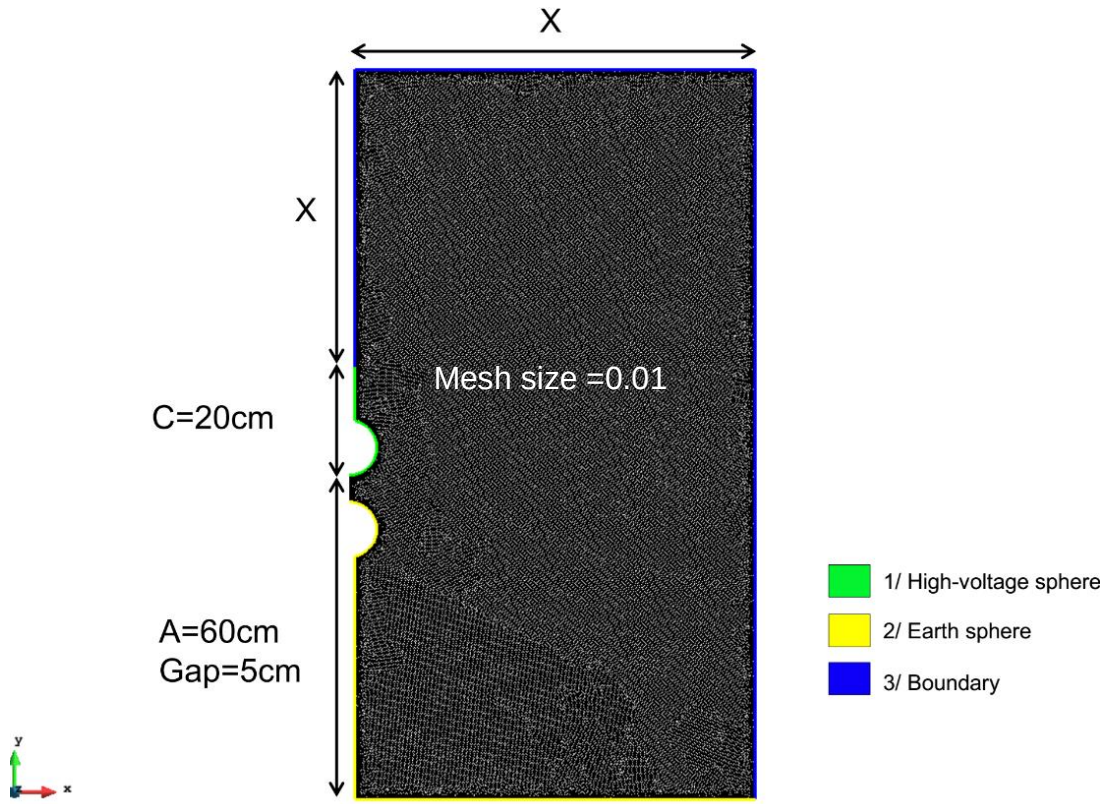

Figure 2-10 Simulation model of vertical sphere-gap

Simulation results:

The electric field distribution along the sphere-gap of each boundary size is plotted in Figure 2-11.

The E_{max} of different boundary size $E_{max,X}$ will compare to $E_{max,300}$ = 0. 3160606 V/cm of initial boundary size X=300 cm. Following the Equation (7), the %Error between each boundary size and initial boundary size is shown in Figure 2-12.

$$\%Error=\frac{E_{max,X}-E_{max,300}}{E_{max,300}}\times 100\% \quad (7)$$

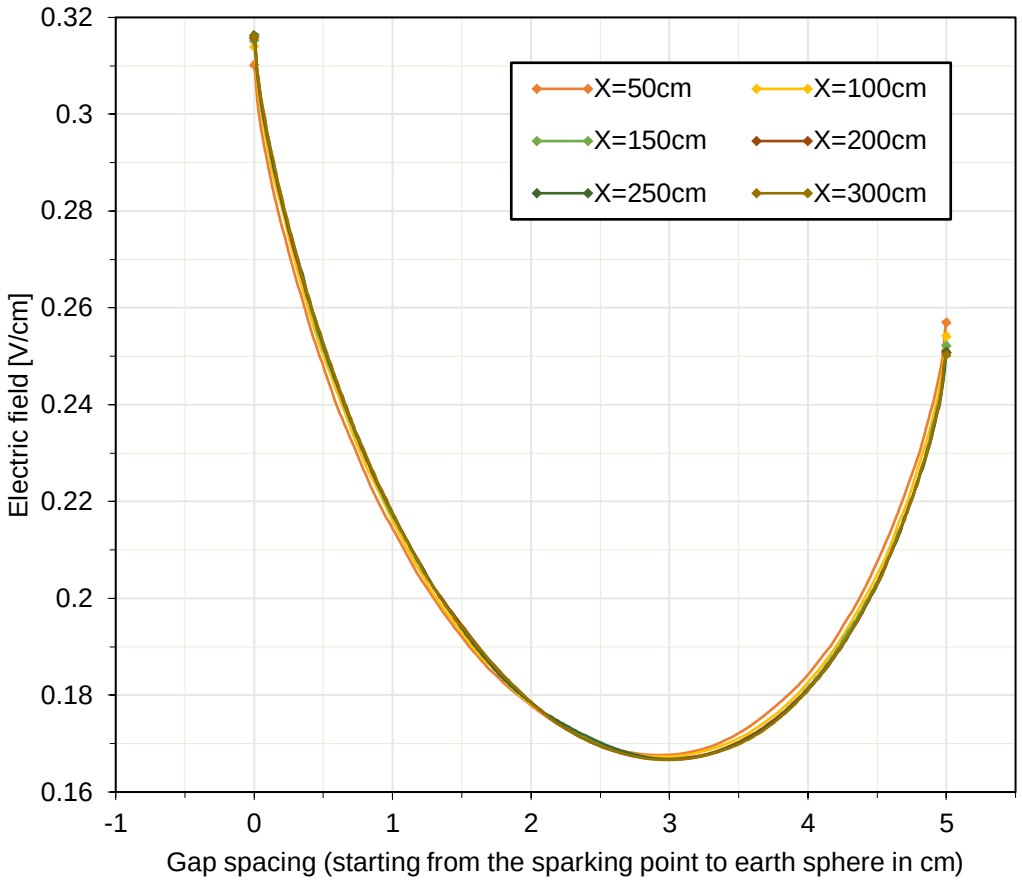

Figure 2-11 The electric field distribution across the sphere-gap with various boundary sizes.

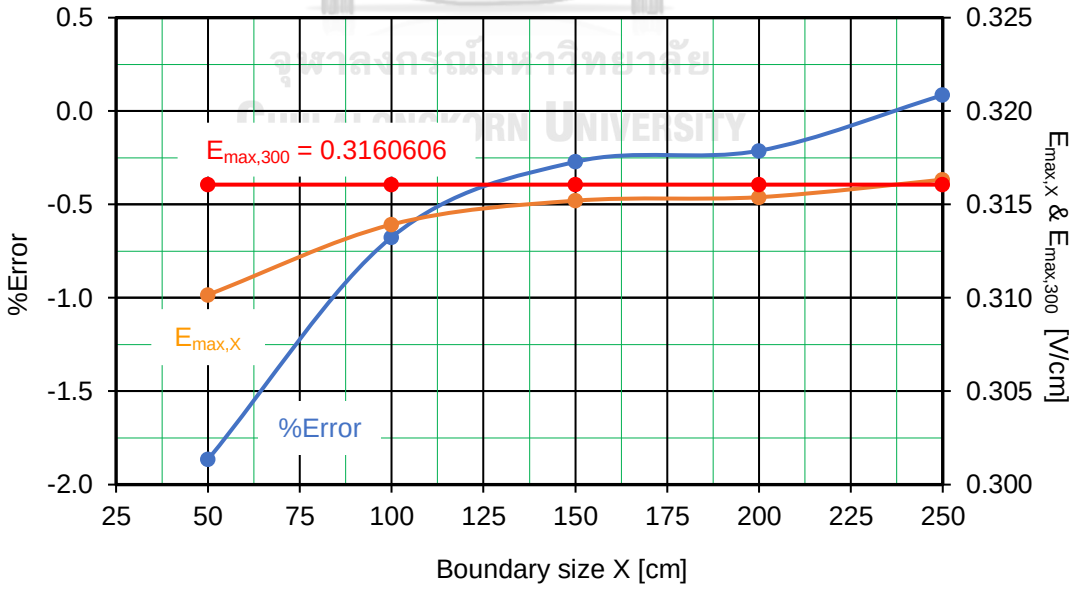

Figure 2-12 %Error of E_{max} with various boundary sizes X.

By considering both the accuracy of the software and the simulation time, the X =**150cm** is chosen as the boundary size for the next effect studies. The E_{max} of 10cm diameter sphere-gap with boundary size **150cm** ($E_{max,150}$ = **0.31520081 v/cm**), while for 5cm diameter sphere-gap, $E_{max,150}$ = **0.63277692 v/cm** as the boundary size X =**150cm**. Hence, the simulation model of sphere-gap with the boundary size of 150cm and the mesh size of **0.005** and **0.01** for 5cm and 10cm sphere-gap, respectively, is considered as the model of sphere-gap without chamber (Table 2-3).

Table 2-3 The E_{max} of sphere-gap without the chamber(reference $E_{max,\ without\ the\ chamber}$ values).

Sphere-gap diameter	Mesh size	Boundary size	$E_{max,\ without\ chamber}$ (v/cm)
∅5cm	0.005	150	0.31520081
∅10cm	0.01	150	0.63277692

2.5 Placing the cylindrical chamber of sphere-gap

There are two steps in order to get a proper size of the chamber:

1. Placing the insulation barrier to find the acceptable size
2. Placing two materials covers: metal and insulation on the barrier, to find which cover material has less influence on the electric field distribution of sphere-gap.

In this implementation, the study is taken for 10cm diameter sphere-gap only as the chamber will be used for both sphere-gap.

2.5.1 Placing the insulation barrier (chamber body)

In this study, the barrier of insulation material that will be used as chamber body material is placed at distance D =60cm, and then it is decreased to analyze the effect on the electric field distribution across gaps of the sphere (Figure 2-13). Actually, the barrier is like a cylindrical chamber without top cover and the purpose of this part is to find the small radius of a cylindrical chamber with less influence on the electric field.

Simulation model:

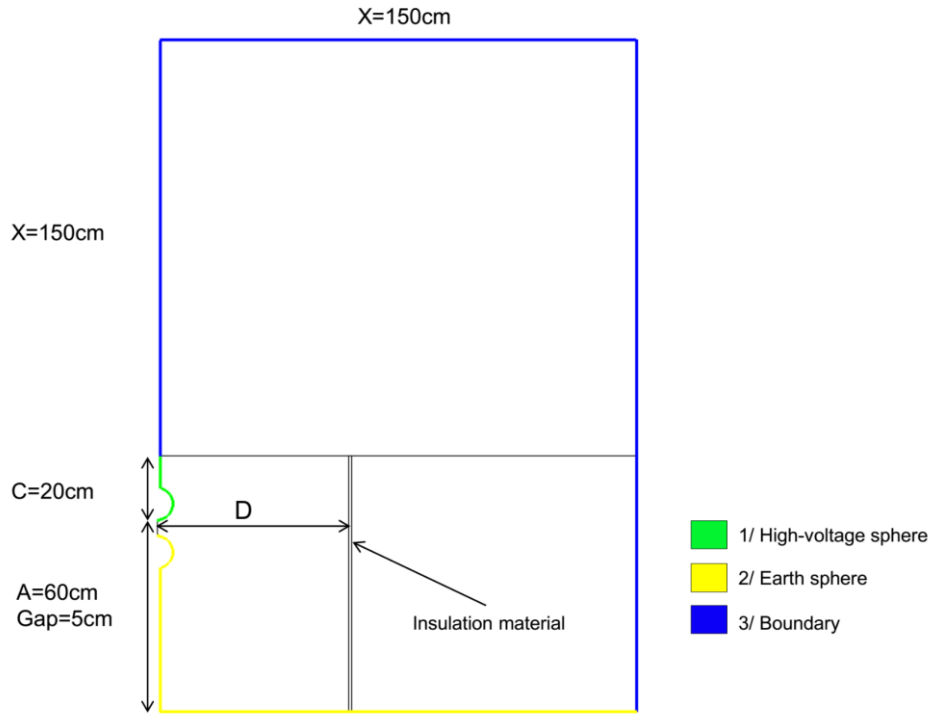

Figure 2-13 simulation model of vertical sphere-gap with insulation barrier.

Simulation results:

After placing the chamber, the electric field distribution along sphere-gap of each distance D is plotted in Figure 2-14. Following the Equation (8), the $\%Error$ of the E_{max} after placing the insulation material at each distance D is shown in Figure 2-15.

$$\%Error=\frac{E_{max,D}-E_{max,without\ chamber}}{E_{max,without\ chamber}}\times 100\% \quad (8)$$

According to Table 2-15, the barrier has not much effect on the $E_{max,without\ chamber}$ of the sphere-gap, the overall $\%Error$ is around 0.2% or less. For the next step, the cover will place on the barrier and the simulation will be made to see the effect.

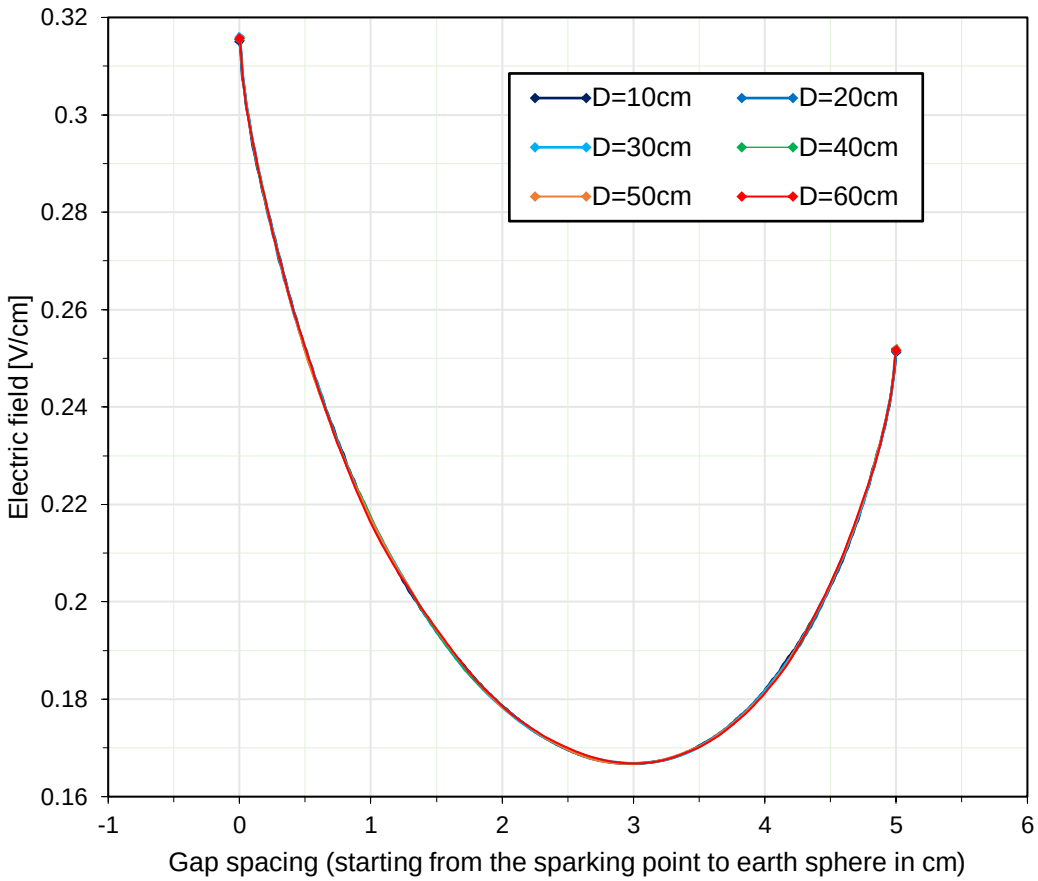

Figure 2-14 The electric field distribution across the gap with different barrier distance.

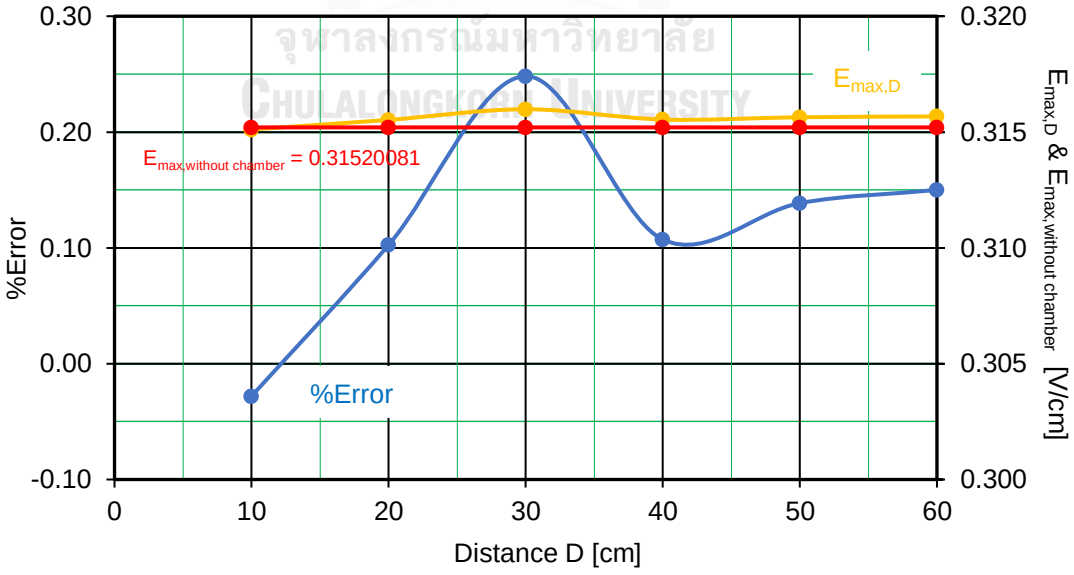

Figure 2-15 %Error of E_{max} with various barrier distance D.

2.5.2 Placing the chamber cover

There are two model options of the chamber that have been taken to study to consider which model has the lowest effects on electric field distribution across the sphere-gap. The distance E&F is the distance from the sparking point of the high-voltage sphere to the chamber top. These two parameters will increase from 20cm to 60cm to study the influence on the electric field distribution across the spheres.

For the bottom part of the chamber, the metal will be used because the metal is convenient for installing the adjusting gear of the earth sphere as well as for connecting the earth connection.

2.5.2.1 First option: Metal cover

Simulation model:

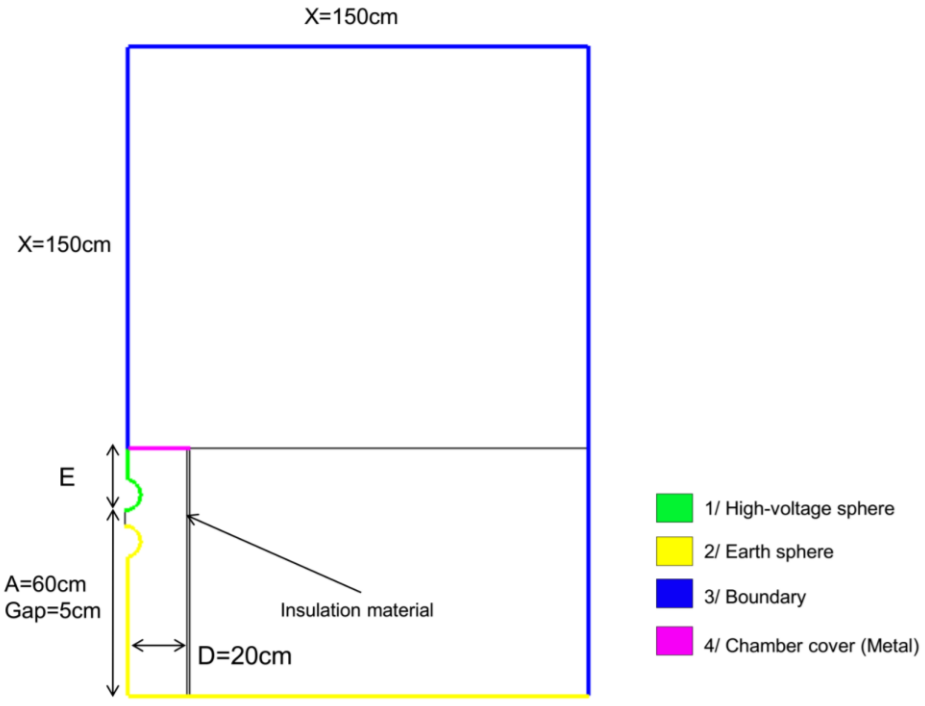

Figure 2-16 Simulation model of vertical sphere-gap with the metal cover chamber.

Simulation results:

Placing the chamber with metal, the electric field distribution along sphere-gap of each distance E is plotted in Figure 2-16. Following the Equation (9), the %Error of the E_{max} after placing the metal cover at each distance E is shown in Figure 2-17.

$$\%Error=\frac{E_{max,E}-E_{max,without\ the\ chamber}}{E_{max,without\ the\ chamber}}\times 100\% \quad (9)$$

With metal cover, the chamber has a strong influence on the E_{max} of the sphere-gap. The %Error for each distance E around -2.5% and the maximum one is -3.23% at distance E = 20cm. With this large %Error, the metal cover seems not able to use for this chamber configuration.

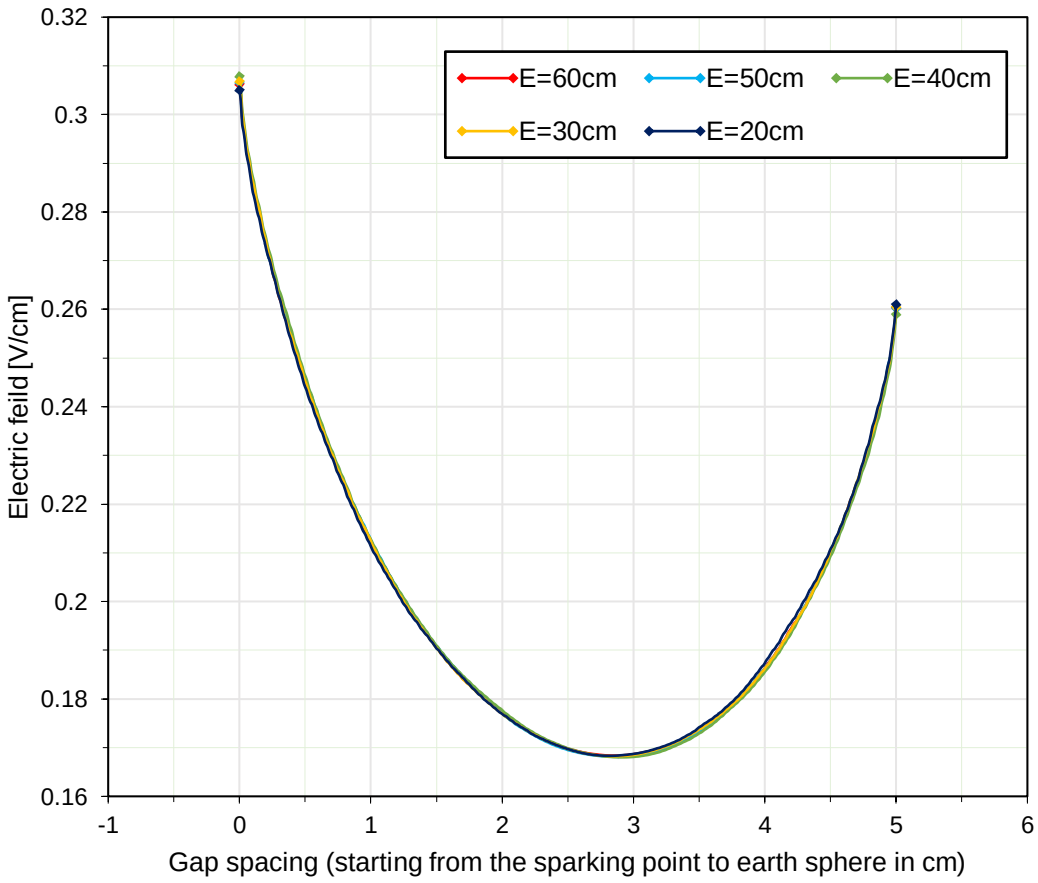

Figure 2-17 Electric field distribution across the gap with different chamber height E.

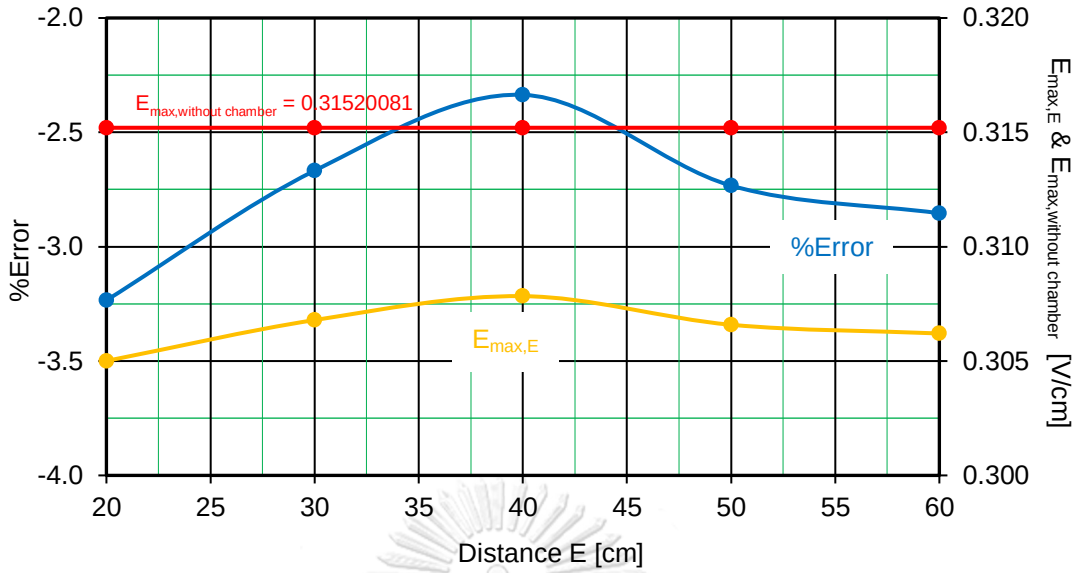

Figure 2-18 %Error of E_{max} with various metal top cover distance E.

2.5.2.2 Second option: Insulation Cover

Simulation model:

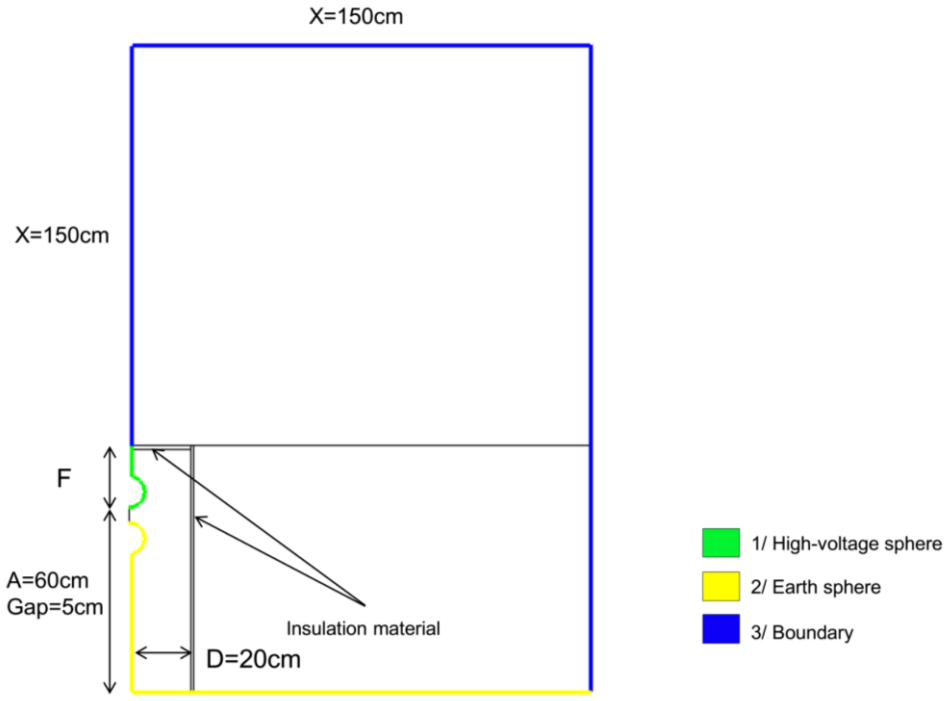

Figure 2-19 Simulation model with insulation cover chamber.

Simulation Results:

Placing the chamber with insulation material cover, the electric field distribution along sphere-gap of each distance F is plotted in Figure 3-20. Following the Equation (10), the %Error of the E_{max} after placing the insulation material cover at each distance F is shown in Figure 2-21.

$$\%Error=\frac{E_{max,F}-E_{max,without\ the\ chamber}}{E_{max,without\ the\ chamber}}\times 100\% \quad (10)$$

According to Table 2-8, the %Error decreases with the distance F, from -2.012% at F =60cm to -0.373% at F=20cm. With an acceptable %Error of -0.373% at F=20cm, the insulation cover with a total height of 80cm is suitable for use.

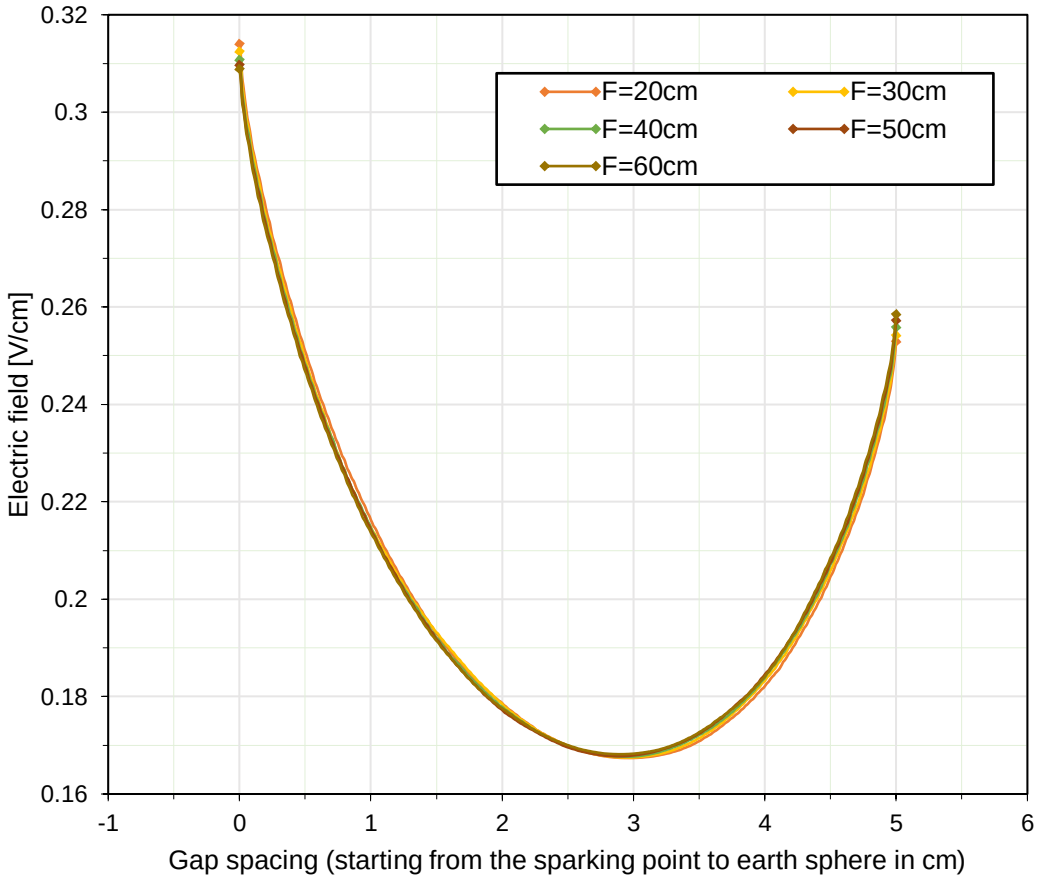

Figure 2-20 Electric field distribution across the gap with different chamber height.

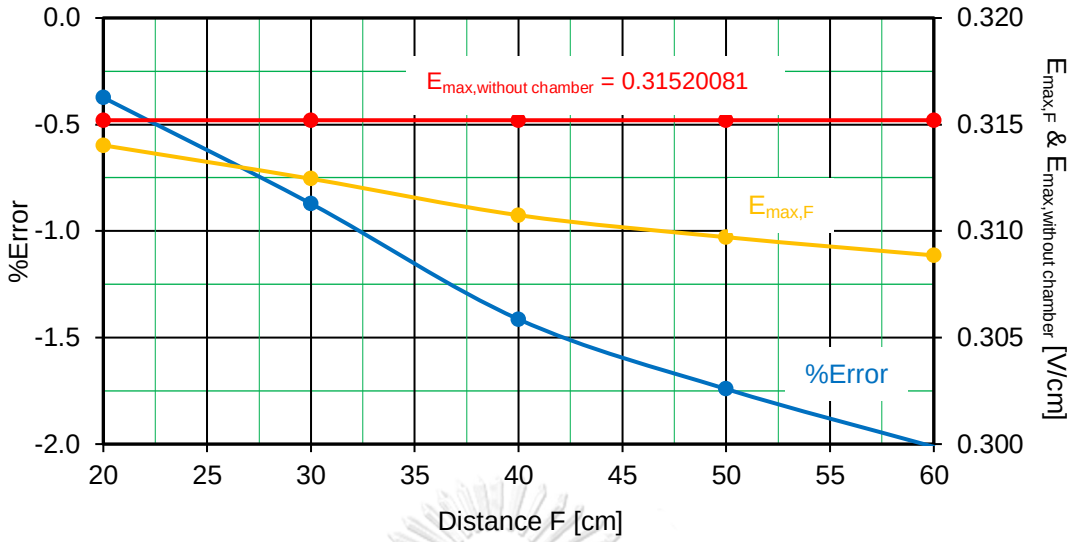

Figure 2-21 %Error of E_{max} with various insulation top cover distance F.

2.5.3 Conclusion

The previous simulation results indicate that:

1. The mesh size and boundary size have a significant effect on the accuracy of simulation results,
2. The insulation body of the chamber has a slight effect on the maximum electric field E_{max} of the sphere-gap,
3. The metal top cover of the chamber has a strong effect on the maximum electric field E_{max}, while the insulation top cover has no significant effect on E_{max}.

Hence, it can be concluded that the chamber should have the body and the cover top made of insulation material while the bottom part is metal material for ease of adjusting gear and earthing connection. The smallest chamber has a height of 80cm and a radius of 20cm with an acceptance %Error of -0.373%.

2.6 The chamber size for 5cm and 10cm diameter sphere-gap

According to the above studies, it shows that the insulation top and metal bottom cylindrical chamber with a height of 80cm and radius of 10cm is suitable to enclose the vertical sphere-gap. However, inside the laboratory, there is an existing chamber with a height of 80 cm and radius of 15cm (Figure 2-22), the body of the chamber is insulation material while the top cover and bottom part are metal. Since the insulation material cover has a small influence on electric field distribution along sphere-gap, the cover top of this old chamber will be replaced by insulation material. Hence the model geometrical of this chamber (Figure 2-23) can be created for the simulation to see if it is acceptable or not to be used.

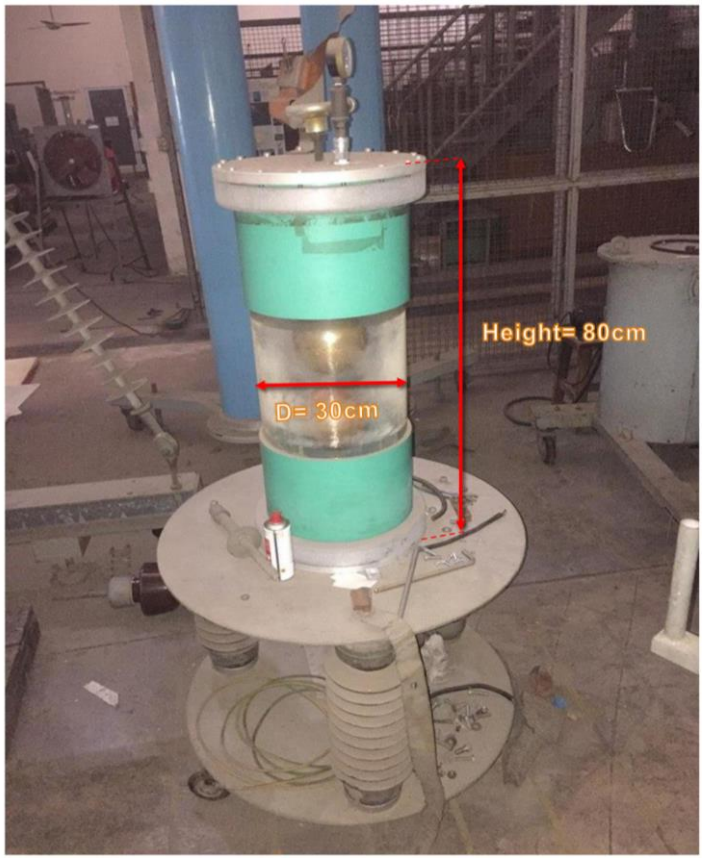

Figure 2-22 The old chamber inside the laboratory.

Simulation model:

The simulation model of ∅5cm and ∅10cm sphere with the cylindrical chamber which has a height of 80cm and the diameter of 30cm. The top and the body of the chamber are insulation material and the chamber bottom is the metal material. The boundary size X is 150cm for both ∅5cm and ∅10cm sphere, where the mesh size is 0.001 and 0.05 for ∅5cm and ∅10cm sphere.

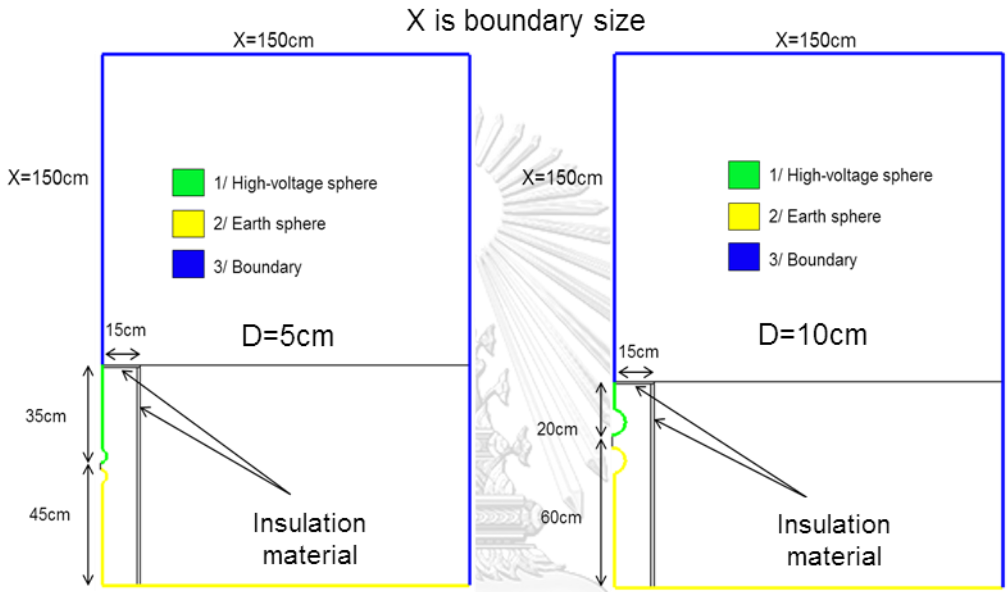

Figure 2-23 Simulation model of D=5cm and D=10cm sphere with the chamber.

Simulation result:

After placing the chamber, the electric field distribution along 5cm and 10 cm sphere-gap without chamber and with chamber are plotted in Figure 2-24 and Figure 2-25, respectively. The %Error of the E_{max} after placing the chamber is described in Table 2-4.

Table 2-4 The %Error of E_{max} of sphere-gap after placing the chamber.

Sphere diameter	$E_{max,\ with\ chamber}$ (v/cm)	$E_{max,\ without\ chamber}$ (v/cm)	%Error
5cm	0.63176012	0.63277692	-0.16%
10cm	0.31514579	0.31520081	-0.017%

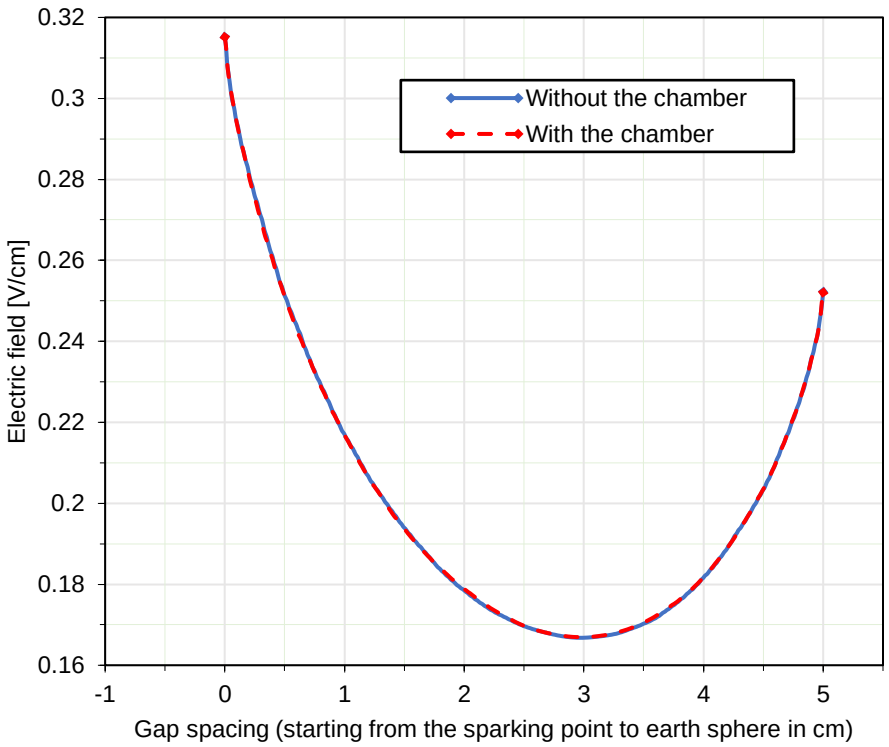

Figure 2-24 The electric field distribution of 10cm diameter sphere-gap with and without the chamber.

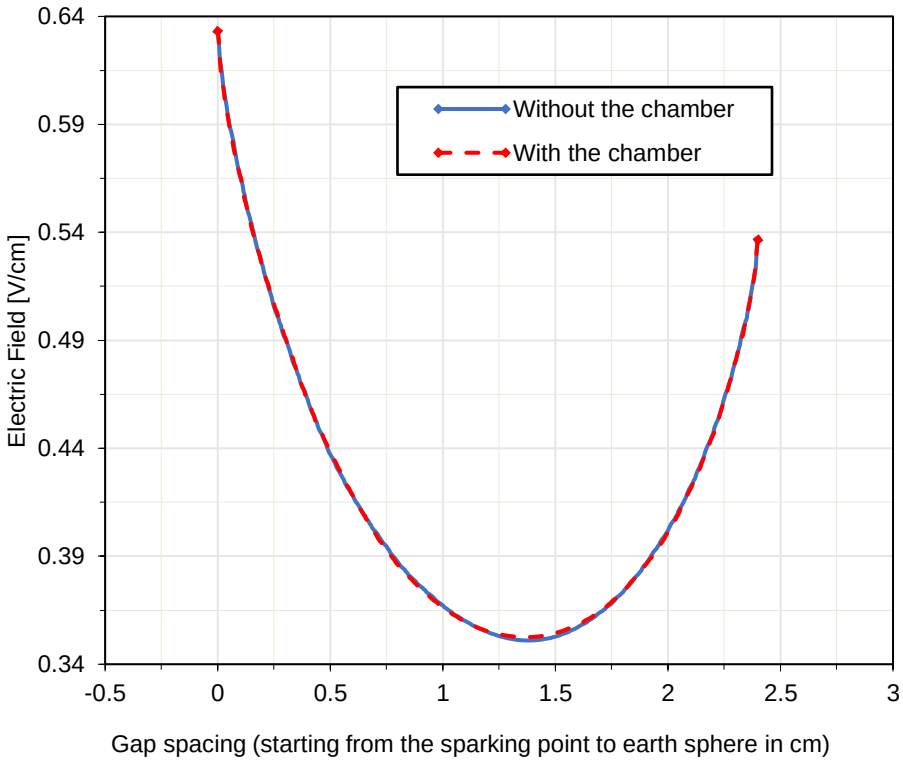

Figure 2-25 The electric field distribution of 5cm diameter sphere-gap with and without the chamber.

2.6.1 CAD drawing of the test chamber

According to Figure 2-24, 2-25 and Table 2-3, the cylindrical chamber size with the 30cm diameter, the height of 80cm, cover and body made of insulation material and the bottom part is made of metal material, has a very low influence on the electric field distribution as well as the E_{max} along the sphere-gap of 5cm and 10cm diameter. Hence, this chamber size is proper to enclosed for the purpose of artificially control the atmospheric condition around the sphere-gap.

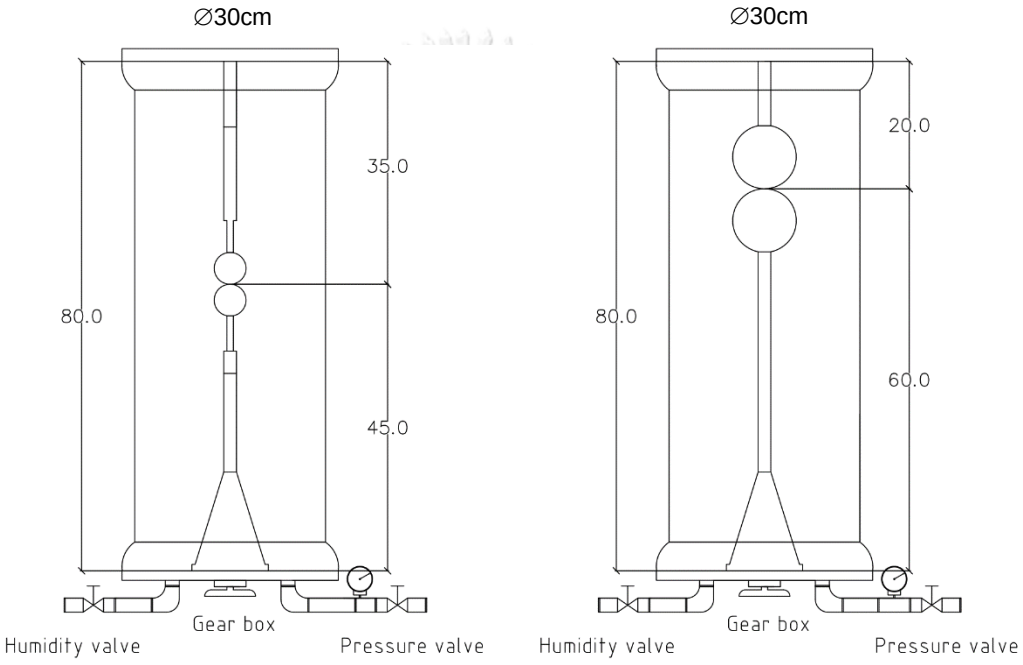

Figure 2-26 CAD drawing of the chamber (earth sphere shows its full length).

Chapter 3
Experiment

3.1 Test equipment

The experiments are set up to investigate the characteristic of lightning impulse breakdown voltage of ∅5cm and ∅10cm sphere with and without irradiation under a various range of humidity. Actually, the experimental setup is a time-consuming task since an impulse voltage test system require many tasks to be done, this process includes setting up control and measuring system, choosing the impulse generator, adjusting internal and external circuit of impulse generator and choosing an accurate measuring device. All the system components have to be prepared to generate the standard lightning impulse voltage 1.2/50μs at a desired voltage level.

The sphere-gap arrangement was prepared according to the standard IEC60052 [5], high voltage sphere is on the top and the bottom sphere is earth. The chamber has a diameter of 30cm and is 80cm in height. Both 5cm and 10cm diameter sphere are made of copper material. The spheres were polished by extra fine sandpaper to ensure the surface smoothness.

3.1.1 The test chambers

The top and body of the chamber are insulation material where the bottom is a metal. The high voltage lead is connected to the high voltage sphere via the bolt attached to the cover top. The chamber is erected on a three-arm base equipped with castor wheels. At the lower end of the chamber, there are one inlet and one outlet for pressuring or evacuating as well as for adjusting the humidity inside the chamber. High precision digital pressure gauge (HC-Y810) with an accuracy of ±0.001MPa is used to measure the pressure inside the chamber. The relative humidity and the temperature inside the chamber are measured by KTJ thermos hygro-meter with the following specifications: relative humidity between 10 and 95%RH (±5%RH accuracy) and temperature between 0 and 10°C (±0.1°C accuracy). The values of relative humidity and the ambient temperature are used to convert to the absolute humidity, using the formula from the IEC60060-1 [3].

The gap spacing is varied by the gearbox at the bottom part of the chamber and the Mitutoyo dial gauge with an accuracy of ±0.01mm is placed below the bottom of the chamber to measure the length of gap spacing between the spheres.

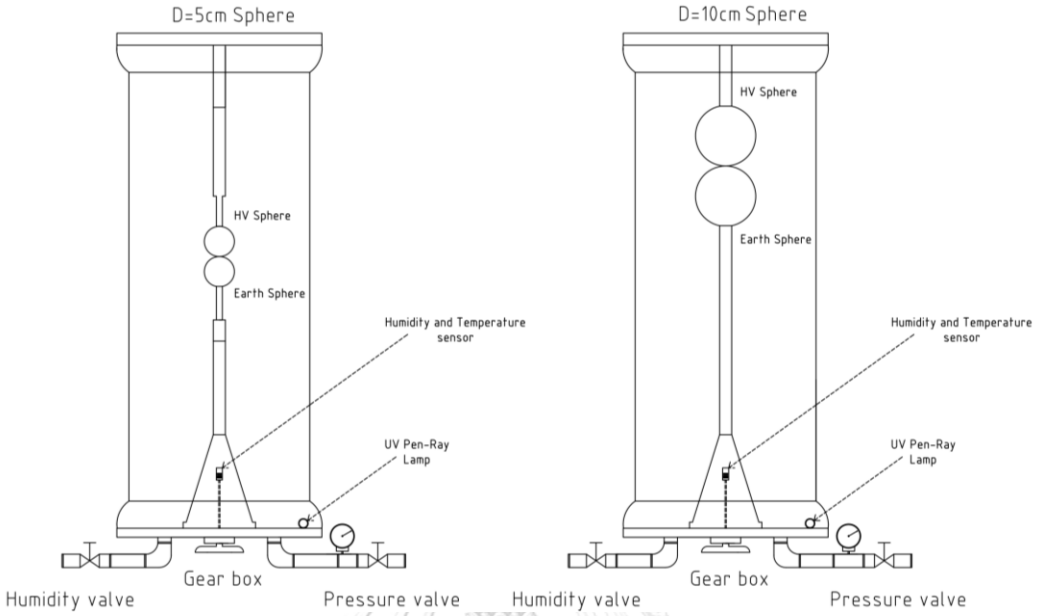

Figure 3-1 Test chamber show (∅5cm and ∅10cm sphere installed).

3.1.2 Humidity control

According to IEC 60061-1[3], the value of relative humidity and the ambient temperature can be used to calculate the absolute humidity, by using the below equation:

$$h = \frac{6.11 \times R \times e^{\frac{17.6 \times t}{243+t}}}{0.4615 \times (273+t)} \quad (11)$$

Where h is the absolute humidity in g/m^3,

R is the relative humidity in per cent and

t is the ambient temperature in °C.

Normally, the relative humidity in the laboratory atmospheric is already high with the value around 60% to 80%. Hence, the chamber valve was opened to maintain equilibrium with the laboratory atmospheric condition. The average temperature which is measured by KTJ thermos hygro-meter was around 32°C.

Following the Equation (11), to achieve the absolute humidity of *10g/m^3* and *18g/m^3* inside the test chamber, the value of relative humidity inside the chamber must be equal

to *~30%* and *~54%*, respectively. For this case, the dry air (contained 79% of N_2 and 21% of 0_2) was pumped into the chamber in order to reduce and maintain those desired relative humidity ranges.

In particular, to achieve the dry air condition, the humidity air existed inside the test chamber was evacuated by vacuum pump after that the dry air was pumped into the chamber. The cycle of this procedure was repeated at least 3-4 time to ensure that the atmospheric condition inside the test chamber is a pure dry air. It can be also determined by KTJ thermos hygro-meter which showed a constant value of relative humidity =10% (the lowest measuring value).

It is also necessary to mention that after adjusting the desired humidity ranges, the chamber was kept for at least 12 hours before the experiment process.

3.1.2.1 The absolute humidity inside the test chamber

For this present experiment, there are 3 absolute humidity ranges which are selected to investigate:

1. Dry air (absolute humidity of 0 g/m^3)
2. The absolute humidity of 10 g/m^3
3. The absolute humidity of 18 g/m^3

The pressure of 8kpa or 60mmhg was added into the chamber; hence, the total pressure was 101.3kPa+8kPa= ***109.3kPa***. The average temperature inside the chamber is around 32℃ (varied between 31-33 ℃).

Following the Equation (1) and (2), the air density correction factor (δ) and humidity correction factor(k) with various absolute humidity range are shown in Table below.

Table 3-1 The air density correction factor (δ) and humidity correction factor (k).

Average temperature=32℃, total pressure=109.3kPa inside test chamber		
The absolute humidity	Air density correction factor (δ)	Humidity correction factor (k)
Dry air	1.036	n/a
$10g/m^3$	1.036	1.002
$18g/m^3$	1.036	1.017

3.1.3 Experiment circuit and components

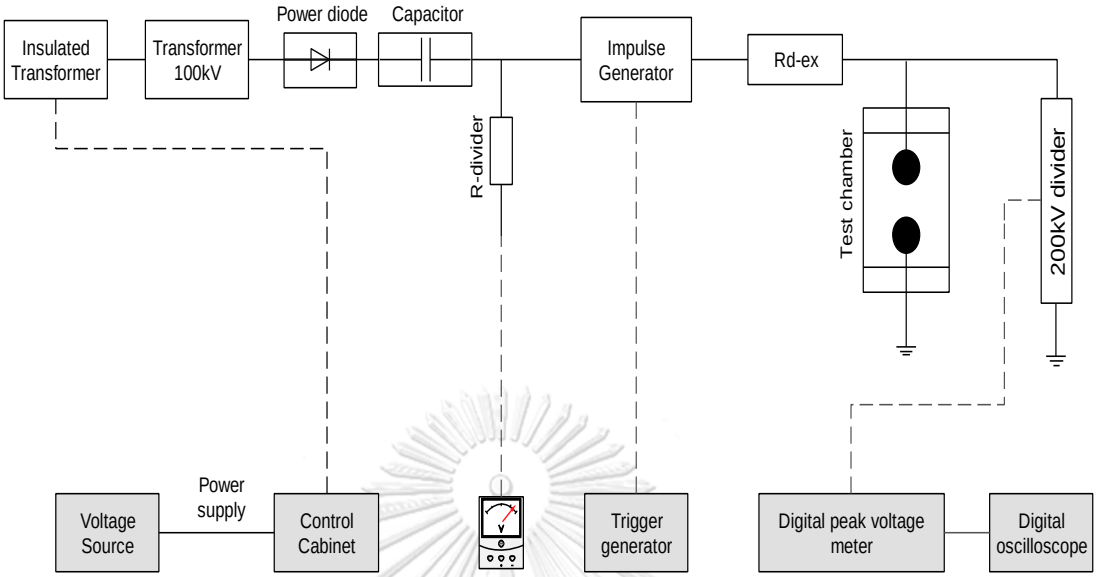

Figure 3-2 The test, control and measuring circuit (for generating voltage ≥35kV).

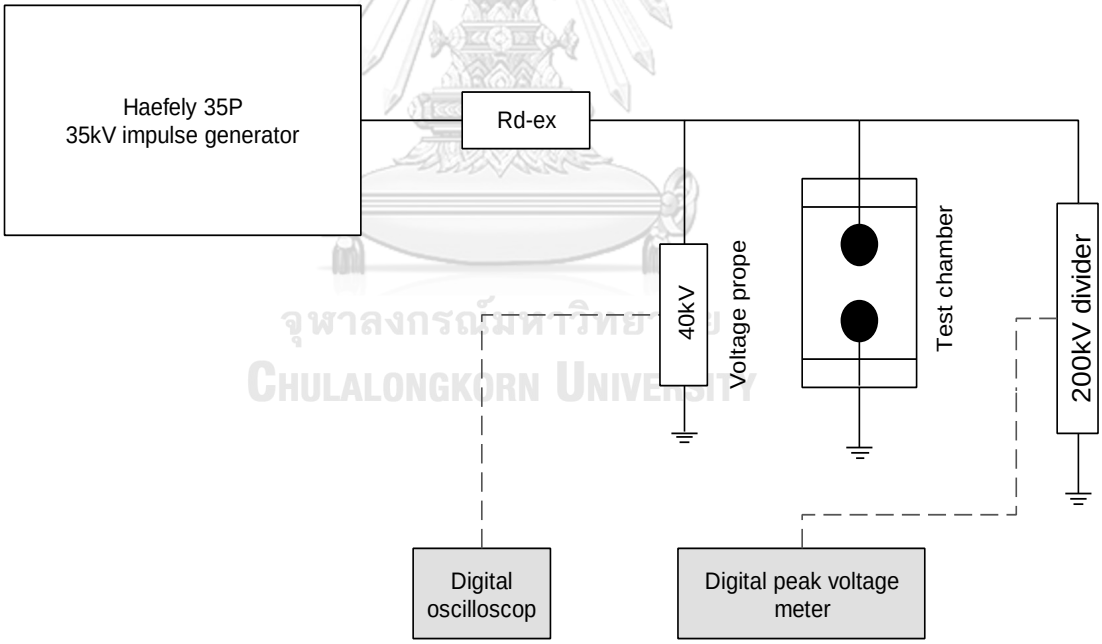

Figure 3-3 The test, control and measuring circuit (for generating voltage ≤35kV).

Control and measuring device:

- Control Cabinet: The impulse test system operates under a control cabinet which charges the impulse generator through the charging unit. This is achieved as the

stages in the impulse generator are connected in parallel via the charging resistors.

- Digital volt-meter: The digital volt-meter is used to view the charging voltage which is measured via a 265kΩ resistive voltage divider with the voltage ratio of 894.73:1.
- Trigger generator: Once the selected charging voltage has been reached, a trigger pulse initiates firing of the first spark-gap of the impulse generator. The resulting over-voltage triggers the successive stages. As all the spark-gaps fire, the stages which are in series now, multiply the charging voltage to reach the test voltage.
- Voltage divider: An impulse voltage divider reduces the impulse voltage to a value that the measuring and recording instruments can operate. In this set-up, the voltage probe (Tektronix P6015a) with 1000:1 voltage division ratio is used to measure the voltage ≤ 35kV, where a higher voltage is measured by a Haefely 200kV voltage divider with a ratio of 151.1:1.
- Digital peak voltmeter and digital oscilloscope: The peak and waveform of impulse test voltage are recorded by these two devices, respectively. In this experiment, Haefely impulse peak voltage meter type 64M and RIGOL DS1022C digital oscilloscope (25MHz 400Msa/s) are used.

Two impulse generators were used in this present study in order to generate difference impulse voltage level.

1. *10-stage, 1000kV Marx generator:*

- The high voltage of 0-100kV with both polarities are generated by DC high voltage power supply, is used to charge the capacitor of the impulse generator.
- Charging capacitor: The maximum charging voltage of 100kV per stage with the energy of 5kJ.
- Internal damping resistors: They are the wave shaping elements of impulse voltage generator. At each stage, the front-time resistor R_d and the tail-time resistor have the value of 12Ω and 68Ω, respectively.

- External damping resistors ($R_{d\text{-}ex}$): The front-time of the impulse voltage wave is convenient to adjust by using the external damping resistors. Two of the external damping resistors $R_{d\text{-}ex}$=406Ω and 286Ω connected in series was added to the circuit in order to generate the impulse voltage wave shape of T_1 =1.269μs and T_2=48μs.

2. *Haefely 35P 35kV impulse generator:* This impulse generator produces both polarities of lightning impulse voltage up to 35kV. The external damping resistors of 600Ω (402Ω+198Ω) were added to the circuit to produce the lightning impulse wave shape of T_1= 1.21μs and T_2=49.3 μs.

3.1.4 The UV irradiation

The UV Pen-Ray® lamp (Figure 3-4) which is used to provide the artificial UV irradiation, is placed at the bottom part of the test chamber (9D from 5cm sphere-gap and 6D from 10cm sphere-gap). With 10mA AC current, this UV lamp has the radiation spectrum of 3600μw/cm^2 and the typical intensity of 254nm at the distance of 19.1mm. The lamp is powered by a power supply which has a primary voltage of 220V/50Hz and secondary open circuit voltage of 2100Vac. Besides the direct irradiation from the bottom of the chamber, there will be some reflection of UV light from the bottom part to the sphere surface.

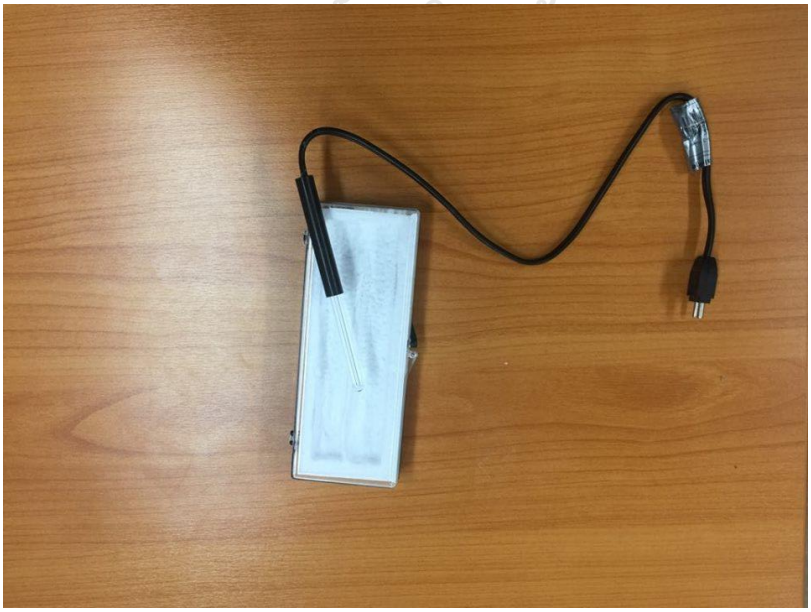

Figure 3-4 UV Pen-Ray® lamp.

3.1.5 Experiment procedure

The workflow of the experiment process can be described by a simple and comprehensive flow-chart. The sequence of steps can be followed in order to obtain the $U_{50\%}$ disruptive discharge voltage of the sphere-gap in a desired atmospheric condition with and without irradiation (Figure 3-5).

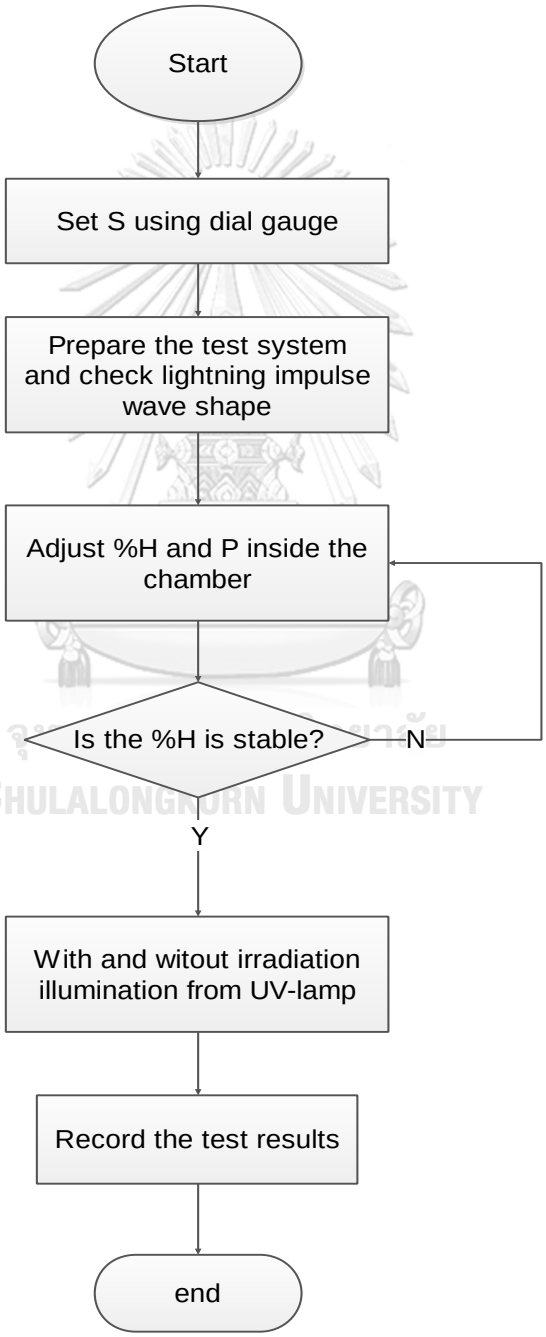

Figure 3-5 The flowchart of the experiment process.

The procedures of conducting the experiment are described as below:

1. Set desired gap spacing and measure it by using dial gauge.
2. Adjust the pressure inside the test chamber and make sure it remains constant. The humidity is modified to meet a desired value via the inlet valves.
3. Choose the number of impulse generator stage to ensure that there is a sufficient voltage for the test. To extend to a lifetime of the capacitors, the charging voltage of each stage is not exceeded 45kV. Therefore, 2-stage is used to generate the impulse voltage for gap spacing of 1.0cm up to 2.4cm while Haefely 35P 35kV impulse generator is used to investigate the S=0.5cm.
4. Choose the measuring device to guarantee the accuracy of the voltage measurement. Since the breakdown voltage of the test gaps is not exceeded 100kV. Hence, voltage probe is used to measure the voltage less than 35kV, while 200kV voltage is used to measure the voltage from 35kV up to 200kV.
5. Choose the voltage polarity by changing the direction of the power diode.
6. Make sure that the generated impulse voltage waveform is corrected according to the standard [3], with a tolerance of 1.2μs±30% for front-time and 50μs±10% for tail-time.
7. Check the UV lamp if it is on or off according to the experiment purpose.
8. Record the test results via digital oscilloscope and digital peak voltage meter.

3.1.6 Treatment of test results

The multilevel method is used in this experimental procedure in order to find the breakdown probability curves under LI with both polarities for all gap spacing. For this method, the guideline is:

- Choosing the $n_i = 10$ voltage applications
- Apply $m = 5$ voltage levels $U_i (i = 1, 2, ..., m)$. Each voltage level, the difference is between 1 to 3% from the previous voltage, $\Delta U = U_{i+1} - U_i (i = 1, 2, ..., m-1)$

- Count the number $(k_i \le n_i)$ of disruptive discharges at each voltage level U_i, disruptive discharge frequency $f_i = k_i / n_i$.
- The $f_i = k_i / n_i$ is plotted against U_i, and $U_{50\%}$ and σ are computed by using curve fitting method on MATLAB program (see APPENDIX A), the typical example is shown in Figure3-6.

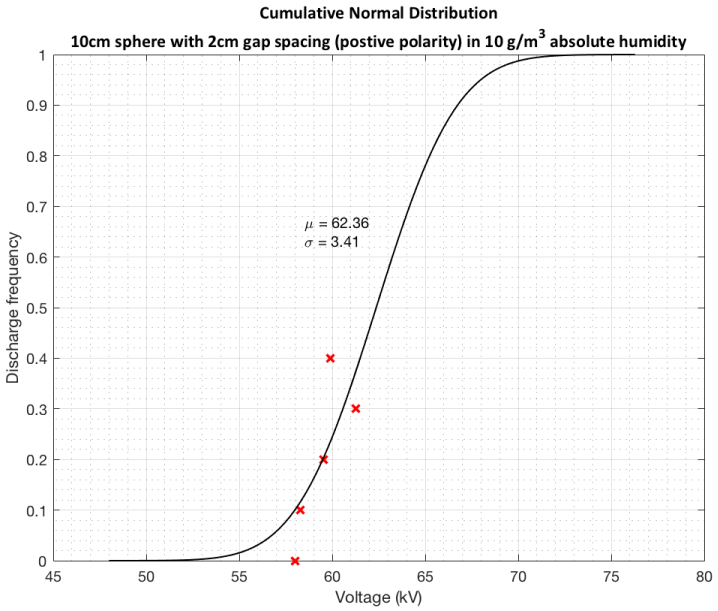

Figure 3-6 Probability of breakdown distribution by using the fitting method on MATLAB program.

Chapter 4
Results and Discussion

4.1 Breakdown probability curves

By using curve fitting method on MATLAB program, the breakdown probability curve was plotted for all value of absolute humidity. In general, the probability curves are regular and have a good fitting with cumulative normal distribution, the typical curves are shown in Figure 4-1 However, there are some probability curves that are irregular in the sense that they deviate from the cumulative normal distribution (Figure 4-2).

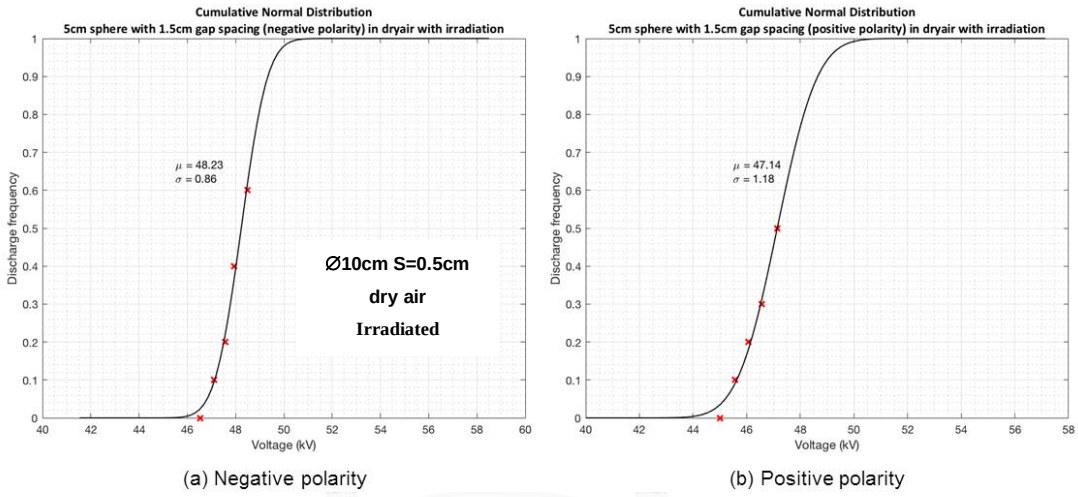

Figure 4-1 The good fitting probability curves with cumulative normal distribution for 10cm sphere with S=0.5cm under LI with both polarities in dry air.

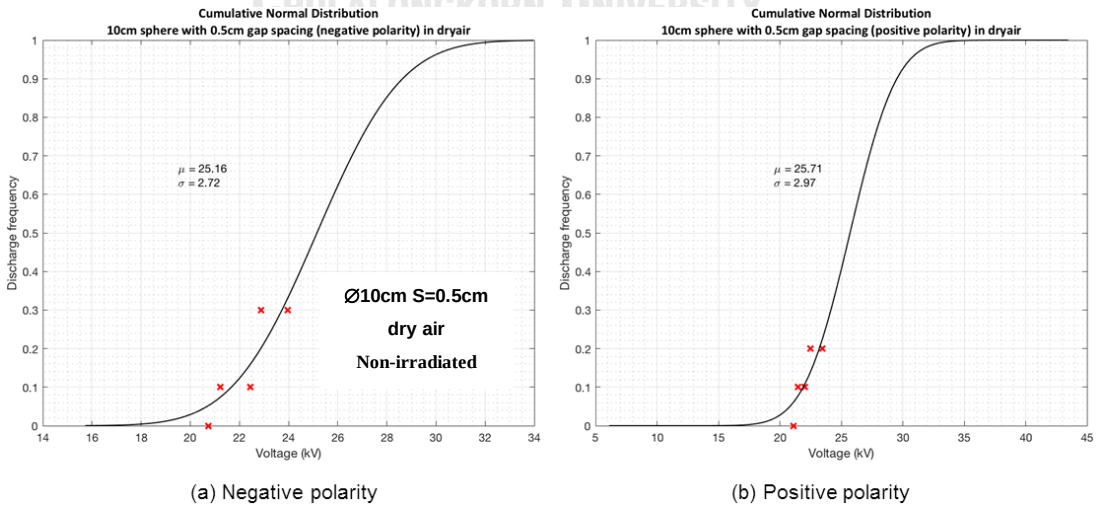

Figure 4-2 The irregular probability curve of 10cm sphere S=0.5cm under LI with both polarities in dry air.

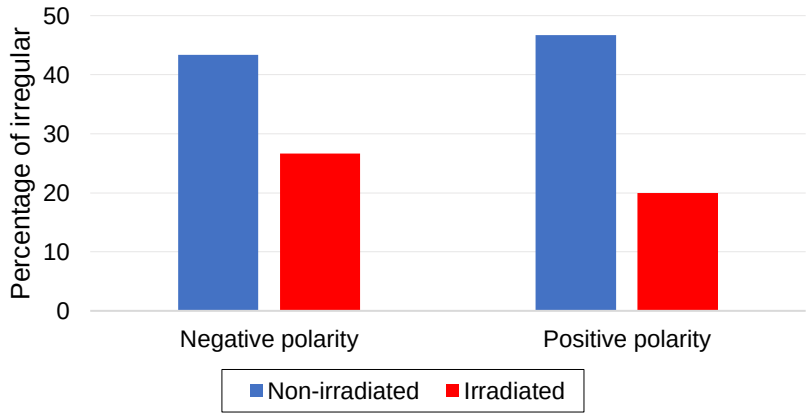

Figure 4-3 The percentage of irregular distribution curve under negative and positive polarity for all gap spacing of 5cm and 10cm sphere-gap.

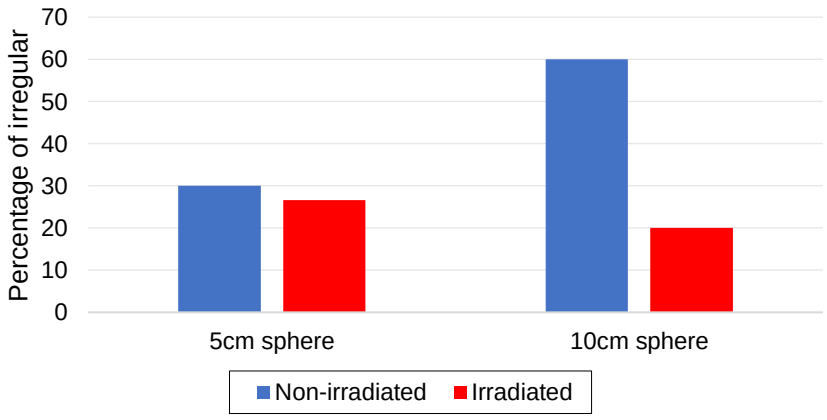

Figure 4-4 The percentage of irregular distribution curves for all gap spacing of 5cm and 10cm sphere-gap under both voltage polarities.

The percentage of irregular distribution curve for 5cm and 10cm diameter sphere-gap with voltage polarity, sphere diameter and irradiation as the parameters, are shown in Figure 4-3 and 4-4, respectively. According to these figures, with the application external irradiation source, the percentage of irregular distribution curves are generally decreased for 5cm and 10cm diameter sphere-gap under both voltage polarities. They also show that the reduction of the percentage of irregular for both ∅5cm and ∅10cm is obvious for positive polarity than for negative polarity. Under both voltage polarities, the influence of irradiation on the percentage of the irregular case seems strong for D=10cm sphere than for D=5cm.

4.2 $U_{50\%}$ disruptive discharge voltage and standard deviation (σ) of 5cm and 10cm diameter sphere-gap

The value of $U_{50\%}$ disruptive discharge voltage ∅5cm and ∅10cm sphere-gap with and without irradiation which are measured under a various range of absolute humidity has been described and studied for the following cases.

4.2.1 The influence of humidity on $U_{50\%}$ disruptive discharge voltage of 5cm and 10cm diameter sphere-gap under both polarities

4.2.1.1 Influence of humidity on $U_{50\%}$ disruptive discharge voltage

Table 4-1 and 4-2, shows the value of $U_{50\%}$ disruptive discharge voltage for the experiment under dry air, absolute humidity of 10g/m^3 and 18g/m^3 for negative and positive LI, respectively. These two tables also show the $U_{50\%}$ disruptive discharge voltage from the IEC standard for 5cm and 10cm diameter sphere-gap. The same values are also plotted against gap spacing (S) in Figure 4-5 and Figure 4-6 for both 5cm and 10cm diameter sphere (measured value is represented by the dot-line and the solid line represents standard value). The value of $U_{50\%}$ of all gap spacing of both 5cm and 10cm diameter sphere-gap are also plotted over this various humidity range under both polarities in Fig 4-7 and 4-8.

It is necessary to mention that the $U_{50\%}$ for non-irradiated gaps was taken for this investigation on the influence of humidity.

Table 4-1 $U_{50\%}$ disruptive discharge lightning impulse voltage of 5cm and 10cm sphere-gap of negative polarity(kV).

Gap spacing (cm)	IEC Standard (kV)		$U_{50\%}$ with various humidity range (kV)					
			Dry air		10g/m^3		18g/m^3	
	5cm	10cm	5cm	10cm	5cm	10cm	5cm	10cm
0.50	17.40	16.80	25.66 (29.80)	25.16 (29.46)	27.20 (31.85)	26.24 (30.33)	28.00 (30.73)	25.88 (29.95)
1.00	32.00	31.70	37.31	36.43	38.02	37.82	37.99	37.91
1.50	45.50	45.50	48.46	48.68	48.64	49.06	50.36	50.64
2.00	57.50	57.90	60.76	60.56	62.37	61.80	62.39	64.34
2.40	65.50	69.50	73.66	72.20	72.50	72.54	74.02	72.48
			Values in the () are measured by voltage probe					

It also necessary to mention again that only gap spacing 0.5cm was measured by both voltage probe and 200kV divider while the S>0.5cm was measured by 200kV divider only.

Table 4-2 $U_{50\%}$ disruptive discharge lightning impulse voltage of 5cm and 10cm sphere-gap of positive polarity(kV).

Gap spacing (cm)	**IEC Standard (kV)**		**$U_{50\%}$ with various humidity range (kV)**					
			Dry air		**10g/m^3**		**18g/m^3**	
	5cm	**10cm**	**5cm**	**10cm**	**5cm**	**10cm**	**5cm**	**10cm**
0.50	17.40	16.80	25.66 (31.58)	25.71 (29.34)	27.65 (32.32)	26.03 (29.93)	27.48 (32.91)	25.68 (29.32)
1.00	32.00	31.70	36.28	36.30	37.31	37.88	38.74	37.80
1.50	46.20	45.50	48.02	48.73	49.42	49.20	50.45	50.43
2.00	59.50	59.00	61.31	61.11	62.93	62.36	63.68	64.84
2.40	69.00	70.00	72.38	72.42	72.96	73.36	74.33	73.60
			Values in the () are measured by voltage probe					

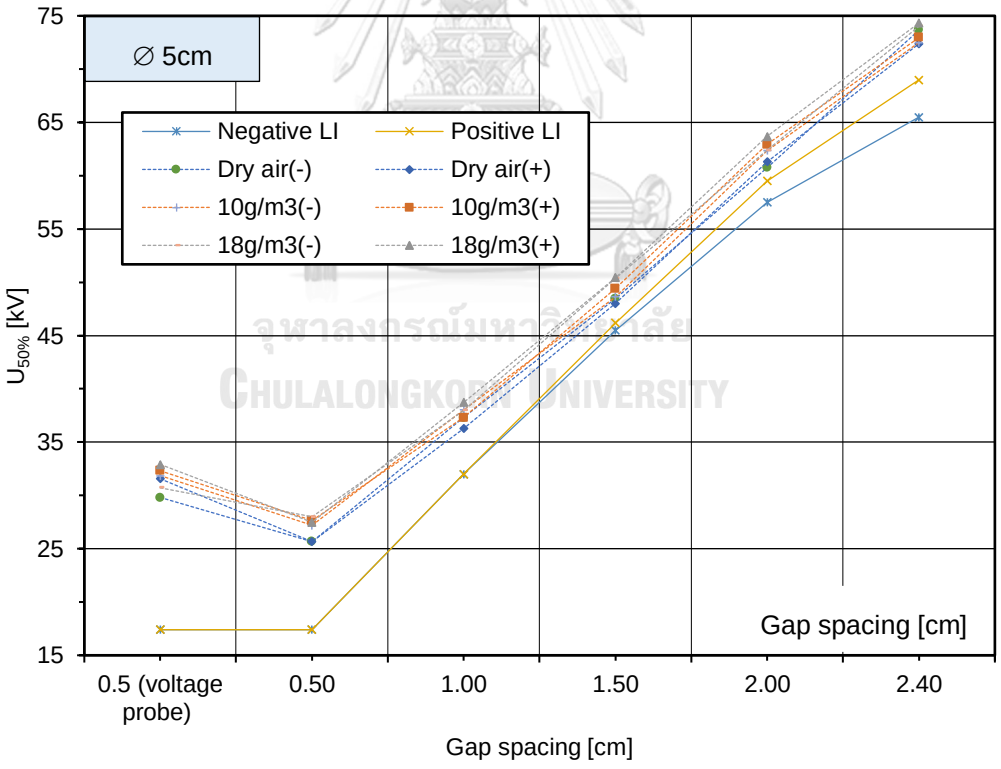

Figure 4-5 $U_{50\%}$ plotted against S for D=5cm under various humidity ranges under both voltage polarities.

From Figure 4-5, it can be seen that there is a difference between the value of the sparkover voltage from the experiments and one of the standards. In general, the

measured $U_{50\%}$ of 5cm diameter sphere-gap are significantly higher than those of the standard under all humidity range for both negative and positive polarity, this trend also occurs for 10cm diameter sphere-gap for both polarities (Figure 4-6). Without the doubt, this phenomenon is caused by the atmospheric condition absolute humidity h and pressure b of the test chamber is higher than the one of the standard atmospheric condition. The difference is obvious for small gap spacing S of both sphere-gap, especially for S=0.5cm which is measured by voltage probe. Actually, the difference of the measured sparkover voltages from the standard value decreases as increasing of gap spacing S for both sphere-gap under negative and positive polarity, except the S=2.4cm for D=5cm under negative polarity, where the difference has a slight increase.

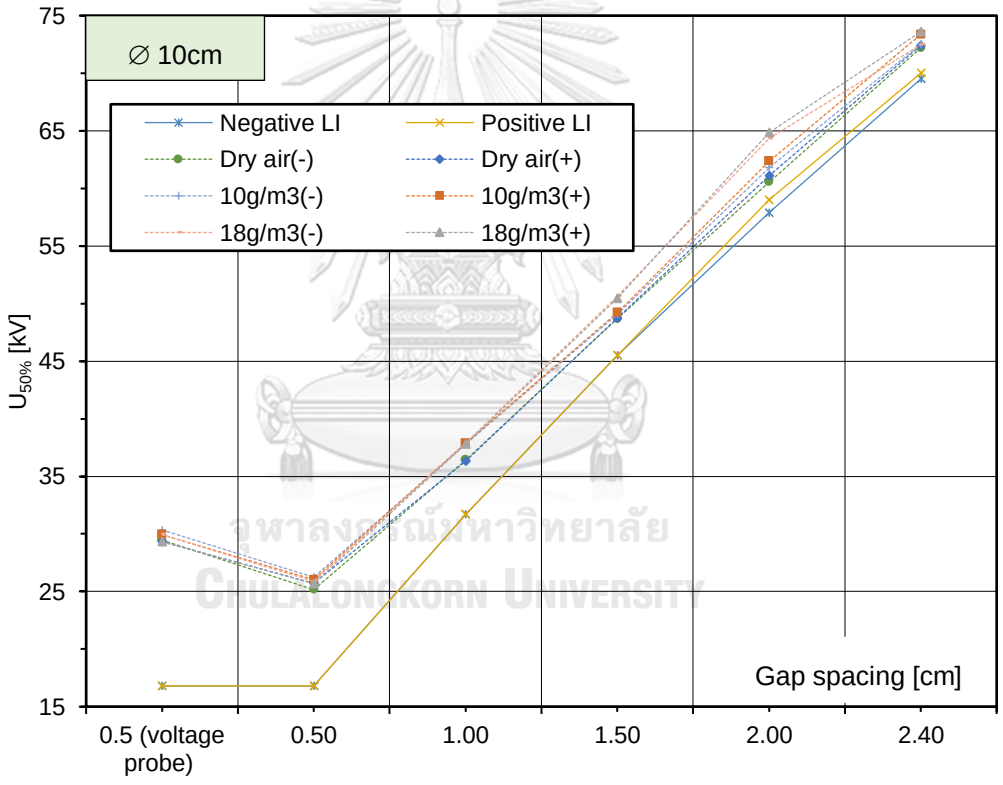

Figure 4-6 $U_{50\%}$ plotted against S for D=10cm under various humidity ranges under both voltage polarities.

The $U_{50\%}$ disruptive discharge voltage of both 5cm and 10cm diameter sphere-gap under various humidity for negative and positive LI (the dot-line represents the negative polarity where positive polarity is represented by the solid line) are shown in Figure 4-7 and 4-8. In general, the $U_{50\%}$ disruptive discharge voltage always tends to have higher

value with the increase of humidity, but the rate of the influence is seemed to depend on gap spacing and voltage polarity.

For 5cm diameter sphere-gap (Figure 4-7), it indicates that upward trend over all the humidity range occurred more frequently for positive polarity than for negative polarity, and it can be seen that the influence is more obvious under both polarities for small gap spacing (S≤1.5cm) than large gap spacing(S≥2.0cm), except the S=0.5 which measured by voltage probe for negative. The influence of humidity is strong for gap spacing of 1.0cm and 1.5cm under positive polarity. But when the gap reached S=2.0cm and 2.4cm, the influence of humidity on the $U_{50\%}$ disruptive discharge voltage is uneven since there are only slightly uptrend and even a downtrend occurs for S=2.4cm under negative polarity.

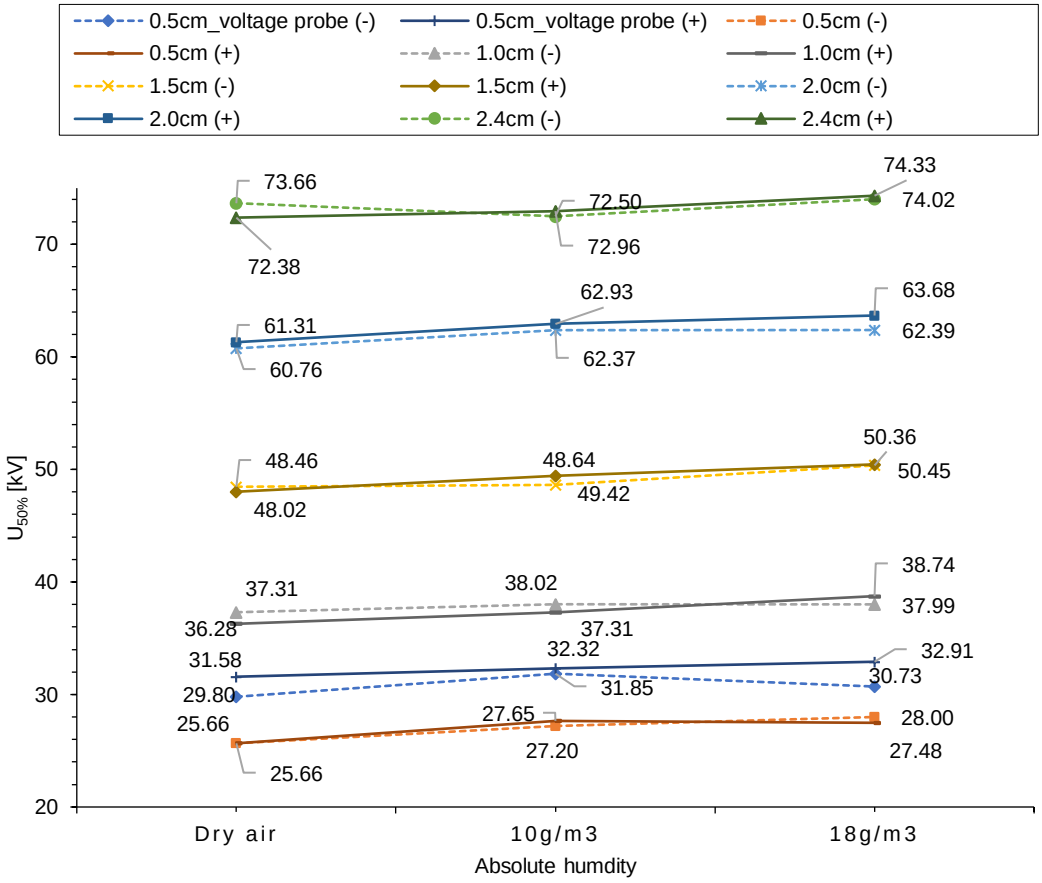

Figure 4-7 $U_{50\%}$ of 5cm diameter sphere-gap for both polarities LI under various absolute humidity without irradiation.

A typical plot is shown in Figure 4-8 referred to 10cm diameter sphere-gap for both polarities. From this figure, it can be seen that the increase in humidity generally causes

the higher value of $U_{50\%}$, the obvious case is the gap spacing of 2.0cm for both polarity. Moreover, the difference of $U_{50\%}$ between negative and positive polarity in relation to the influence of humidity, is relatively low, except the gap spacing of 2.4cm. This trend is also similar to the standard value where there is no significant difference $U_{50\%}$ of positive from negative polarity for 10cm diameter sphere. This occurrence may be caused by the uniformity of filed across the gap of 10cm sphere, which shows that the voltage polarity has no effect on $U_{50\%}$[9, 24].

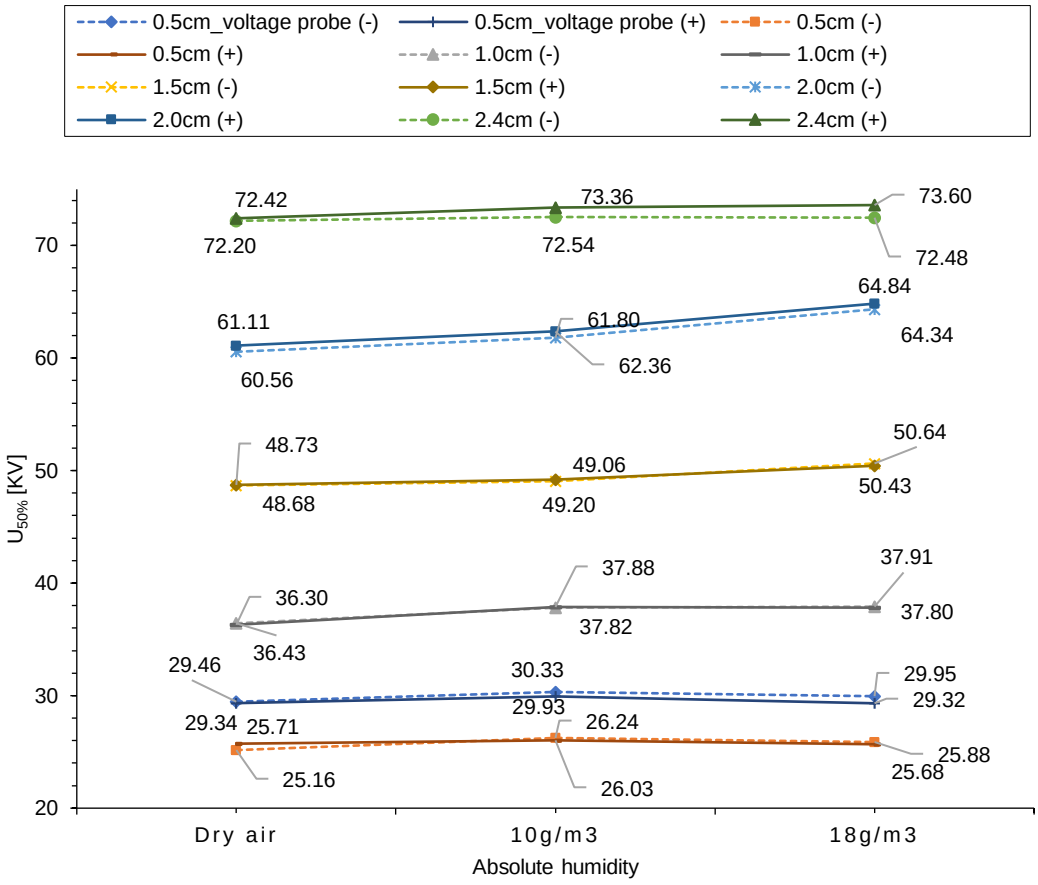

Figure 4-8 $U_{50\%}$ of 10cm diameter sphere-gap for both polarities LI under various absolute humidity without irradiation.

From Figure 4-7 and 4-8, it shows that the influence of humidity on the value of $U_{50\%}$ is not so strong[24]; however, it can be seen that the influence of humidity is obvious for ∅10cm than for ∅5cm diameter sphere-gap at the same gap spacing, the uptrend line of $U_{50\%}$ over the humidity range occurred more frequent for D=10cm sphere than for D=5cm. Moreover, the influence of humidity on the value of $U_{50\%}$ is irregular for D=5cm, especially for large spacing (S ≥ 2.0cm). This occurrence may be caused by

the influence of the gap spacing[9, 24], where large gap spacing (S = 2.0 and 2.4cm) for D=5cm is considered as small gap spacing (S < 0.25D) for D=10cm.

From these figures, it can be also seen that the influence of humidity on $U_{50\%}$ for this present study tends to depend on gap spacing S and the voltage polarity. The influence becomes weaker as gap spacing S increased. For small gap spacing, the relative abundance of the primary electrons is the main mechanism that controls the influence of humidity because the increase of humidity slowdowns the breakdown process in a sense that the attachment of water vapour molecules increases the scarcity of primary electrons [9]. The reason that the influence of humidity on $U_{50\%}$ increases for larger D is may due to "higher field values with smaller D resulting in the easier availability of primary electron"[24].

4.2.1.2 The influence of humidity on standard deviation (σ)

The value of σ for 5cm diameter sphere-gap over the absolute humidity range with and without irradiation for negative and positive polarity is shown in Table 4-3 and 4-4, respectively. The one for 10cm diameter sphere is shown in Table 4-5 and 4-6. The average value of σ for full range of humidity (hereafter $\sigma_{average}$), is also added to these tables. The same value of σ and $\sigma_{average}$ (for the non-irradiated gap) with the same parameters for D=5cm and D=10cm is also plotted in Figure 4-9 and 4-10, respectively.

5cm diameter sphere:

Table 4-3 Standard deviation σ for lightning impulse voltage of 5cm sphere-gap of negative polarity.

Gap spacing (cm)	Standard deviation σ with various humidity range (%)							
	Without irradiation				With irradiation			
	Dry air	10g/m^3	18g/m^3	$\sigma_{average}$	Dry air	10g/m^3	18g/m^3	$\sigma_{average}$
0.50	8.51 (8.20)	13.41 (13.48)	15.58 (8.62)	12.50 (10.10)	6.78 (7.28)	7.76 (8.13)	3.86 (4.56)	6.13 (6.66)
1.00	8.51	13.41	15.58	4.87	2.68	1.89	2.71	2.43
1.50	3.40	7.01	4.19	3.62	1.77	2.69	4.79	3.08
2.00	2.11	3.47	5.27	2.30	3.01	2.53	1.80	2.45
2.40	2.29	3.12	1.49	2.25	1.44	1.89	2.39	1.91
	Values in the () are measured by voltage probe							

Table 4-4 Standard deviation σ for lightning impulse voltage of 5cm sphere-gap of positive polarity.

Gap spacing (cm)	Standard deviation σ with various humidity range (%)							
	Without irradiation				With irradiation			
	Dry air	10g/m^3	18g/m^3	$\sigma_{average}$	Dry air	10g/m^3	18g/m^3	$\sigma_{average}$
0.50	8.44 (8.25)	14.25 (10.92)	14.26 (11.57)	12.32 (10.25)	4.64 (4.46)	7.96 (3.37)	4.33 (4.98)	5.64 (4.27)
1.00	4.41	3.19	4.00	3.87	3.78	2.89	2.71	3.13
1.50	3.25	2.43	3.35	3.01	2.46	2.12	2.52	2.37
2.00	3.80	1.36	2.52	2.56	2.66	1.62	1.35	1.88
2.40	1.74	2.23	1.86	1.94	2.22	1.18	1.08	1.49
	Values in the () are measured by voltage probe							

10cm diameter sphere:

Table 4-5 Standard deviation σ for lightning impulse voltage of 10cm sphere-gap of negative polarity.

Gap spacing (cm)	Standard deviation σ with various humidity range (%)							
	Without irradiation				With irradiation			
	Dry air	10g/m^3	18g/m^3	$\sigma_{average}$	Dry air	10g/m^3	18g/m^3	$\sigma_{average}$
0.50	10.81 (10.62)	11.97 (10.95)	20.21 (17.06)	14.33 (12.88)	7.25 (8.21)	8.73 (7.96)	13.71 (12.23)	9.89 (9.47)
1.00	4.34	8.36	7.73	6.81	5.25	7.50	3.79	5.52
1.50	3.59	4.57	6.24	4.80	3.59	5.71	4.28	4.53
2.00	6.82	6.29	4.76	5.96	4.54	3.75	3.01	3.76
2.40	3.66	4.54	2.95	3.71	3.05	1.84	3.72	2.87
	Values in the () are measured by voltage probe							

Table 4-6 Standard deviation σ for lightning impulse voltage of 10cm sphere-gap of positive polarity.

Gap spacing (cm)	Standard deviation σ with various humidity range (%)							
	Without irradiation				With irradiation			
	Dry air	10g/m^3	18g/m^3	$\sigma_{average}$	Dry air	10g/m^3	18g/m^3	$\sigma_{average}$
0.50	11.55 (6.31)	9.64 (5.91)	5.22 (10.85)	12.14 (7.69)	8.45 (7.11)	7.19 (3.76)	10.51 (4.55)	8.71 (5.14)
1.00	4.71	7.73	7.65	6.70	7.87	8.8	5.97	7.55
1.50	3.86	4.00	7.04	4.97	5.64	5.99	5.30	5.64
2.00	3.50	5.47	3.61	4.19	3.21	3.64	3.35	3.40
2.40	4.40	5.47	4.36	4.74	3.55	4.08	3.80	3.81
	Values in the () are measured by voltage probe							

It is necessary to mention that the standard σ of the breakdown probability curve which is generated by MATLAB program, is derived from the following equation: $\sigma=\frac{U_{50\%}-U_{16\%}}{U_{50\%}}\times 100\%$. And the values of σ for the influence of humidity and influence of irradiation studies are obtained from the breakdown probability curves which are measured by 200kV voltage divider only.

5cm diameter sphere:

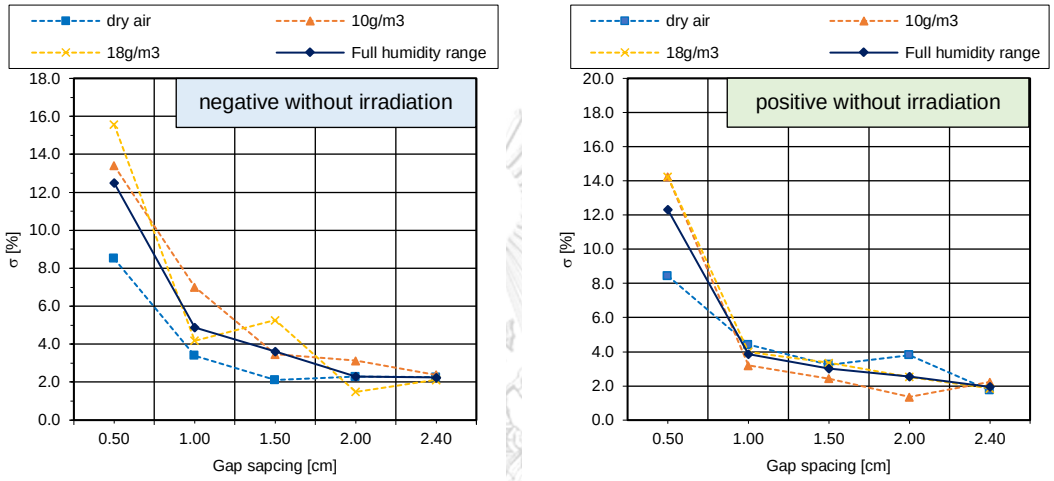

Figure 4-9 The value of σ for various humidity range and the $\sigma_{average}$ for full humidity range against gap spacing under both polarity.

10cm diameter sphere:

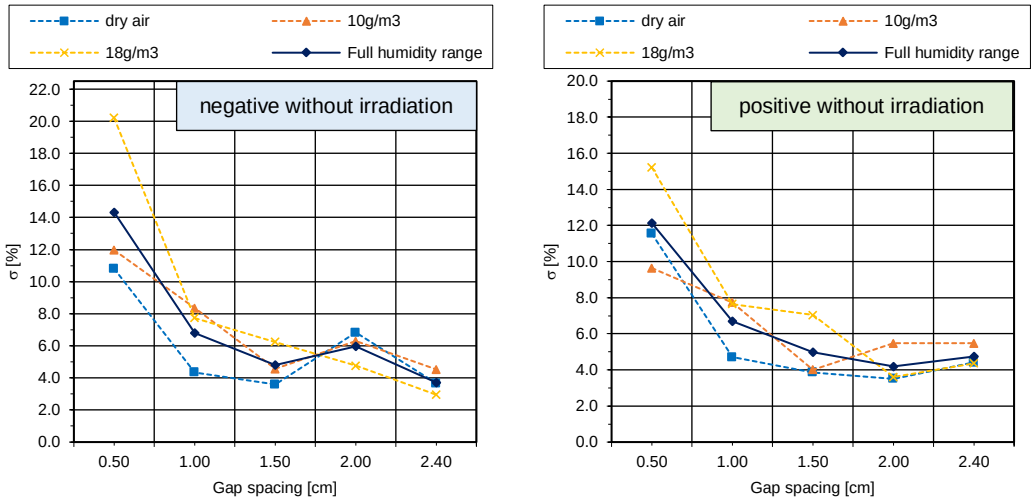

Figure 4-10 The value of σ for various humidity range and the average value of $\sigma_{average}$ for full humidity range against gap spacing under both polarity.

From Figure 4-9, it can be seen that the influence of humidity on the value of σ is so irregular for D=5cm of both polarities. For negative polarity, the value of σ shows the downtrend over gap spacing for dry air and absolute humidity of $10g/m^3$ and the value of σ under $10g/m^3$ of all gap spacing is always higher than the one under dry air; however, the zig zag occurs when the absolute humidity reached $18g/m^3$. For positive polarity, the influence of humidity on the value of σ is less marked, especially when S is higher than 1.0cm. In general, the $\sigma_{average}$ for full humidity range of both polarities decreases with increasing of gap spacing. At gap spacing of 0.5cm under both polarities, $\sigma_{average}$ is relatively large (around 12%) but when S≥0.1 the $\sigma_{average}$ drops rapidly with the value around 2%-4%.

For D=10cm of both polarity (Figure 4-10), the influence of humidity on σ is also not equal and for each humidity range, the curves of σ against the gap spacing shows a zig-zag trend for all gap spacing, except negative polarity under absolute humidity of $18g/m^3$ where the curve shows a downtrend. For full humidity range, the value of $\sigma_{average}$ decreases with the increase of gap spacing, except the gap spacing 2.0cm. Similar to D=5cm, the $\sigma_{average}$ is significantly large at S=0.5cm with a value around 14% for negative polarity and 12% for positive polarity but when S≥1.0cm the $\sigma_{average}$ for both voltage polarity remains within the value of 4%-6%.

The $\sigma_{average}$ for D=5cm and 10cm generally decreases as the gap spacing increases. The comparison between the value of σ for D=5cm and 10cm, indicates that the value of σ for D=5cm sphere-gap tends to be smaller than the one for D=10cm. From Figure 4-9 and 4-10, it can be deduced that the value of σ seems not strongly depend on the influence of absolute humidity, but it tends to depend on the gap spacing and sphere diameter.

4.2.2 The influence of irradiation on $U_{50\%}$ disruptive discharge voltage of 5cm and 10cm diameter sphere-gap under both polarities

4.2.2.1 The influence of irradiation on $U_{50\%}$ disruptive discharge voltage

The IEC standard [5] claimed that in order to measure the voltage < 50kV for all sphere diameters, and to measure voltage with D ≤ 12.5cm for all voltage shapes, it usually requires the additional external irradiation. In this part, the application of external irradiation was used in order to study the effect of irradiation on the value of $U_{50\%}$.

Table 4-7 and 4-8, show the value of $U_{50\%}$ disruptive discharge voltage of both 5cm and 10cm diameter sphere-gap with and without the application of external irradiation source from UV-lamp for negative and positive polarity, respectively. While the $U_{50\%}$ with and without irradiation against gap spacing S over the humidity range for negative and positive polarity are plotted in Figure 4-11 and 4-12 for ∅5cm sphere-gap and Figure 4-13 and Figure 4-14 for ∅10cm sphere-gap. It is important to mention that $U_{50\%}$ sparkover voltage over the humidity range is not yet converted by IEC correction method [5]. Hence, the influence of irradiation on the value of $U_{50\%}$ can be studied by adding into account the rate of absolute humidity.

Table 4-7 $U_{50\%}$ disruptive discharge lightning impulse voltage of 5cm and 10cm sphere-gap of negative polarity with and without irradiation.

Gap spacing (cm)	**IEC Standard (kV)**		**$U_{50\%}$ with various humidity range with irradiation (kV)**					
			Dry air		**10g/m^3**		**18g/m^3**	
	5cm	**10cm**	**5cm**	**10cm**	**5cm**	**10cm**	**5cm**	**10cm**
0.50	17.40	16.80	24.33 (28.29)	24.15 (28.62)	25.21 (29.67)	24.98 (29.01)	24.46 (29.11)	24.37 (28.46)
1.00	32.0	31.70	35.93	35.98	37.07	36.92	37.72	37.44
1.50	45.50	45.50	48.23	45.99	48.45	47.26	50.08	49.10
2.00	57.50	57.90	60.64	60.61	62.09	61.88	62.55	63.16
2.40	65.50	69.50	72.69	71.70	71.85	72.75	73.14	73.40
Gap spacing (cm)	**IEC Standard (kV)**		**$U_{50\%}$ with various humidity range without irradiation (kV)**					
			Dry air		**10g/m^3**		**18g/m^3**	
	5cm	**10cm**	**5cm**	**10cm**	**5cm**	**10cm**	**5cm**	**10cm**
0.50	17.40	16.80	25.66 (29.80)	25.16 (29.46)	27.20 (31.85)	26.24 (30.33)	28.00 (30.73)	25.88 (29.95)
1.00	32.00	31.70	37.31	36.43	38.02	37.82	37.99	37.91
1.50	45.50	45.50	48.46	48.68	48.64	49.06	50.36	50.64
2.00	57.50	57.90	60.76	60.56	62.37	61.80	62.39	64.34
2.40	65.50	69.50	73.66	72.20	72.50	72.54	74.02	72.48
			Values in the () are measured by voltage probe					

Table 4-8 $U_{50\%}$ disruptive discharge lightning impulse voltage of 5cm and 10cm sphere-gap of positive polarity with and without irradiation.

Gap spacing (cm)	IEC Standard (kV)		$U_{50\%}$ with various humidity range with irradiation (kV)					
			Dry air		10g/m^3		18g/m^3	
	5cm	10cm	5cm	10cm	5cm	10cm	5cm	10cm
0.50	17.40	16.80	23.92 (29.92)	24.15 (29.25)	25.12 (29.02)	24.91 (29.02)	24.06 (29.99)	24.83 (28.55)
1.00	32.00	31.70	35.34	36.87	36.04	37.34	38.52	37.84
1.50	46.20	45.50	47.14	47.88	48.97	47.61	49.59	49.27
2.00	59.50	59.00	60.49	60.82	62.38	62.28	62.21	63.20
2.40	69.00	70.00	72.40	73.28	71.32	73.59	73.01	73.91
Gap spacing (cm)	**IEC Standard (kV)**		**$U_{50\%}$ with various humidity range without irradiation (kV)**					
			Dry air		**10g/m^3**		**18g/m^3**	
	5cm	**10cm**	**5cm**	**10cm**	**5cm**	**10cm**	**5cm**	**10cm**
0.50	17.40	16.80	25.66 (31.58)	25.71 (29.34)	27.65 (32.32)	26.03 (29.93)	27.48 (32.91)	25.68 (29.32)
1.00	32.00	31.70	36.28	36.30	37.31	37.88	38.74	37.80
1.50	46.20	45.50	48.02	48.73	49.42	49.20	50.45	50.43
2.00	59.50	59.00	61.31	61.11	62.93	62.36	63.68	64.84
2.40	69.00	70.00	72.38	72.42	72.96	73.36	74.33	73.60
			Values in the () are measured by voltage probe					

5cm diameter sphere-gap:

From Figure 4-11 and 4-12 show the value of $U_{50\%}$ of D=5cm (with and without irradiation) for negative and positive polarity, respectively, while one of D=10cm is shown in Figure 4-13 and 4-14. From these figures, it can be seen that they share a common trend that the value of $U_{50\%}$ disruptive discharge of both 5cm and 10cm sphere for negative and positive polarity generally have a slight decrease when the application of external irradiation source is presented.

For D=5cm (Figure 4-11 and 4-12), it can be seen that the value of $U_{50\%}$ for both polarities of the irradiated gap is generally lower than the one of the non-irradiated gaps. From these figures, they also show that reduction of the value of $U_{50\%}$ is more obvious for positive polarity than for negative polarity. For both voltage polarities, the influence of irradiation is stronger for small gap spacing (S≤1.0cm) than for large gap spacing, except the gap spacing of 2.4cm under positive polarity.

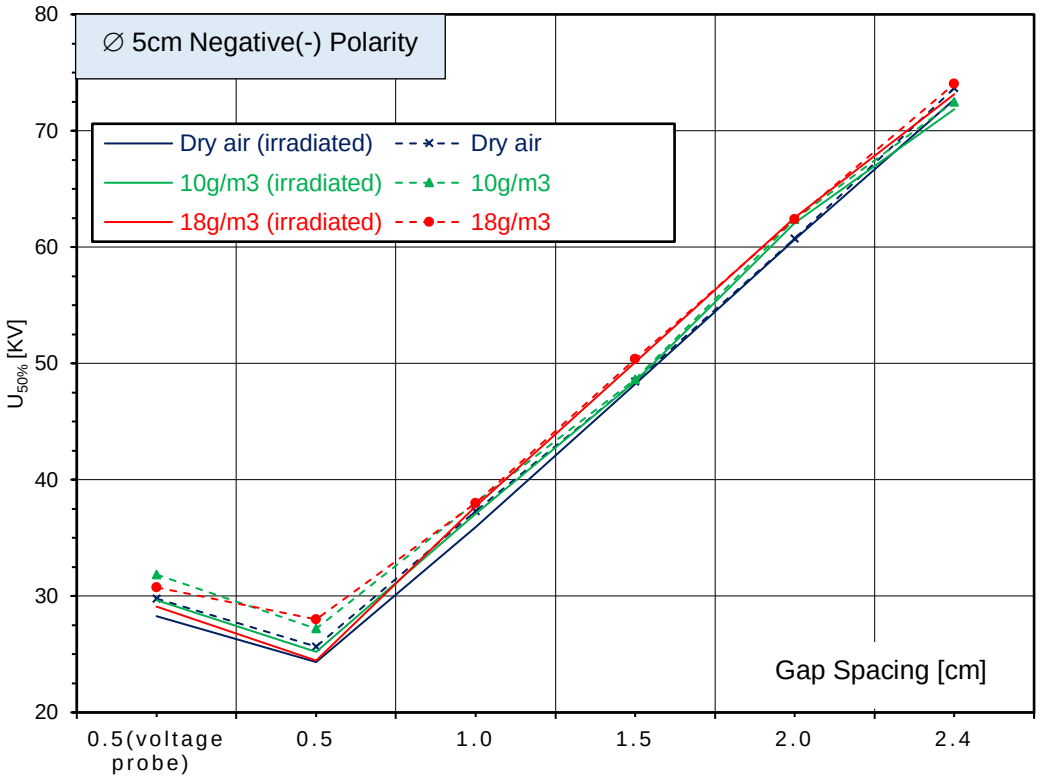

Figure 4-11 Plot of $U_{50\%}$ of negative LI voltage for 5cm diameter sphere against gap spacing under various humidity range with irradiation.

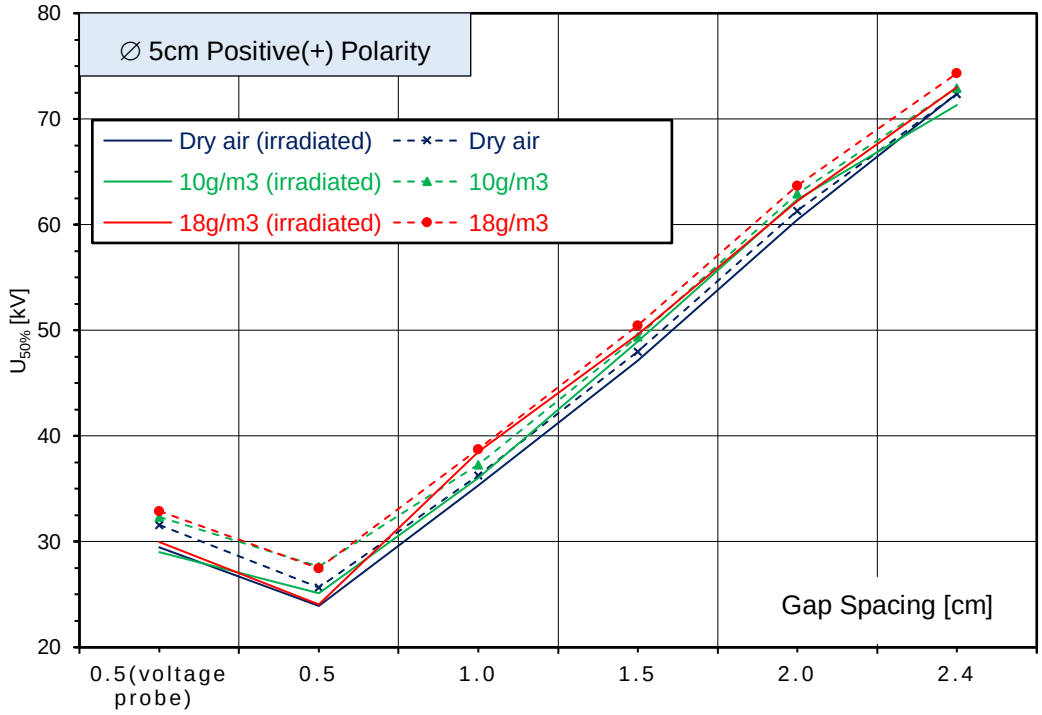

Figure 4-12 Plot of $U_{50\%}$ of positive LI voltage for 5cm diameter sphere against gap spacing under various humidity range with irradiation.

10cm diameter sphere:

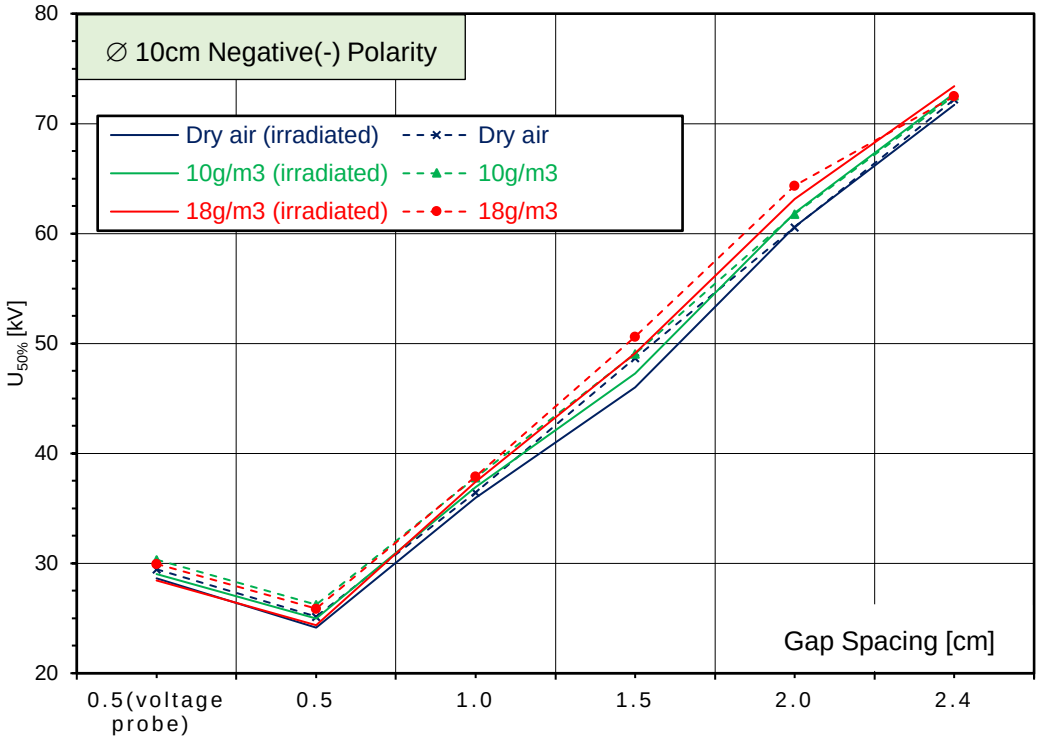

Figure 4-13 Plot of $U_{50\%}$ of negative LI voltage for 10cm diameter sphere against gap spacing under various humidity range with irradiation.

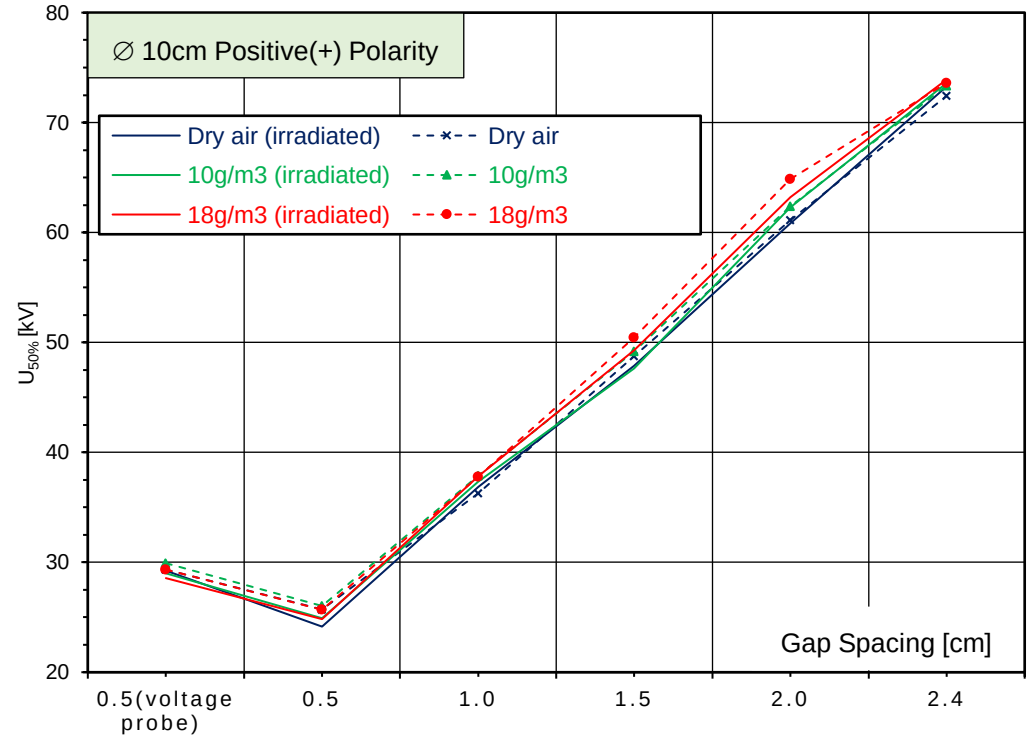

Figure 4-14 Plot of $U_{50\%}$ of positive LI voltage for 10cm diameter sphere against gap spacing under various humidity range with irradiation.

In particular in Figure 4-13 and 4-14, for D=10cm under both polarities, the reduction of $U_{50\%}$ of the irradiated gap is generally not equal over the all humidity range and the influence of irradiation on the value of $U_{50\%}$ exists for all gap spacing except the gap spacing of 2.0cm and 2.4 cm for both polarities. The reduction is obvious for gap spacing of 1.5cm under both polarities. However, for S= 0.5 and 1.0cm, it can be seen that the difference seems more obvious for negative than for positive polarity.

4.2.2.2 The influence of irradiation on standard deviation (σ)

The value of σ with irradiation for each humidity range of 5cm and 10cm diameter sphere are plotted in Figure 4-15 and 4-17 against gap spacing S with voltage polarity as the parameter. Figure 4-16 and 4-18, show the plot of $\sigma_{average}$ for full humidity range of 5cm and 10cm diameter sphere, with and without irradiation against gap spacing S with voltage polarity as the parameter.

From Figure 4-15, it can be seen the curve of σ with irradiation of each humidity range is fluctuation over the gap spacing S with negative polarity. However, for positive the curves of each humidity range are close to each other and the curves over gap spacing show a slight decrease with increasing of S and the overall value of σ between ~1% to ~4% except the S=0.5cm for 10g/m^3 where σ is relatively large ≈8%. For 10cm diameter sphere-gap (Figure 4-17), the fluctuation of the curve of σ over the gap spacing for each humidity is less significant for positive polarity. Similar to the non-irradiation case, for both D=5cm and 10cm the value of $\sigma_{average}$ with irradiation sphere also tend to decreases when the gap spacing increases.

In irrespective of D and S, the value of $\sigma_{average}$ for negative and positive polarity (Figure 4-16 and 4-18) of the irradiated gap is always smaller than the one of non-irradiated, the significant case is the gap spacing S=0.5cm for both D=5cm and 10cm spheres under both voltage polarities. For S ≥ 1.0cm of D=5cm (Figure 4-16), the reduction of $\sigma_{average}$ of the irradiated gap is less marked, especially the S=2.0cm of negative polarity. However, there are some reverse trends for S= 1.0 and 1.5cm of D=10cm under positive where these irradiated gaps gain higher value of $\sigma_{average}$ than non-irradiated gaps.

5cm diameter sphere-gap:

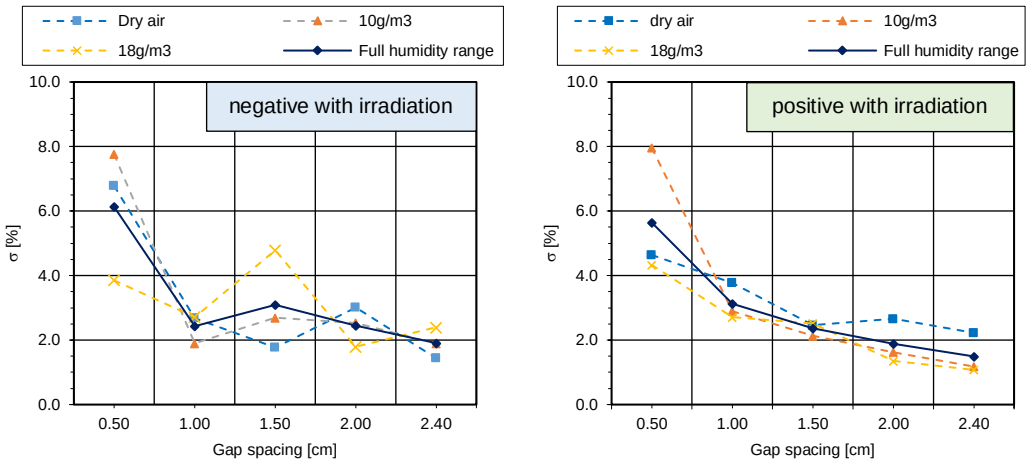

Figure 4-15 The value of σ with irradiation of D=5cm for various humidity range and the average value of σ for full range of humidity against gap spacing.

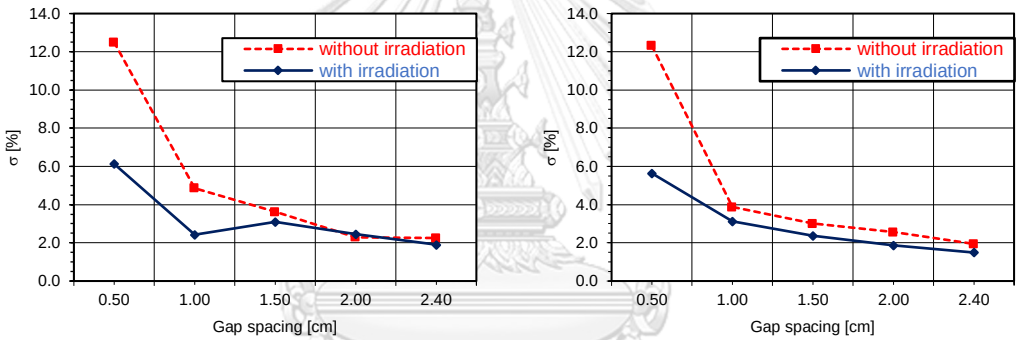

Figure 4-16 The value of $\sigma_{average}$ of D=5cm with and without for full humidity range against gap spacing under negative and positive polarity.

10cm diameter sphere-gap:

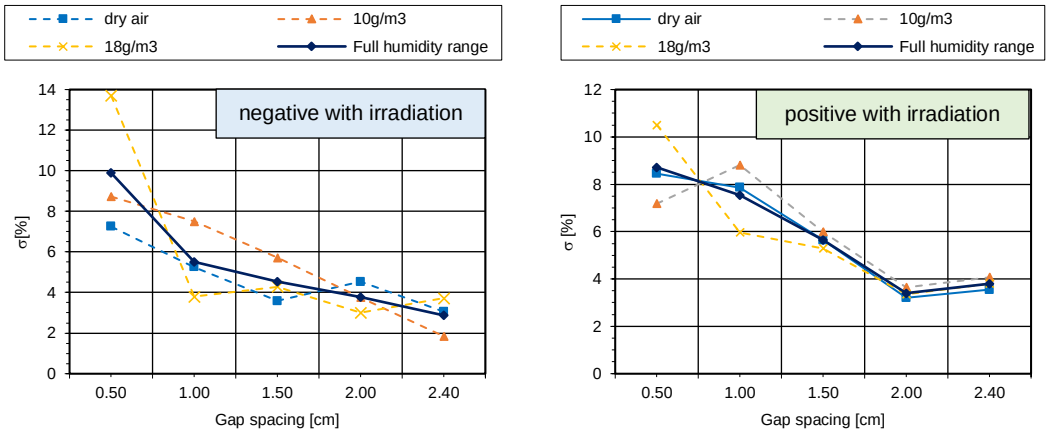

Figure 4-17 The value of σ for D=10cm with irradiation under various humidity range and the average value of σ for full range of humidity against gap spacing.

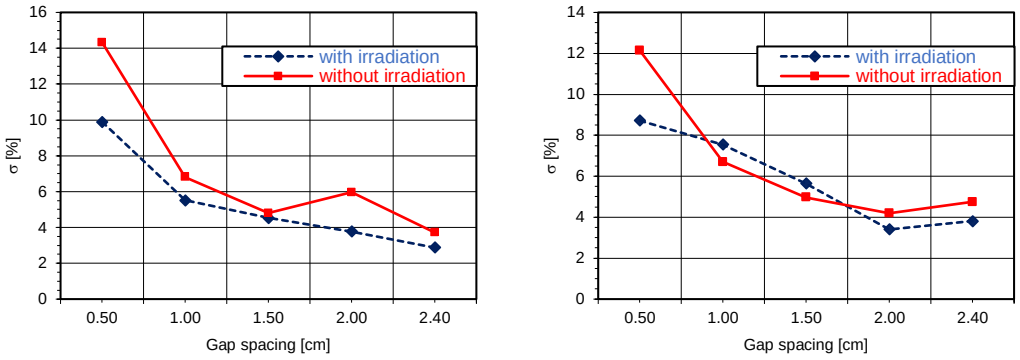

Figure 4-18 The value of $\sigma_{average}$ of D=10cm with and without irradiation for full humidity range against gap spacing under negative and positive polarities.

To sum up the influence of irradiation on $U_{50\%}$ and σ, the usage of external irradiation source from UV-Lamp generally lower the value of $U_{50\%}$ and σ, and the influence is valid for all range of humidity. The reason for this phenomenon is due to the enhancement of the number of initiated electrons, hence the flashover of irradiated gap occurred regularly as the applied voltage increase.

However, it can be also seen that the influence is less marked as the increasing of gap spacing. The reason for this phenomenon is that "the higher applied voltage increases the critical volume and therefore enhance the availability of primary electrons to the inception of electron avalanches" [10]. Moreover, the irradiation also reduces the percentage of the irregular curve of the breakdown probability (Figure 4-3 and 4-4), which mean that the breakdown probability curve that has a good fitting the Cumulative Normal Distribution is increased as the gaps of the sphere were irradiated.

4.2.3 $U_{50\%,\ corrected}$ of 5cm and 10cm diameter sphere-gap with and without irradiation

The $U_{50\%}$ obtained under the atmospheric condition inside the test chamber, are corrected to standard reference $U_{50\%,corrected}$ as follows:

$$U_{50\%,corrected} = \frac{U_{50\%}}{\delta \times k} \tag{12}$$

By using air density correction factor δ and humidity correction factor k from Table 3-1 and by following the Equation (12), the $U_{50\%,corrected}$ are obtained and described in bellowing tables:

4.2.3.1 $U_{50\%,\ corrected}$ of 5cm and 10cm diameter sphere-gap without irradiation

By using air density correction factor δ and humidity correction factor k from Table 3-1 and by following the Equation (12), the $U_{50\%\ corrected}$ without irradiation of D=5cm and D=10cm sphere-gap for both polarities, are obtained and shown in Table 4-9 and 4-10, respectively. The same values from the tables are also plotted against gap spacing S in Figure 4-21 and 4-22. The dot-lines represent the value of $U_{50\%,\ corrected}$ under each humidity range for negative and positive polarity, where the $U_{50\%}$ of standard LI under negative and positive polarity is represented by solid-line.

Table 4-9 $U_{50\%,\ corrected}$ disruptive discharge lightning impulse voltage of 5cm sphere-gap of negative and positive polarity(kV).

Gap spacing (cm)	IEC Standard (kV)		$U_{50\%,\ corrected}$ with various humidity range (kV)					
			Dry air		10g/m^3		18g/m^3	
	(-)	(+)	(-)	(+)	(-)	(+)	(-)	(+)
0.50	17.40	17.40	24.76 (28.75)	24.76 (30.47)	26.18 (30.66)	26.62 (31.11)	26.54 (29.13)	26.05 (31.20)
1.00	32.00	32.00	36.00	35.00	36.60	35.91	36.01	36.73
1.50	45.50	46.20	46.75	46.33	46.82	47.57	47.74	47.83
2.00	57.50	59.50	58.62	59.15	60.04	60.57	59.15	60.37
2.40	65.50	69.00	71.07	69.83	69.79	70.23	70.17	70.47
			Values in the () are measured by voltage probe					

Table 4-10 $U_{50\%,\ corrected}$ disruptive discharge lightning impulse voltage of 10cm sphere-gap of negative and positive polarity(kV).

Gap spacing (cm)	**IEC Standard (kV)**		**$U_{50\%,\ corrected}$ with various humidity range (kV)**					
			Dry air		**10g/m^3**		**18g/m^3**	
	(-)	**(+)**	**(-)**	**(+)**	**(-)**	**(+)**	**(-)**	**(+)**
0.50	16.80	16.80	24.27 (28.42)	24.80 (28.31)	25.27 (29.19)	25.06 (28.81)	24.53 (28.39)	24.36 (27.80)
1.00	31.70	31.70	35.15	35.02	36.40	36.46	35.94	35.83
1.50	45.50	45.50	46.97	47.01	47.22	47.36	48.01	47.81
2.00	57.90	59.00	58.43	58.96	59.49	60.03	60.99	61.47
2.40	69.50	70.00	69.66	69.87	69.82	70.61	68.71	69.77
			Values in the () are measured by voltage probe					

Follow the Equation (13), the difference of $U_{50\%,\ corrected}$ from $U_{50\%}$ (hereafter %Error) of 5cm and 10cm sphere-gap for both voltage polarities, are shown in Table 4-11 and 4-12, respectively. The same values are also plotted against gap spacing S in Figure 4-21 and 4-22.

$$\%Error = \frac{U_{50\%,corrected} - U_{50\%}}{U_{50\%}} \tag{13}$$

Table 4-11 The difference of $U_{50\%,\ corrected}$ from $U_{50\%}$ of 5cm sphere-gap for both voltage polarities (%).

Gap spacing (cm)	**IEC Standard (kV)**		**The difference of $U_{50\%,\ corrected}$ from $U_{50\%}$ (%Error)**					
			Dry air		**10g/m^3**		**18g/m^3**	
	(-)	**(+)**	**(-)**	**(+)**	**(-)**	**(+)**	**(-)**	**(+)**
0.50	17.40	17.40	42.28 (65.23)	42.28 (75.10)	50.47 (76.19)	52.96 (78.79)	52.55 (67.43)	49.72 (79.30)
1.00	32.00	32.00	12.49	9.38	14.37	12.23	12.55	14.77
1.50	45.50	46.20	2.75	0.28	2.90	2.97	4.93	3.52
2.00	57.50	59.50	1.95	-0.59	4.41	1.81	2.86	1.46
2.40	65.50	69.00	8.50	1.20	6.54	1.78	7.13	2.12
			Values in the () are measured by voltage probe					

Table 4-12 The difference of $U_{50\%,\ corrected}$ from $U_{50\%}$ of 10cm sphere-gap for both voltage polarities (%).

Gap spacing (cm)	IEC Standard (kV)		The difference of $U_{50\%,\ corrected}$ from $U_{50\%}$ (%Error)					
			Dry air		10g/m^3		18g/m^3	
	(-)	(+)	(-)	(+)	(-)	(+)	(-)	(+)
0.50	16.80	16.80	44.49 (69.18)	47.65 (68.49)	50.34 (73.78)	49.14 (71.49)	46.04 (69.00)	44.91 (65.45)
1.00	31.70	31.70	10.87	10.48	14.84	15.02	13.37	13.04
1.50	45.50	45.50	3.22	3.33	3.79	4.08	5.51	5.07
2.00	57.90	59.00	0.91	-0.07	2.74	1.74	5.34	4.18
2.40	69.50	70.00	0.23	-0.19	0.47	0.88	-1.13	-0.32
			Values in the () are measured by voltage probe					

From Table 4-11, 4-12 and Figure 4-19, 4-20, it can be seen that $U_{50\%,\ corrected}$ of D=5cm and 10cm for both voltage polarities which is converted by using IEC humidity correction method, is generally still higher than the standard value. However, the difference of $U_{50\%,\ corrected}$ for both 5cm and 10cm sphere-gap from the standard value decreases as increasing of gap spacing, except the gap spacing of 2.4cm for D=5cm of negative polarity only.

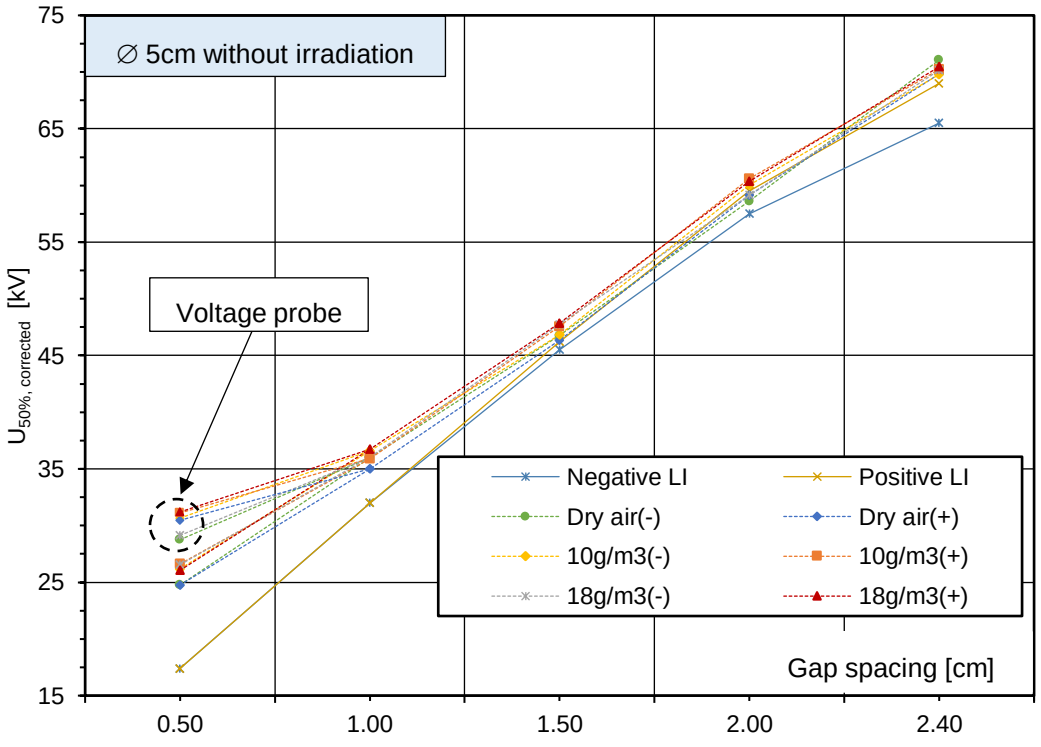

Figure 4-19 $U_{50\%,\ corrected}$ plotted against S for D=5cm under various humidity range under both voltage polarities.

The %Error of $U_{50\%,\ corrected}$ from the standard value for 5cm and 10cm sphere-gap are represented by Figure 4-21 and 4-22, respectively, which have voltage polarity and absolute humidity as the parameters. The negative polarity is represented by the solid-line and the dot-line represents the positive polarity.

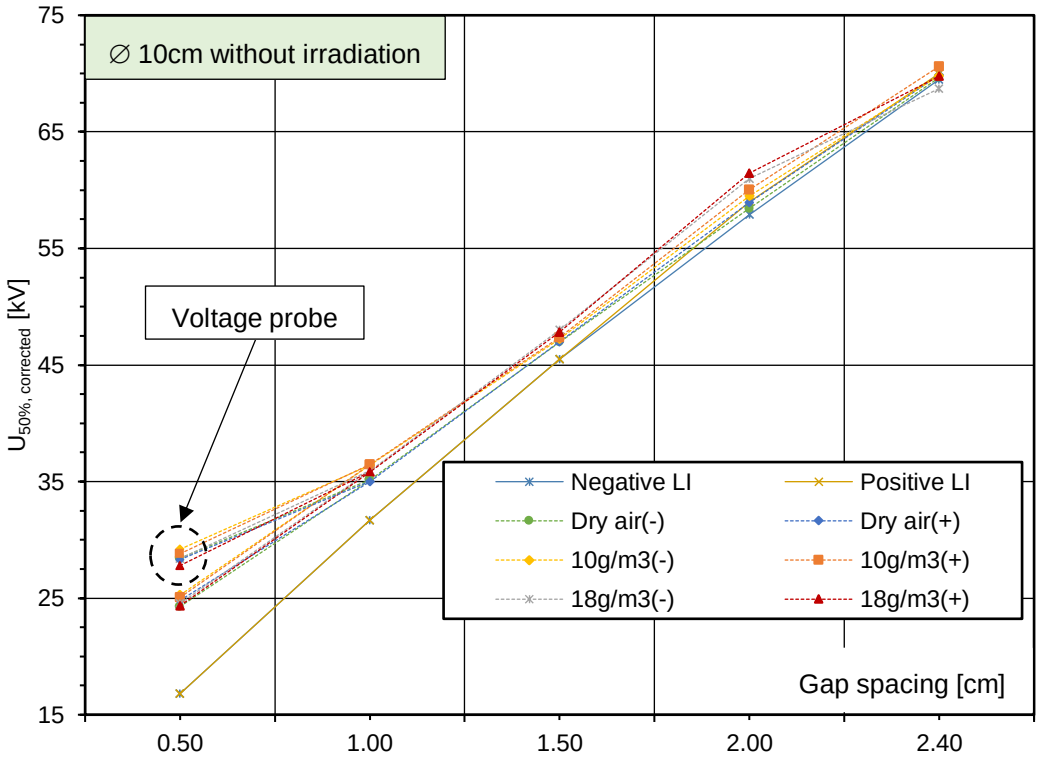

Figure 4-20 $U_{50\%,\ corrected}$ plotted against S for D=10cm under various humidity range under both voltage polarities.

For S ≥ 1.5cm of D=5cm, the %Error of each humidity range for both voltage polarities is generally small with the overall value remains within ±3%, except the negative polarity of S=1.5cm under 18g/m^3, S=2.0 under 10g/m^3 and S= 2.4cm under all humidity range which has the value around 4.93%, 4.43% and between 6.54% to 8.5%, respectively. For small gap spacing (S ≤ 1.0cm) of both voltage polarities, the %Error of each humidity range is relatively large with the overall value between 9.38% to 14.77% or for S=1.0cm and between 42.28% to 52.96% or less for S=0.5cm. The worst case is for S=0.5cm for all humidity range which is measured by voltage probe with the %Error between 65.23% to 79.30%.

For large gap spacing D=10cm of both voltage polarities under all humidity range, the %Error is less than the one of D=5cm, the overall %Error is less than 1% for S=2.4cm, between -0.07% and 5.34% for S=2.0cm and between 3.22% and 5.51% for S=1.5cm.

For smaller gaps, the %Error is between 10.48% and 15.02% for S=1.0cm, between 44.91% and 50.34% for S=0.5cm and the worst case also occurs for S=0.5cm measured by voltage probe which has %Error between -73.78% and 65.45%.

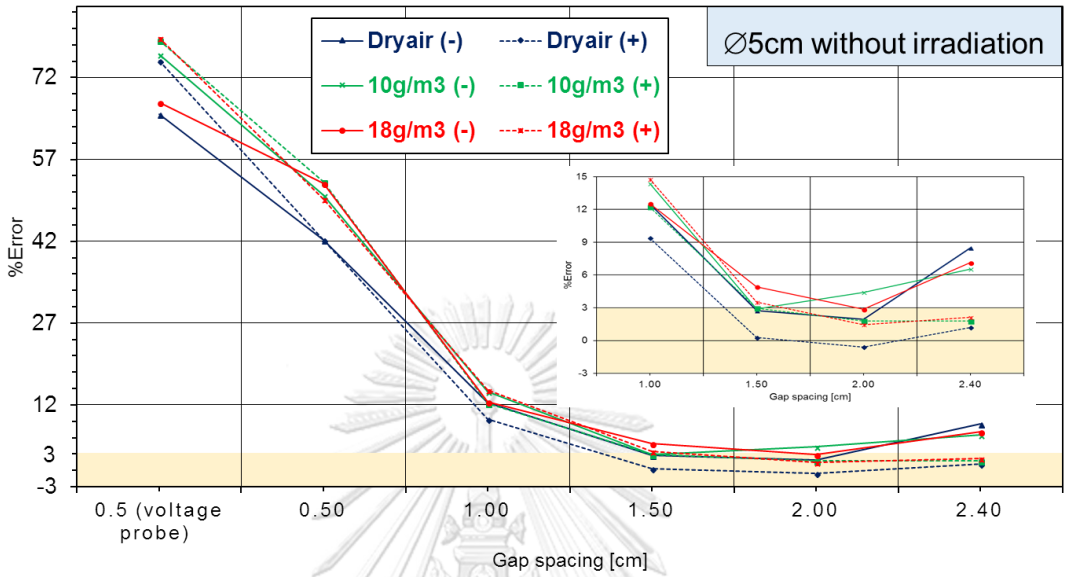

Figure 4-21 The %Error of $U_{50\%,\ corrected}$ from the standard value for D=5cm against S under both voltage polarities.

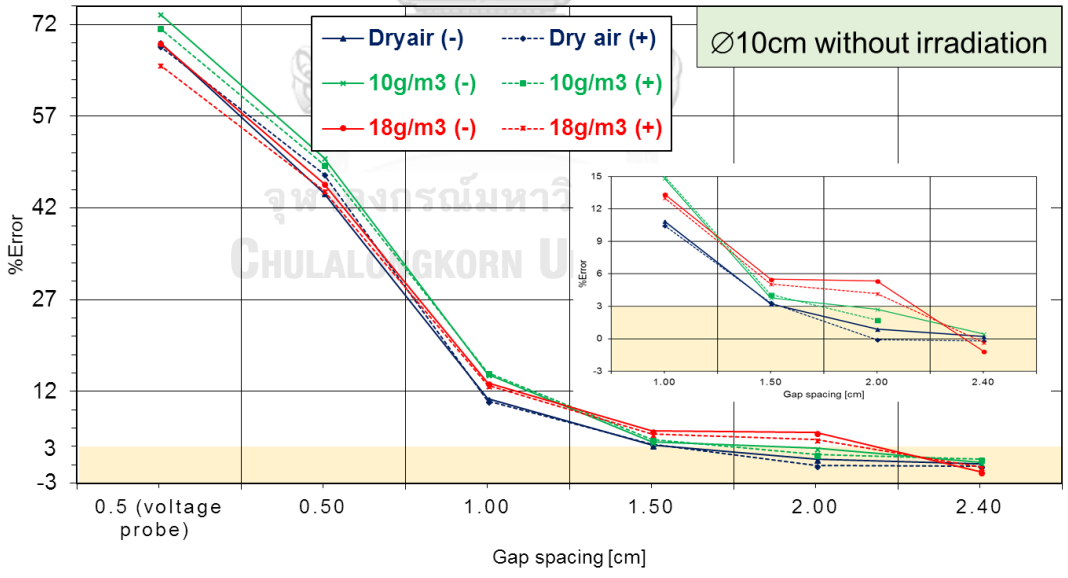

Figure 4-22 The %Error of $U_{50\%,\ corrected}$ from the standard value for D=10cm against S under both voltage polarities.

By using IEC correction method, the $U_{50\%,\ corrected}$ from the experiment is converted and it gets closer to the standard value with acceptable %Error for the larger gap spacing (S ≥1.5cm). However, the undesirable %Error occurs for small gap spacing. As the

difference between the measured value and the standard value is significantly huge, it can be assumed that the reason that lead to such huge difference for small S, it may not come from the failure of IEC correct method but it is surely come from other effects.

4.2.3.2 $U_{50\%,\ corrected}$ of 5cm and 10cm diameter sphere-gap with irradiation

By using air density correction factor δ and humidity correction factor k from Table 3-1 and by following the Equation (13), the $U_{50\%,corrected}$ with irradiation for 5cm and 10cm sphere-gap are obtained and described in the Table 4-13 and 4-14. The same values are also plotted against gap spacing S for ∅5cm and ∅10cm sphere-gap (Figure 4-23 and 4-24).

Table 4-13 $U_{50\%,\ corrected}$ disruptive discharge lightning impulse voltage of 5cm sphere-gap of negative and positive polarity(kV).

Gap spacing (cm)	**IEC Standard (kV)**		**$U_{50\%}$ with various humidity range (kV)**					
			Dry air		**10g/m^3**		**18g/m^3**	
	(-)	**(+)**	**(-)**	**(+)**	**(-)**	**(+)**	**(-)**	**(+)**
0.50	17.40	17.40	23.47 (27.29)	23.08 (28.43)	24.27 (28.56)	24.18 (27.93)	23.19 (27.60)	22.81 (28.42)
1.00	32.00	32.00	34.66	34.10	35.68	34.69	35.76	36.52
1.50	45.50	46.20	46.53	45.48	46.64	47.14	47.48	47.01
2.00	57.50	59.50	58.50	58.36	59.77	60.05	59.30	58.98
2.40	65.50	69.00	70.13	69.85	69.16	68.65	69.34	69.21
			Values in the () are measured by voltage probe					

Table 4-14 $U_{50\%,\ corrected}$ disruptive discharge lightning impulse voltage of 10cm sphere-gap of negative and positive polarity(kV).

Gap spacing (cm)	**IEC Standard (kV)**		**$U_{50\%}$ with various humidity range (kV)**					
			Dry air		**10g/m^3**		**18g/m^3**	
	(-)	**(+)**	**(-)**	**(+)**	**(-)**	**(+)**	**(-)**	**(+)**
0.50	16.80	16.80	23.30 (27.61)	23.30 (28.22)	24.05 (27.92)	23.98 (27.93)	23.10 (26.98)	23.54 (27.07)
1.00	31.70	31.70	34.71	35.57	35.54	35.94	35.49	35.87
1.50	45.50	45.50	44.37	46.19	45.49	45.83	46.55	46.71
2.00	57.90	59.00	58.48	58.68	59.56	59.95	59.88	59.91
2.40	69.50	70.00	69.18	70.70	70.03	70.84	69.58	70.07
			Values in the () are measured by voltage probe					

Follow the Equation (13), the %Error of 5cm and 10cm sphere-gap for both voltage polarities, are shown in Table 4-15 and 4-16, respectively. The same values are also plotted against gap spacing S in Figure 4-25 and 4-26.

Table 4-15 The difference of $U_{50\%,\ corrected}$ from $U_{50\%}$ of 5cm sphere-gap for negative and positive voltage polarities.

Gap spacing (cm)	**IEC Standard (kV)**		**The difference of $U_{50\%,\ corrected}$ from $U_{50\%}$ (%Error)**					
			Dry air		**10g/m^3**		**18g/m^3**	
	(-)	**(+)**	**(-)**	**(+)**	**(-)**	**(+)**	**(-)**	**(+)**
0.50	17.40	17.40	34.90 (56.86)	32.63 (63.40)	39.46 (64.14)	38.96 (60.54)	33.27 (58.60)	31.09 (63.39)
1.00	32.00	32.00	8.33	6.55	11.51	8.41	11.75	14.12
1.50	45.50	46.20	2.27	-1.56	2.50	2.03	4.34	1.76
2.00	57.50	59.50	1.75	-1.92	3.94	0.92	3.13	-0.88
2.40	65.50	69.00	7.07	1.23	5.59	-0.51	5.86	0.31
			Values in the () are measured by voltage probe					

Table 4-16 The difference of $U_{50\%,\ corrected}$ from $U_{50\%}$ of 10cm sphere-gap for negative and positive voltage polarities.

Gap spacing (cm)	**IEC Standard (kV)**		**The difference of $U_{50\%,\ corrected}$ from $U_{50\%}$ (%Error)**					
			Dry air		**10g/m^3**		**18g/m^3**	
	(-)	**(+)**	**(-)**	**(+)**	**(-)**	**(+)**	**(-)**	**(+)**
0.50	16.80	16.80	38.69 (64.36)	38.69 (67.98)	43.13 (66.22)	42.72 (66.27)	37.52 (60.60)	40.11 (61.10)
1.00	31.70	31.70	9.50	12.21	12.11	13.38	11.97	13.16
1.50	45.50	45.50	-2.48	1.53	-0.02	0.72	2.30	2.66
2.00	57.90	59.00	-0.89	-0.55	0.96	1.61	1.48	1.55
2.40	69.50	70.00	-0.47	1.00	0.76	1.19	0.12	0.10
			Values in the () are measured by voltage probe					

From Figure 4-23 and 4-24, it can be seen that $U_{50\%,\ corrected}$ with irradiation of 5cm and 10cm sphere-gap attain closer to the standard value than the one without irradiation. The significant case is for large gap spacing (S≥1.5cm) of both sphere-gap where the $U_{50\%,\ corrected}$ with irradiation seems to reach the same value as the reference standard. The detail information can be obtained in Figure 2-25 and 2-26 which clearly indicate the %Error of $U_{50\%,\ corrected}$ with irradiation from the standard value under each humidity range of both voltage polarities for D=5cm and D=10cm, respectively.

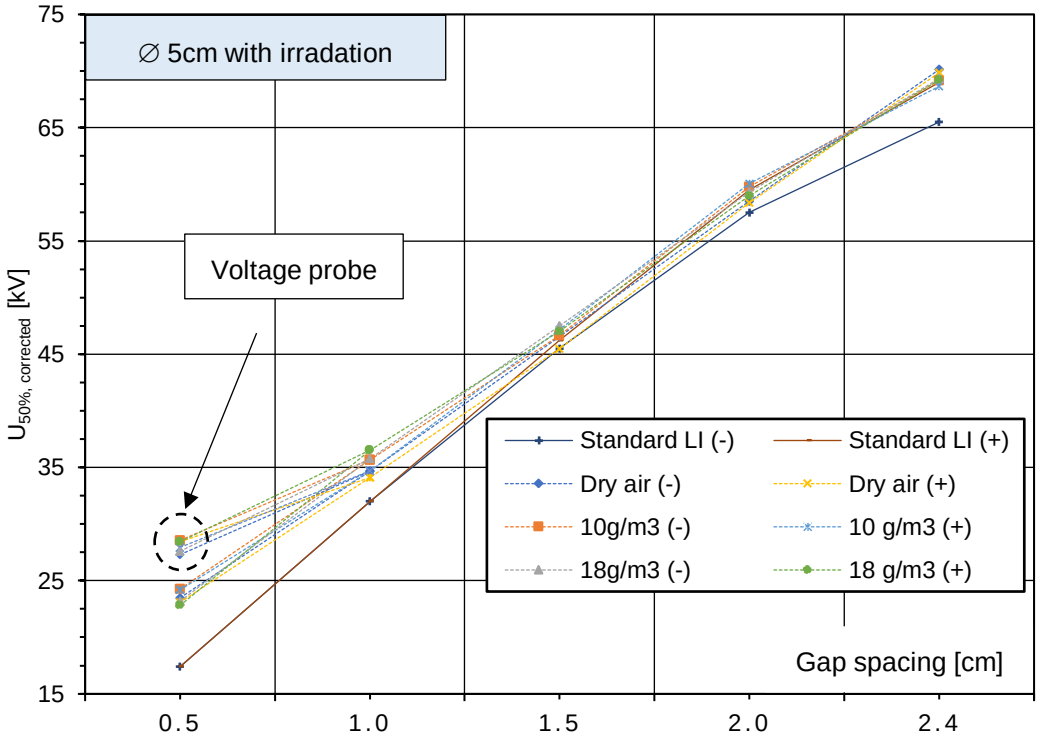

Figure 4-23 $U_{50\%, corrected}$ plotted against S for D=5cm under various humidity range under both voltage polarities.

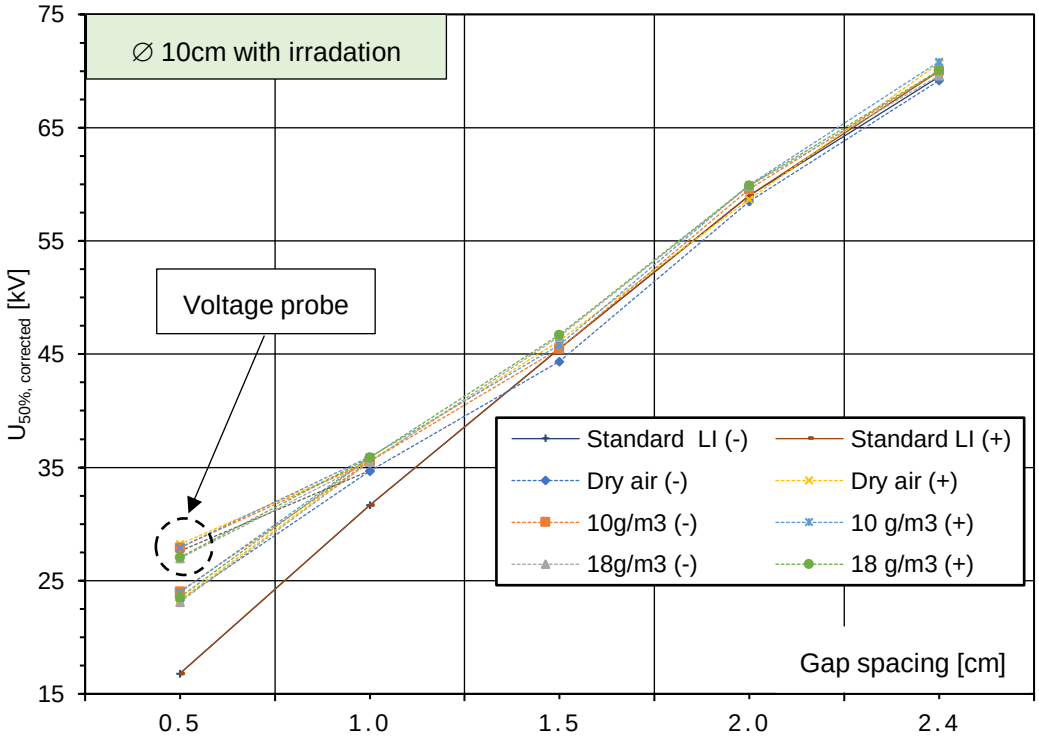

Figure 4-24 $U_{50\%, corrected}$ plotted against S for D=10cm under various humidity range under both voltage polarities.

From Figure 4-25 and 4-26, it can be seen that there are some differences between the $U_{50\%,\ corrected}$ with irradiation and the standard value. Generally, the value of the present experiment is higher than the one of the standards. However, $U_{50\%,\ corrected}$ of 5cm and 10cm diameter sphere-gap attain closer to the standard value as the gap spacing increases. The significant case is for large gap spacing ($S \geq 1.5$cm) of both sphere-gap where %Error generally remains within the value of ±3%, except D=5cm for negative polarity under dry air, absolute humidity of 10g/m3 and 18 g/m3, which is higher than the standard value by 7.07%, 5.59% and 5.56% respectively. The reason for this can be observed that the curve of negative LI of standard $U_{50\%}$ against S for 5cm deviates at S=2.4cm. For both voltage polarities of 5cm and 10cm sphere the huge difference occurred for small gap spacing ($S \leq 1.0$cm), the $U_{50\%,\ corrected}$ is higher than the standard value by more than 10%.

For $S \geq 1.5$cm, D=5cm of negative polarity, the %Error for each humidity range is between 2.27% to 4.34%, 1.75% to 3.94% and 5.86% to 7.07% for S= 1.5, 2.0 and 2.4cm, respectively. For the same gap spacing under the positive voltage of D=5cm, the overall %Error is around 2.0% or less. For small gap spacing ($S \leq 1.0$cm), under negative polarity, the %Error is relatively large, 33.27% to 39.46% and 8.33% to 11.5% for S= 0.5cm and 1.0cm, respectively. For same S of positive polarity, the %Error is between 31.09% to 38.96% and 6.55% to 14.14% The worst case is S=0.5cm measured by voltage probe where the %Error under each humidity range of negative and positive polarity are between 56.86% to 64.14% and 60.54% to 63.40%, respectively.

In particular, for $S \geq 1.5$cm of D=10cm, the %Error for both voltage polarities under each humidity range achieved much better than the one of D=5cm with the overall value between -2.48% to 2.66%. For $S \leq 1.0$ of both polarity, the overall %Error is between 37.52% to 43.13% and 9.5% to 13.38% for S=0.5cm and 1.0cm, respectively. In particular, for both voltage polarities of 0.5cm measured by voltage probe, the overall %Error is between 60.60% to 67.98%.

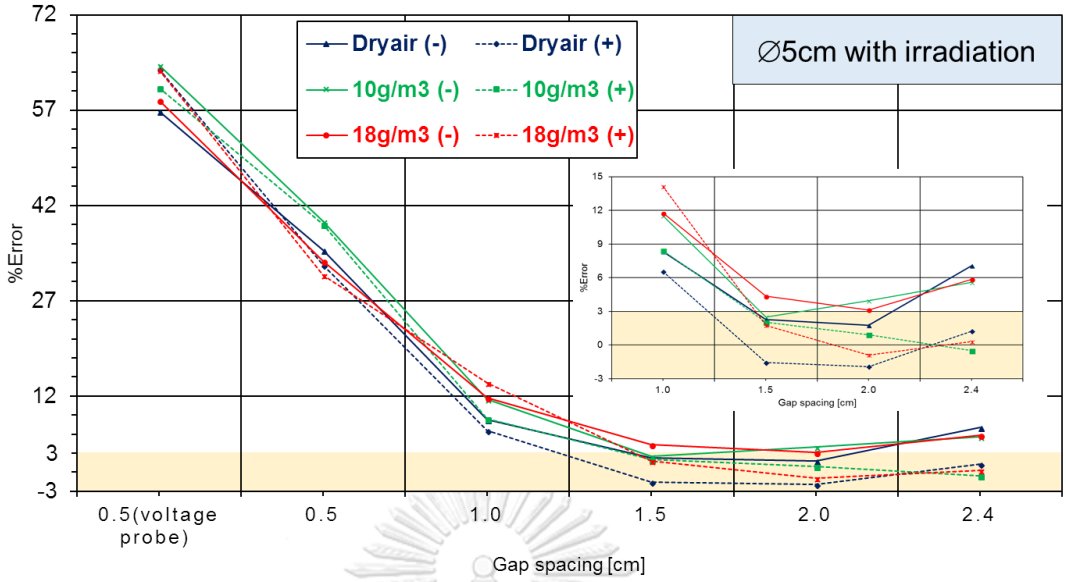

Figure 4-25 The %Error of $U_{50\%,\ corrected}$ from the standard value for D=5cm against S under both voltage polarities.

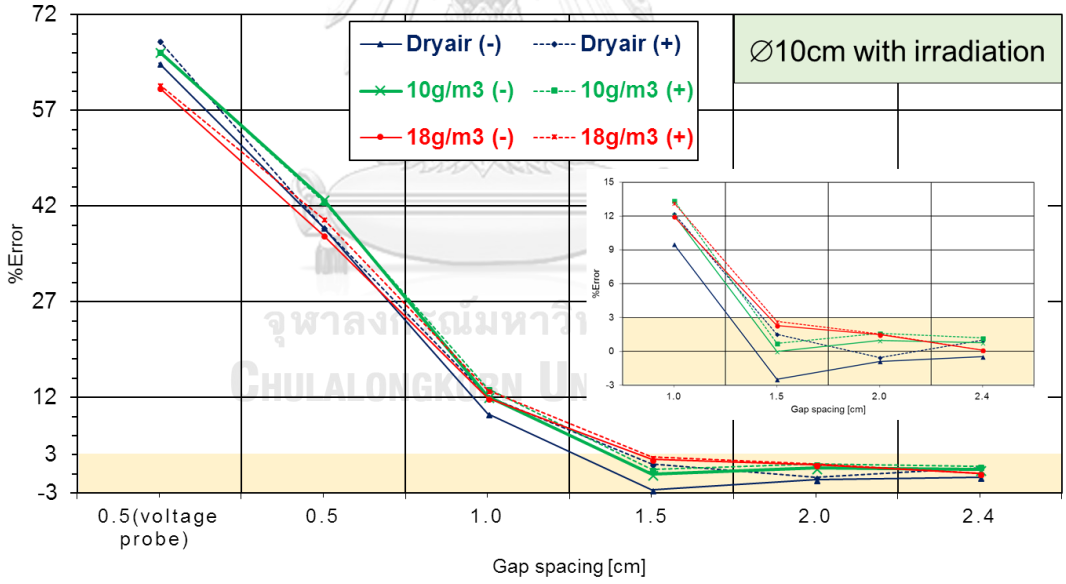

Figure 4-26 The %Error of $U_{50\%,\ corrected}$ from the standard value for D=10cm against S under both voltage polarities.

From Figure 4-25 and 4-26 and Figure 4-21 and 4-22, it can be seen that the irradiated gaps generally attain closer to the standard value than the non-irradiated gaps. For both with and without irradiation, the acceptable difference occurs only for S ≥1.5cm but for smaller S, it shows a huge difference from the standard value. Drew an attention from

small S, it can be deduced that the IEC correction method and the application irradiation is not the main factor that causes such undesirable difference.

Moreover, it can be clearly seen that there is the difference between the value of $U_{50\%,\ corrected}$ measured from voltage probe and the one from 200kV voltage divider. The measured values from the voltage probe (rated voltage of 40kV) always show the higher value than the one from 200kV voltage divider (rated voltage of 200kV). From this case, it can be assumed that the different measuring devices may lead to the difference in voltage measurement of sphere-gap. However, the IEC standard does not indicate the measurement devices which are used in their experiment process. Hence, the measuring device is a reasonable factor that leads the difference between the experiment value and the standard value since the $U_{50\%}$ from the voltage probe, 200kV voltage divider and IEC standard show the different value from each other. Furthermore, the uncertainty of measuring device may be guaranteed for measuring the voltage level at 20% up to a maximum voltage of the measuring device itself (the selected calibration voltage level is around 20% up to maximum rated voltage). It is due to linearity effect in the calibration process of the measuring device [6]. So, the measurement uncertainty of 200kV voltage divider for measuring the peak voltage stressed on the sphere-gap may be increased for gap spacing of 0.5cm ($U_{50\%}$ of S=0.5cm is smaller than 20% of 200kV).

4.2.3.3 The comparison between $U_{50\%,\ corrected}$ of 5cm and 10cm diameter sphere-gap

In this part, the value $U_{50\%,\ corrected}$ with irradiation of D=5cm and D=10cm for both voltage polarities under a various range of humidity was taken to study. Figure 4-27, 4-28 and 4-29, show the plots of $U_{50\%,\ corrected}$ with irradiation for both voltage polarities under dry air, absolute humidity of 10g/m^3 and 18g/m^3. The value $U_{50\%,\ corrected}$ of both sphere under various humidity range for negative and positive polarity is shown in Figure 4-30 and Figure 4-31, respectively.

Following the Equation (14), the difference between $U_{50\%}$ of ∅5cm and of ∅10cm (hereafter %ΔU) sphere for negative and positive polarity are plotted against gap, are shown in Figure 4-32 and 4-33, respectively.

$$\%\Delta U = \frac{U_{50\%,5cm} - U_{50\%,10cm}}{U_{50\%,10cm}} \times 100\% \qquad (14)$$

In the Figures 4-32 and 4-33, the dot-line represents the %ΔU for each humidity ranges and the red solid-line represents the average value of %ΔU of the experiment for full humidity range, while the %ΔU of the standard value is represented by the blue solid-line.

It is also necessary to mention that the only $U_{50\%,\ corrected}$ with irradiation (hereafter $U_{50\%,\ corrected}$) was used for this comparison study.

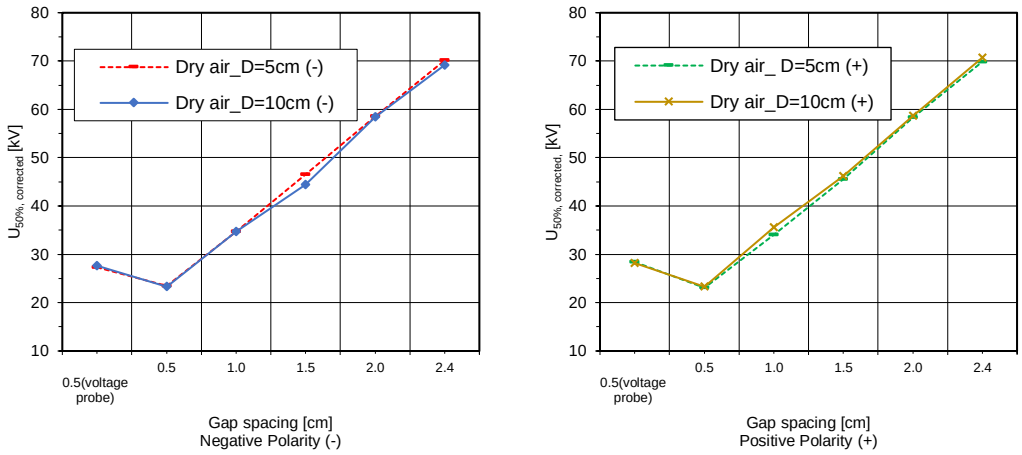

Figure 4-27 Plot of $U_{50\%,\ corrected}$ of 5cm and 10cm sphere-gap against gap spacing for LI under dry air.

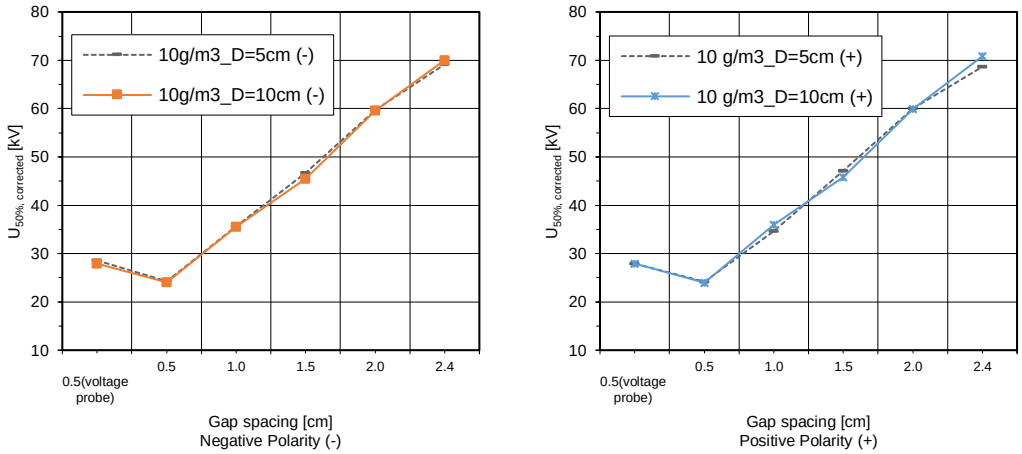

Figure 4-28 Plot of $U_{50\%,\ corrected}$ of 5cm and 10cm sphere-gap against gap spacing for LI under absolute humidity of $10g/m^3$.

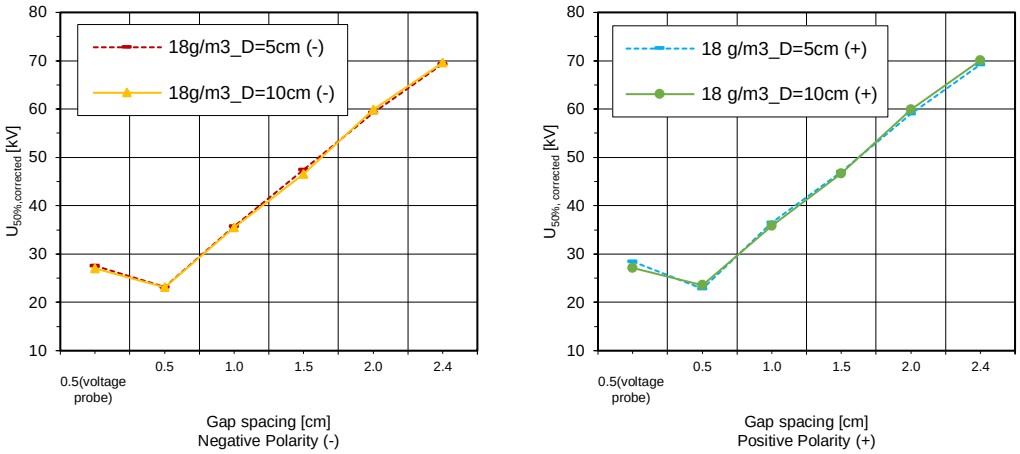

Figure 4-29 Plot of $U_{50\%,\ corrected}$ of 5cm and 10cm sphere-gap against gap spacing for LI under absolute humidity of 18g/m^3.

Figure 4-30 and 4-31 show the plots of $U_{50\%,\ corrected}$ of both sphere-gap over the gap spacing under for all range of humidity for negative and positive polarity, respectively. Under dry air for both voltage polarities, the $U_{50\%,\ corrected}$ for D=5cm have a good fitting with D=10cm for both voltage polarities. However, there are some diversion at S=1.5cm for negative polarity and S=1.0cm for positive polarity. Under absolute humidity of 10g/m^3 for both voltage polarities, it indicates that the curve of $U_{50\%,\ corrected}$ against the gap spacing for 5cm sphere also fits well with the one for 10cm sphere, a fair amount of diversion occurred at S=2.4cm under positive polarity. For both voltage polarities under absolute humidity of 18g/m^3, shows that the curve of $U_{50\%,\ corrected}$ against the gap spacing for D=5cm and 10cm also have a good fitting with each other, but there is a significant diversion at S=1.0cm under negative polarity.

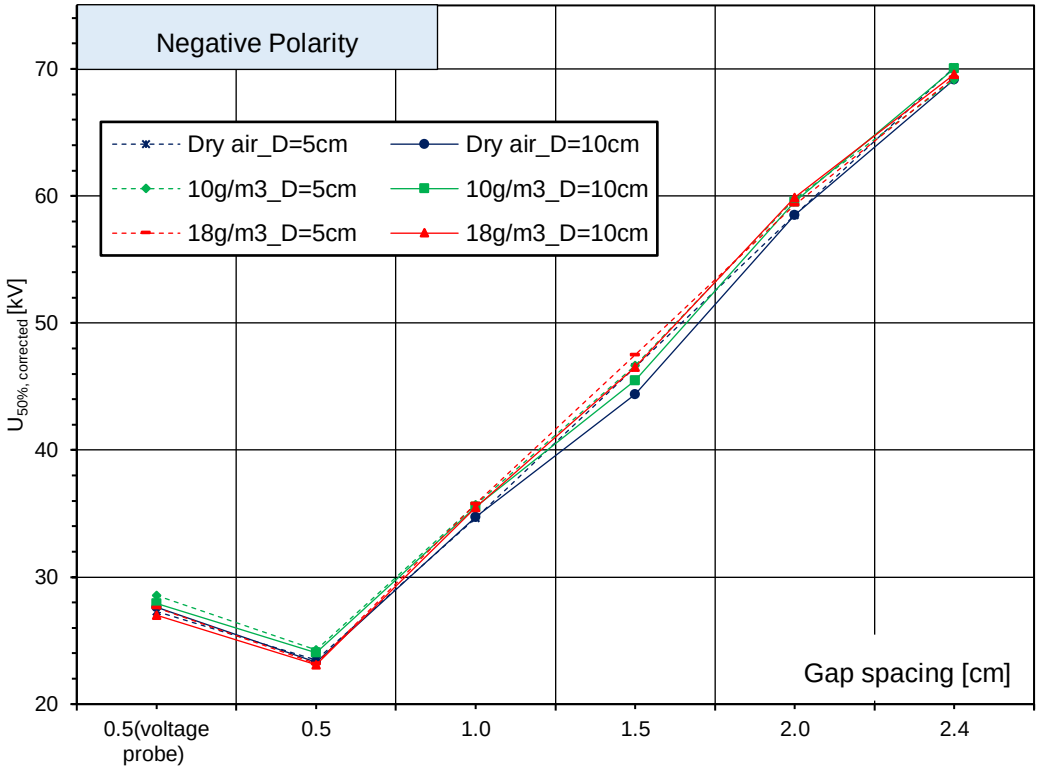

Figure 4-30 Plot of $U_{50\%,\ corrected}$ of 5cm and 10cm sphere-gap for negative LI under various humidity range against gap spacing.

From Figure 4-32, under negative polarity, the %ΔU of $U_{average}$ of the experiment tend to close to 0%, except the gap spacing S=1.5cm, while %ΔU of the standard value decrease from value around 3.6% to -5.7%.

Under positive polarity (Figure 4-33), the %ΔU of the standard value always higher than 0%, except S=2.4cm, while %ΔU of the experiment is generally lower than 0%, except gap S= 0.5cm (measured by voltage probe) and S=1.5cm.

From Figure 4-32 and 4-33, it can be seen that %ΔU of the experiment generally attains the lower value than %ΔU of the IEC standard and %ΔU of the experiment gets closer to 0% than one of the IEC standards.

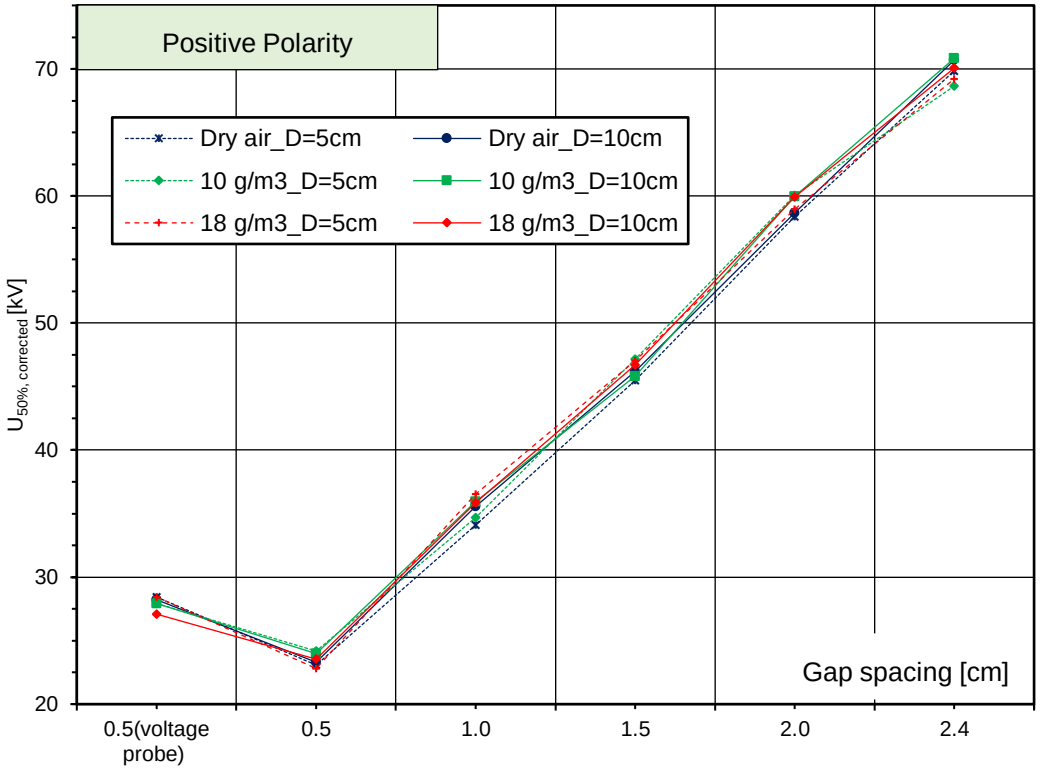

Figure 4-31 Plot of $U_{50\%,\ corrected}$ of 5cm and 10cm sphere-gap for positive LI under various humidity range against gap spacing.

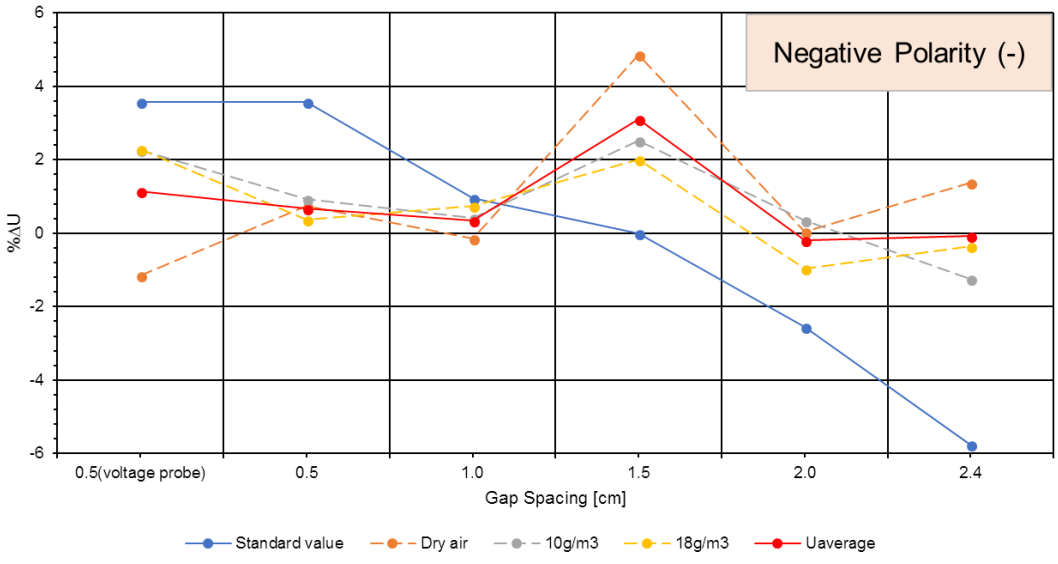

Figure 4-32 Plot of %ΔU of the measured values and of standard values against gap spacing for negative polarity.

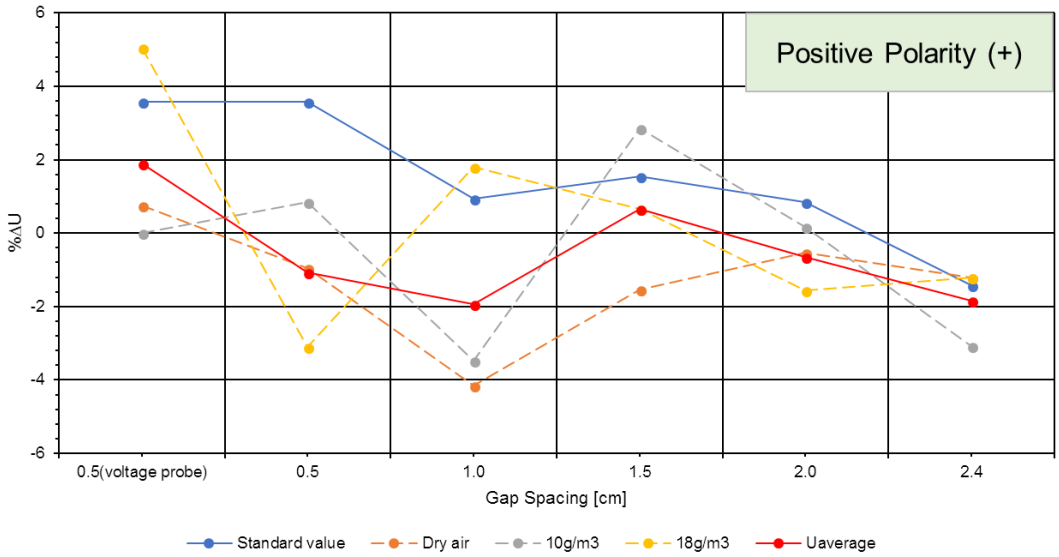

Figure 4-33 Plot of %ΔU of the measured values and of standard values against gap spacing for positive polarity.

To sum up of this part, for both voltage polarities, under all range of humidity the curve of $U_{50\%,\ corrected}$ against gap spacing for D= 5cm and D=10cm from this present experiment generally have a good fitting with each other and the values of $U_{50\%}$ for D=5cm and D=10cm are close to each other. Moreover, it can be seen that the %Error between the measured value and the standard value for D=10cm is smaller than the one for D=5cm. Hence it can be deduced that the values of $U_{50\%}$ for both D=5cm and D=10cm spheres from this experiment tend to close the 10cm standard sphere-gap than 5cm standard sphere gap.

However, there are some values of $U_{50\%}$ in the standard that may be interpolated [25]. In this case, the gap spacing which is suspected to be interpolated occur for both D=5cm and D=10cm, and the significant one is for D=10cm under negative polarity with S=1.5, 2.0 and 2.4cm. From Figure 4-24, it can be seen that the $U_{50\%}$ of 10cm standard sphere-gap show a linear increase over the gap spacing, while the one of 5cm standard sphere gap shows a diversion at gap spacing of 2.4cm under negative polarity (Figure 4-23).

Chapter 5
Conclusion

For this present work, it can be seen that $U_{50\%}$ increases as increasing of humidity but this influence is not so strong. The influence of humidity on $U_{50\%}$ seems to depend on gap spacing S and voltage polarity. This influence becomes weaker as gap spacing S increases. While, the standard deviation σ seems not strongly depend on the rate of humidity, but it tends to depend on the gap spacing and sphere diameter. For all range of humidity, the IEC correction method seems proper for $S \geq 1.5$cm, but there is an undesirable difference between the measured and the standard value for S=0.5cm and 1.0cm.

For $S \leq 1.5$cm of both 5cm and 10cm diameter sphere ($D \leq 12.5$cm and $U_{50\%} < 50$kV), the value of $U_{50\%}$ and standard deviation σ of the breakdown curve with irradiation is lower than the one without irradiation. This case confirms with the IEC standard which suggests that the additional irradiation is required for the sphere with a diameter smaller than 12.5cm and for voltage below 50kV. Moreover, in this present work, the application of irradiation is still valid for S=2.0 and 2.4cm ($U_{50\%} > 50$kV).

For both voltage polarities of $U_{50\%, \text{ corrected}}$ with and without irradiation (Figure 4-23 and 4-24 and Figure 4-19 and 4-20), it can be seen that the gap spacing of 1.5, 2.0 and 2.4cm shows an acceptable diversion from the IEC standard but the undesirable difference occurred for S=0.5 and 1.0cm. However, for S=0.5cm that was measured by both voltage probe and 200kV divider, the value $U_{50\%}$ measured by voltage probe is always higher than the one measured by 200kV voltage divider. In this case, it can be deduced that the different measuring devices that were used to measure the same sphere-gap may obtain the different value from each other. From this, it can be assumed that the IEC correction method and the application of irradiation is not the main reason that caused such a huge difference but the measuring device that was used to measure the standard sphere-gap is the main cause that leads the different measuring value since the breakdown voltage $U_{50\%}$ for S=0.5cm of both 5cm and 10cm sphere-gap that is obtained from voltage probe, 200kV divider and IEC standard, show the different values from each other.

For both voltage polarities under all range of humidity, the value of $U_{50\%}$ for 5cm and 10cm sphere of the experiments (Figure 4-30 and 4-31) tends to be close to each other. However, this occurrence is opposite to the IEC standard which shows that the value of $U_{50\%}$ for 5cm and 10cm sphere have a significant difference from each other, especially under negative polarity (Figure 1-4). However, some values of $U_{50\%}$ for 10cm standard sphere-gap under negative polarity are suspected to be assumed by the method of interpolation. With this matter, the difference between $U_{50\%}$ of 5cm and 10cm sphere-gap in the standard may be in a doubt.

The conclusion, the uncertainty of 5cm and 10cm diameter sphere-gap may be increased and the ability to use this standard value in purpose calibration or for checking the measuring device is in a doubt, especially for small gap spacing.

REFERENCES

[1] *IEC 60071-1 "Insulation Co-ordination" Part 1*, 2006.

[2] *IEEE Standard 4 "IEE Standard for High-Voltage Testing Techniques"*, 2013.

[3] *IEC 60060-1 "High voltage test techniques" Part 1: General definitions and test requirements*, 2000.

[4] W. Hauschild and E. Lemke, High-voltage test and measuring techniques, Heidelberg: Springer,, 2014, pp. 1 online resource (xxii, 505 pages). [Online]. Available: SpringerLink http://dx.doi.org/10.1007/978-3-642-45352-6 MIT Access Only.

[5] *IEC 60052-2002 "Voltage measurement by means of standard air gaps"*, 2002.

[6] *IEC 60060-2 "High-voltage test techniques" – Part 2: Measuring systems*, 2010.

[7] F. Peek, "The sphere gap as a means of measuring high voltage," *Transactions of the American Institute of Electrical Engineers*, vol. 33, no. 1, pp. 923-949, 1914.

[8] E. Kuffel, "Influence of humidity on the breakdown voltage of sphere-gaps and uniform-field gaps," *Proceedings of the IEE-Part A: Power Engineering*, vol. 108, no. 40, pp. 295-301, 1961.

[9] D. Gourgoulis, P. Mikropoulos, and C. Stassinopoulos, "Sparkover voltage of sphere gaps under standard lightning and switching impulse voltages," *IEE Proceedings-Science, Measurement and Technology*, vol. 143, no. 3, pp. 187-194, 1996.

[10] D. Gourgoulis and C. Stassinopoulos, "Influence of irradiation on impulse breakdown of sphere gaps and sphere–rod gaps," *IEE Proceedings-Science, Measurement and Technology*, vol. 145, no. 4, pp. 147-151, 1998.

[11] O. Fujii, T. Hayakawa Student, Y. Mizuno, and K. Naito, "Evaluation of Humidity Correction Factor of Disruptive Discharge Voltage of Standard Sphere Air Gaps," *IEEJ Transactions on Electrical and Electronic Engineering*, vol. 3, no. 1, pp. 100-105, 2008.

[12] Y. Mizuno, M. Masuda, O. Fujii, and K. Naito, "Effect of absolute humidity on disruptive discharge voltage of standard sphere air gaps," in *Electrical Insulation and Dielectric Phenomena (CEIDP), 2010 Annual Report Conference on*, 2010, pp. 1-4: IEEE.

[13] J. Li, Z. Peng, and X. Yang, "Potential calculation and grading ring design for ceramic insulators in 1000 kV UHV substations," *IEEE Transactions on Dielectrics and Electrical Insulation*, vol. 19, no. 2, 2012.

[14] S. Gutiérrez, I. Sancho, L. Fontán, and M. Martínez-Iturralde, "Influence of irregularities within electric fields in high voltage cables," in *Electrical Insulation and Dielectric Phenomena (CEIDP), 2011 Annual Report Conference on*, 2011, pp. 752-755: IEEE.

[15] L. Xie, J. Zheng, Z. Li, W. Dong, K. P. Zha, and G. Tang, "Optimization of grading ring design for a new UHV equipotential shielding capacitor voltage transformer," in *Electrical Insulation and Dielectric Phenomena (CEIDP), 2011 Annual Report Conference on*, 2011, pp. 748-751: IEEE.

[16] S. M. Kumar and L. Kalaivani, "Electric field distribution analysis of 110 kV composite insulator using Finite Element Modeling," in *Circuit, Power and Computing Technologies (ICCPCT), 2014 International Conference on*, 2014, pp. 136-141: IEEE.

[17] GID. (2017). *GID reference manual*. Available: https://www.gidhome.com/cgi-bin/referencemanual/PREPROCESSING/Mesh+Menu/Unstructured

[18] ElmerSolver. *Elmer user manual*. Available: https://www.csc.fi/web/elmer-/documentation

[19] S. T. More and R. Bindu, "Effect of Mesh Size on Finite Element Analysis of Plate Structure," 2015.

[20] A. Dutt, "Effect of Mesh Size on Finite Element Analysis of Beam," *SSRG International Journal of Mechanical Engineering (SSRG-IJME)*, vol. 2, no. 12, p. 8, 2015.

[21] M. MICHELARAKIS, "Electric field distribution of sphere-plane gaps," Master Master Thesis project, KTH School of Electrical Engineering, KTH Royal Institute OF Technology, 2016.

[22] E. Kuffel, W. S. Zaengl, and J. Kuffel, *High voltage engineering : fundamentals*, 2nd ed. Oxford ; Boston: Butterworth-Heinemann, 2000, pp. xiii, 239 p.

[23] A. Maglaras and L. Maglaras, "Modeling and analysis of electric field distribution in air gaps, stressed by breakdown voltages," 2004.

[24] D. Gourgoulis and C. Stassinopoulos, "Spark breakdown of sphere gaps stressed by standard impulse voltages," *IEE Proceedings-Science, Measurement and Technology*, vol. 144, no. 6, pp. 273-279, 1997.

[25] K. Petcharaks, "Applicability of the Streamer Breakdown Criterion to Inhomogeneous Gas Gaps," PhD diss., ETH Zurich, ETH Zurich, 1995.

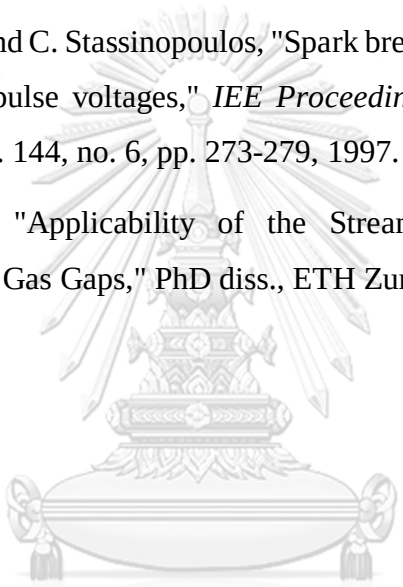

APPENDIX A

The code in MATLAB which is used to plot the breakdown probability curve, is describe as below:

Example for D=10cm, S=1.0cm of negative polarity under absolute humidity of 18g/m^3 and without irradiation

```
X = [45.01, 46.24, 46.99, 48.06, 49.82];              % Applied voltage
Y = [0, 10, 20, 30, 40];                              % Discharge frequency
fcn = @(b,x) normcdf(x, b(1), b(2));                  % Objective Function
NRCF = @(b) norm(Y/100 - fcn(b,X));            % Norm Residual Cost Function
B = fminsearch(NRCF, [40; 60]);                       % Estimate Parameters
Xplot = linspace(min(X)-15, max(X)+15);
Z = fcn(B,Xplot);
figure(1)
plot(X, Y/100,'xr', 'Linewidth', 2)
hold on
plot(Xplot, Z, 'k', 'Linewidth', 1)
hold off
grid on,
grid minor
title({'Cumulative Normal Distribution'...
    '10cm sphere with 1.5cm gap spacing (positive polarity) in 18 g/m^3 absolute
humidity'}, 'FontName', 'Calibri', 'FontSize', 12)
xlabel('Voltage (kV)')
ylabel('Discharge frequency')
text(46, 0.65, sprintf('\\mu = %.2f\n\\sigma = %.2f', B))
```

From the above code, the $U_{50\%}$ disruptive discharge voltage and the standard deviation (σ) of the breakdown probability curve are shown and computed (i.e. D=10cm, S=1.5cm of positive polarity under 18g/m^3 of absolute humidity):

In the following breakdown probability curve, the μ is the 50% disruptive discharge voltage and σ is the standard deviation which is obtained from the equation: $\sigma = U_{50\%} - U_{16\%}$.

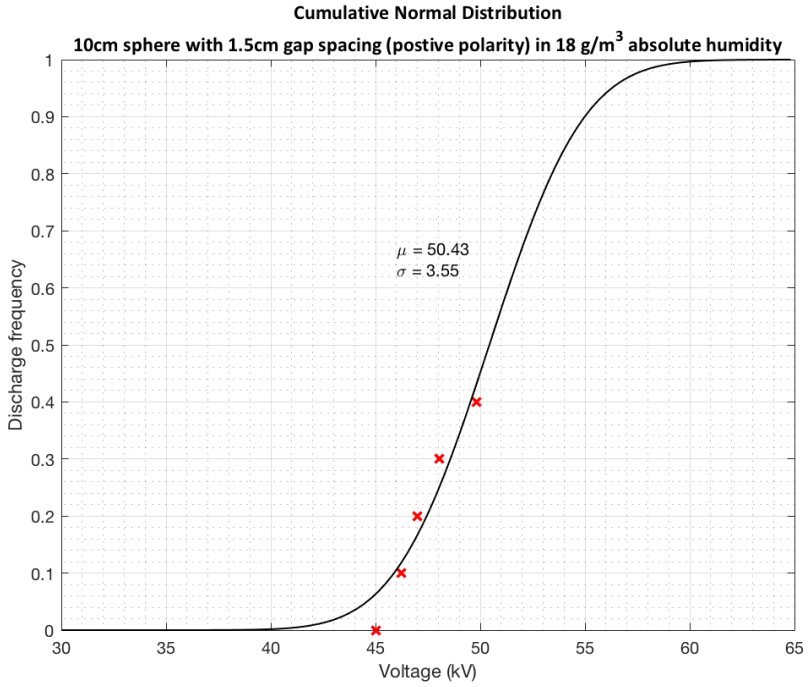

APPENDIX B

I. The breakdown probability curve of 5cm sphere for negative and positive polarity under various range of humidity:

1) Dry air:

a) Without irradiation

➢ S= 0.5cm (negative and positive LI)

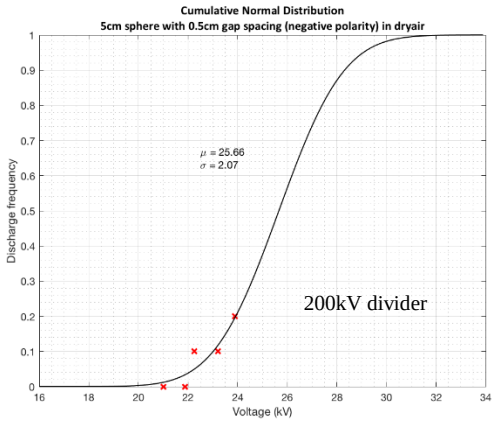

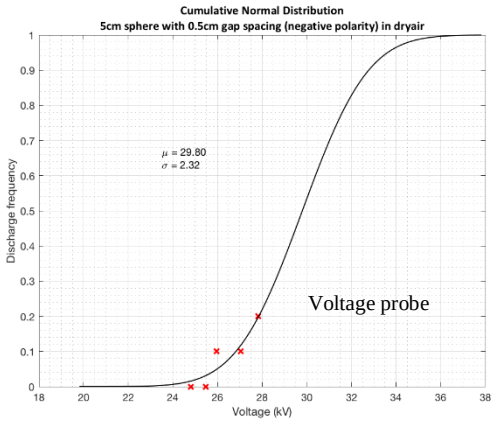

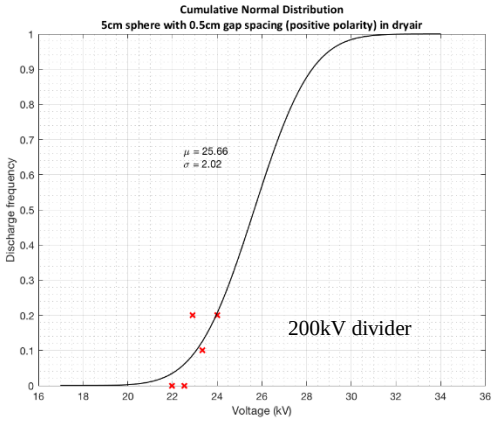

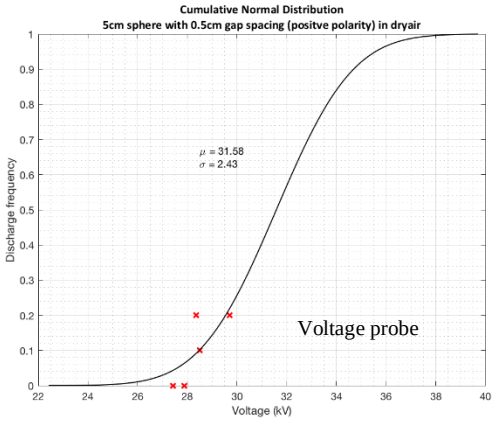

- S=1.0cm (negative and positive polarity)

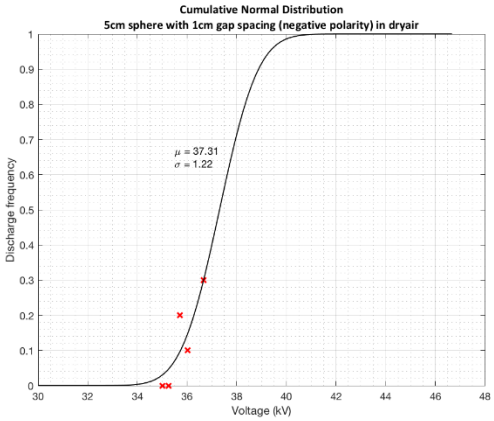

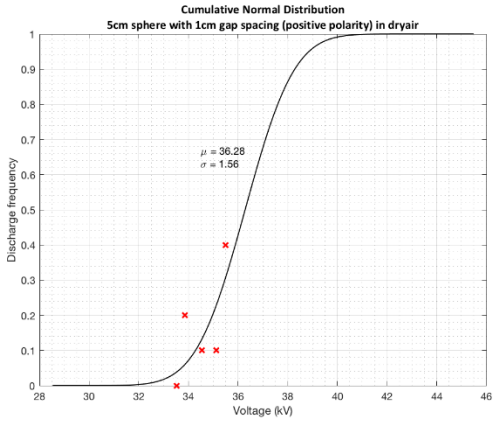

- S=1.5cm (negative and positive polarity)

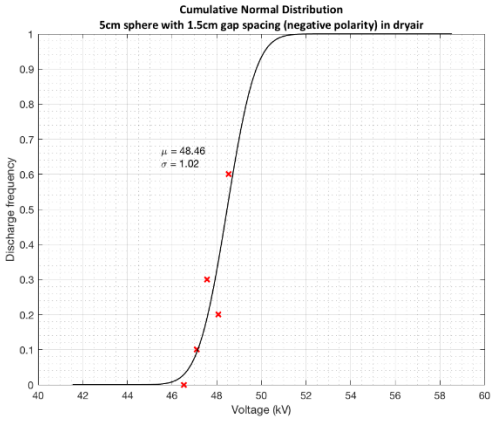

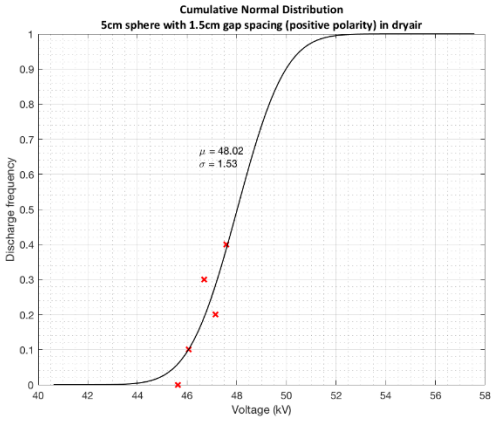

- S=2.0 (negative and positive polarity)

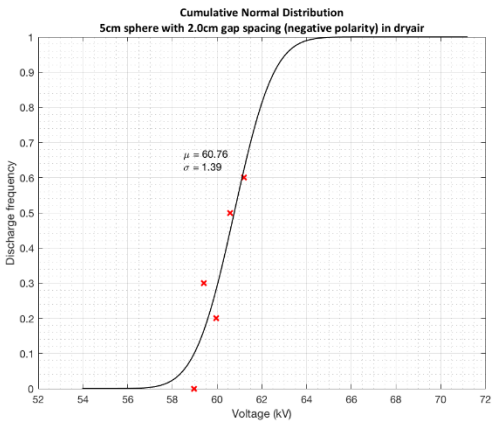

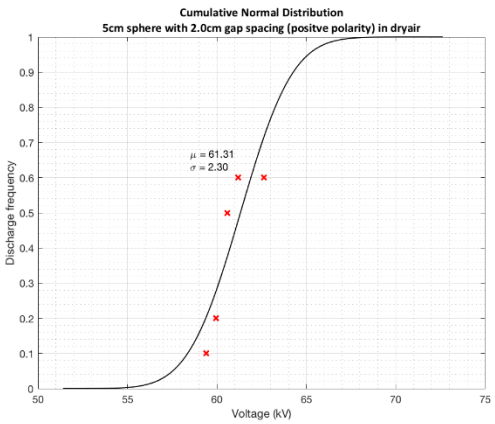

- S=2.4cm (negative and positive polarity)

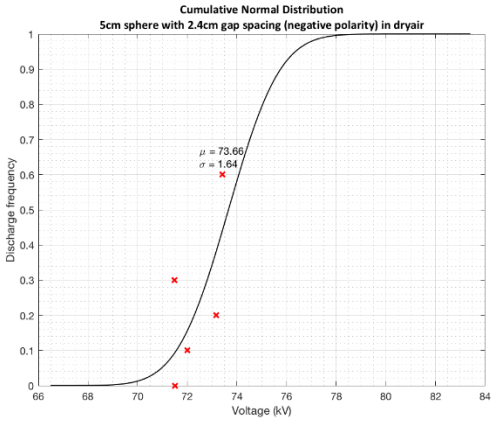

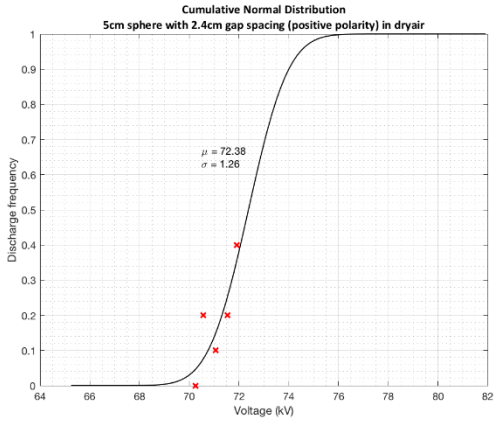

b) With irradiation

- S=0.5cm (negative and positive polarity)

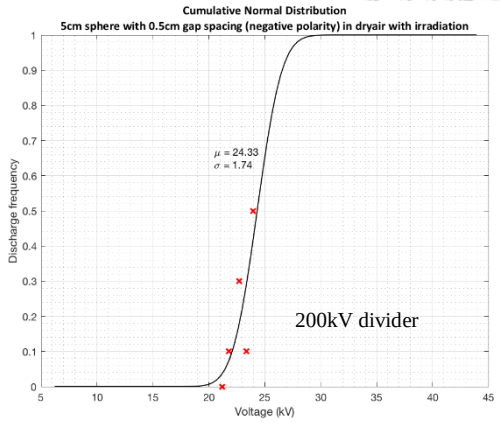

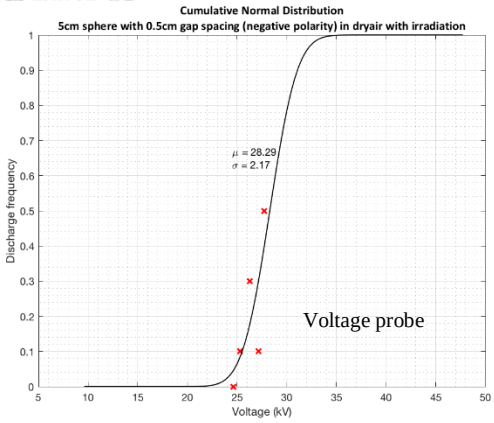

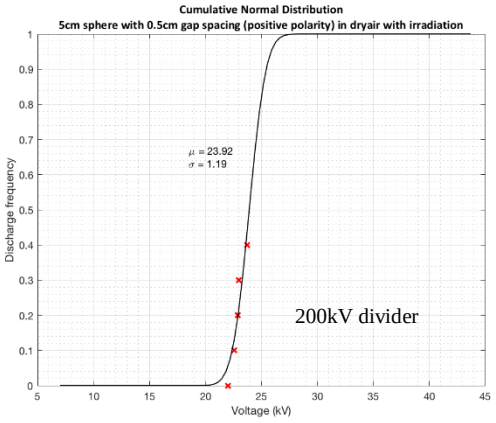

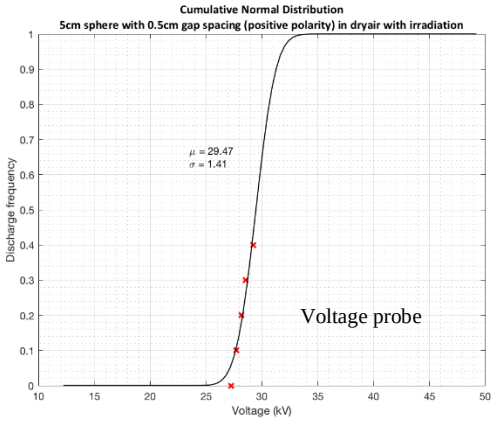

- S=1.0cm (negative and positive polarity)

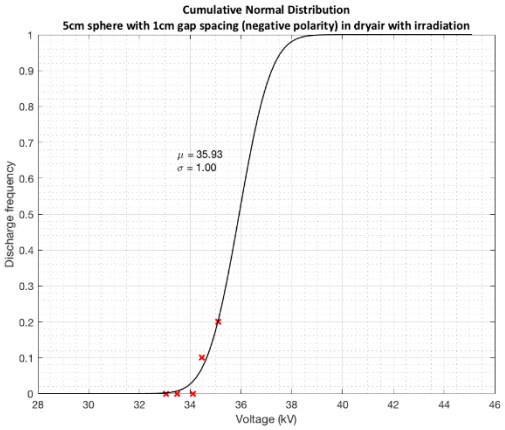

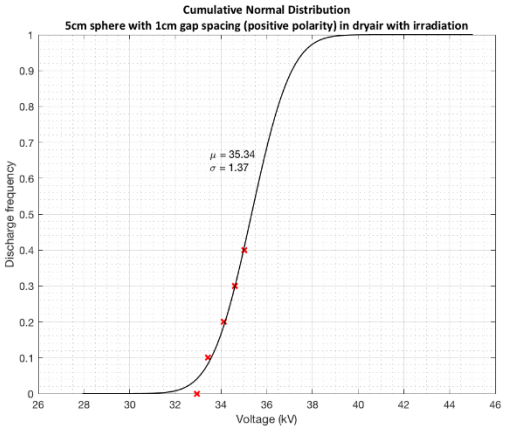

- S=1.5cm (negative and positive polarity)

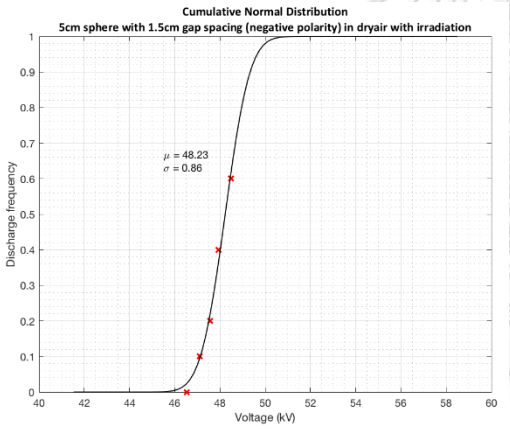

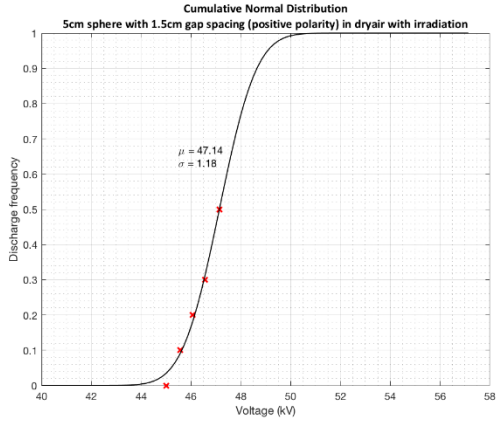

- S=2.0cm (negative and positive polarity)

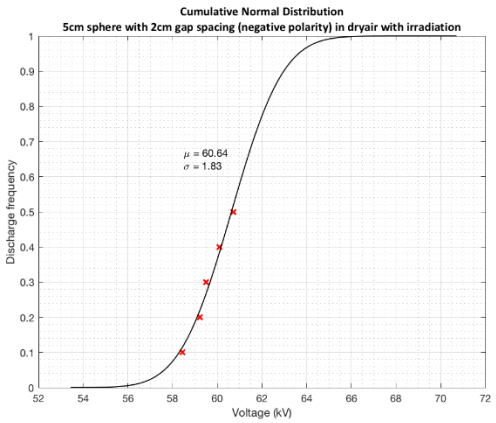

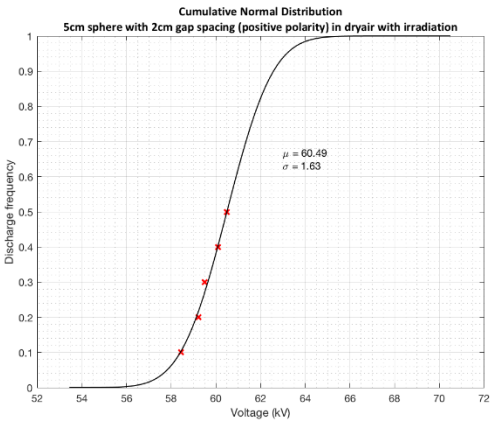

- S=2.4cm (negative and positive polarity)

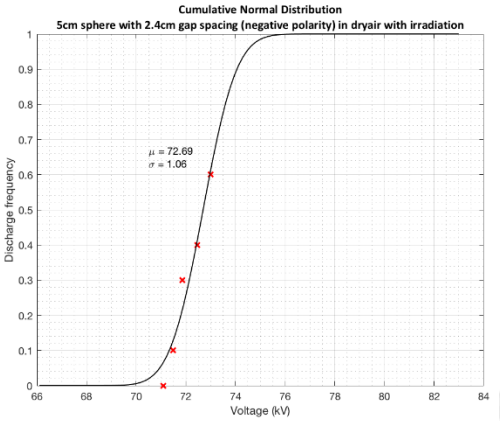

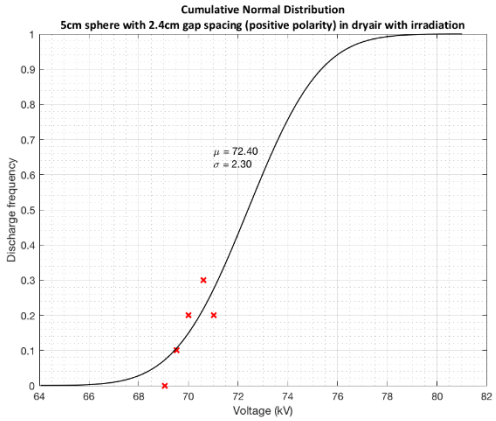

2) The absolute humidity of 10g/m^3

a) Without irradiation

- S=0.5cm (negative and positive polarity)

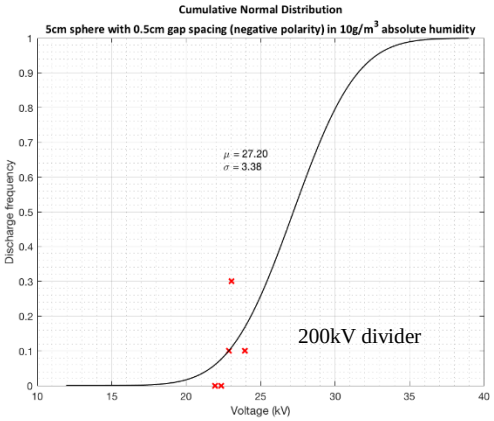

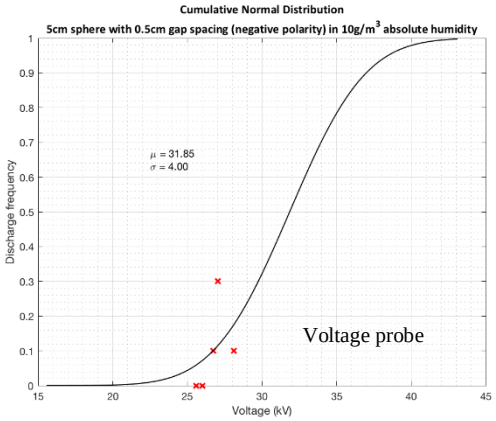

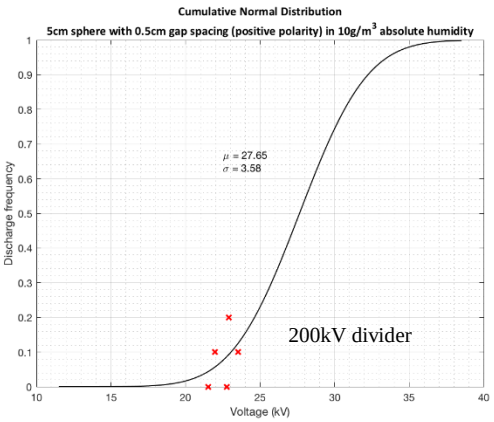

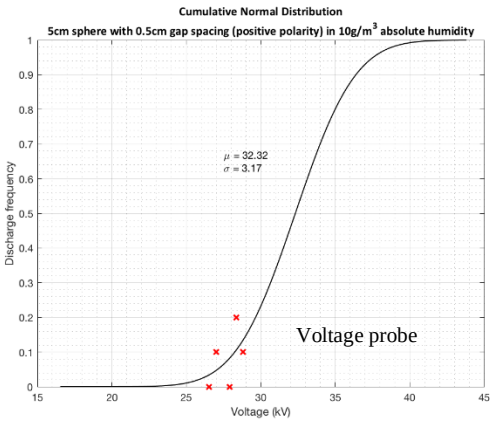

- S=1.0cm (negative and positive polarity)

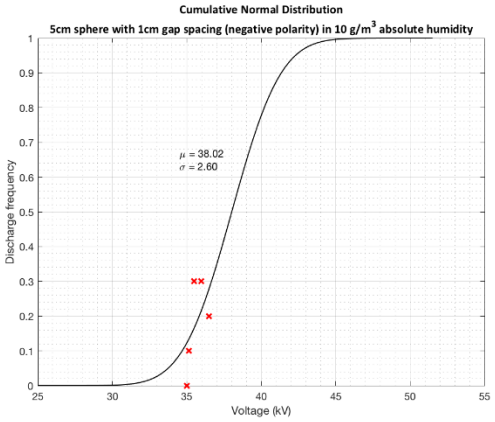

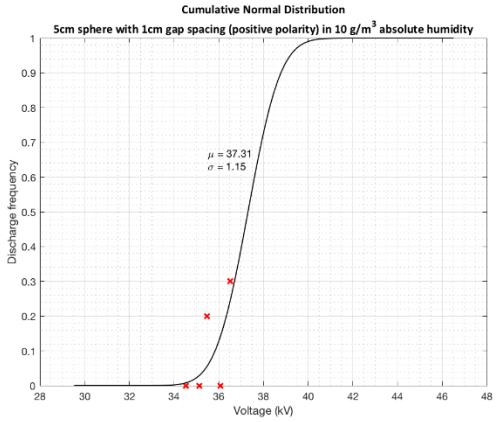

- S=1.5cm (negative and positive polarity)

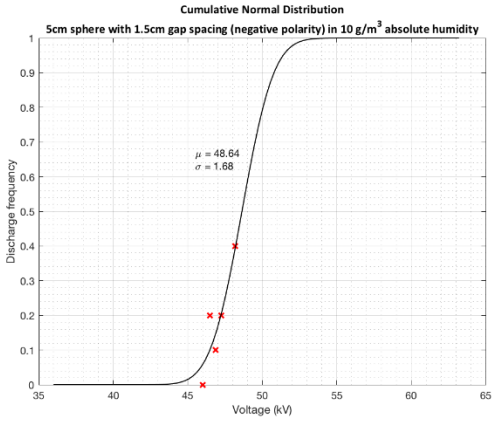

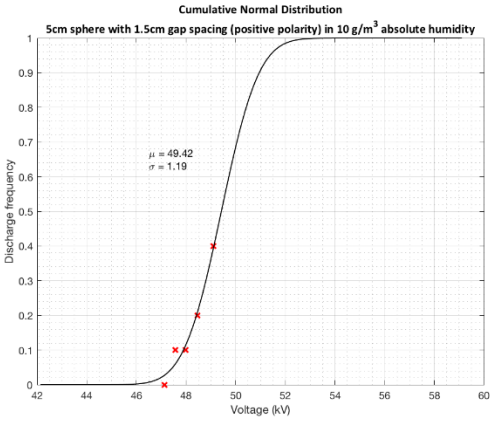

- S=2.0cm (negative and positive polarity)

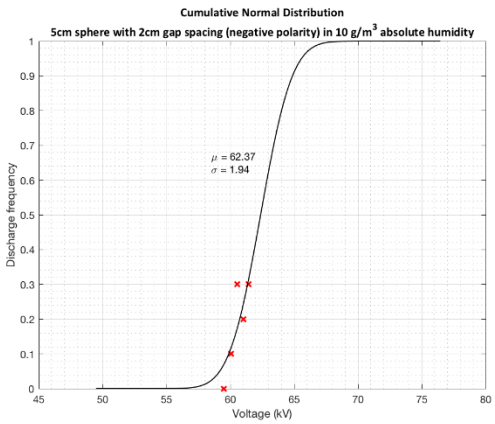

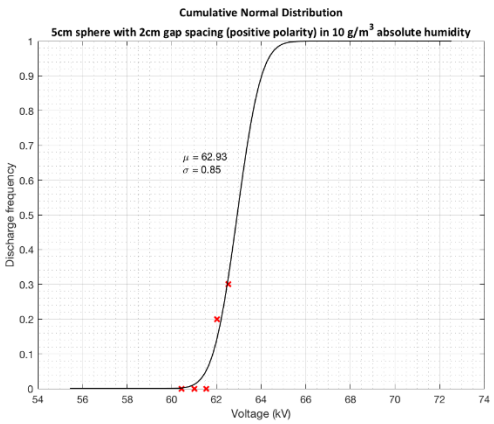

- S=2.4cm (negative and positive polarity)

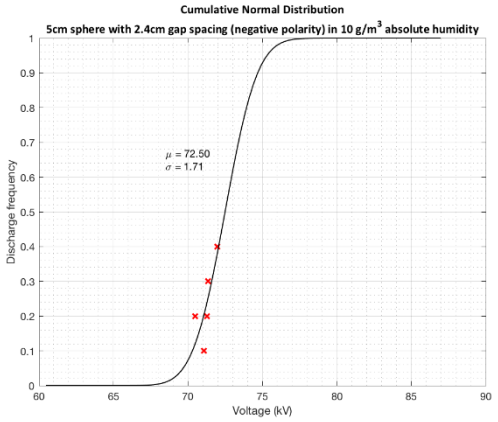

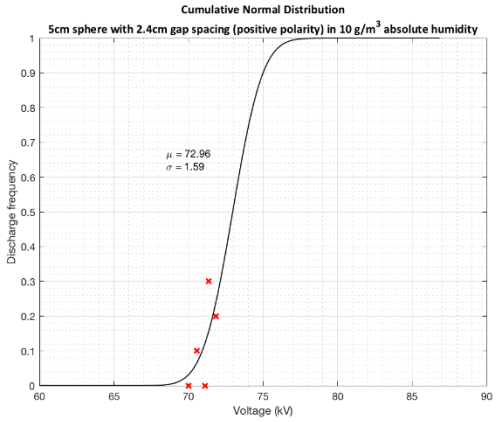

b) With irradiation

- S=0.5cm (negative and positive polarity)

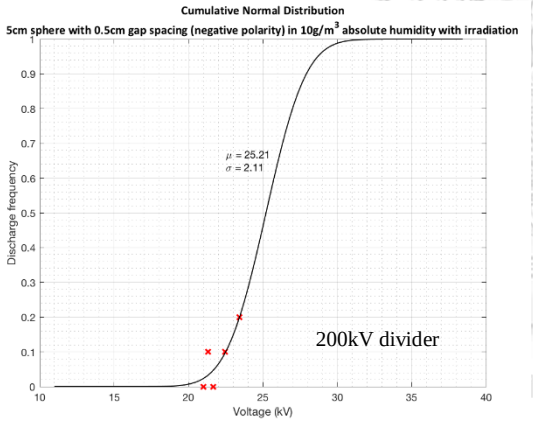

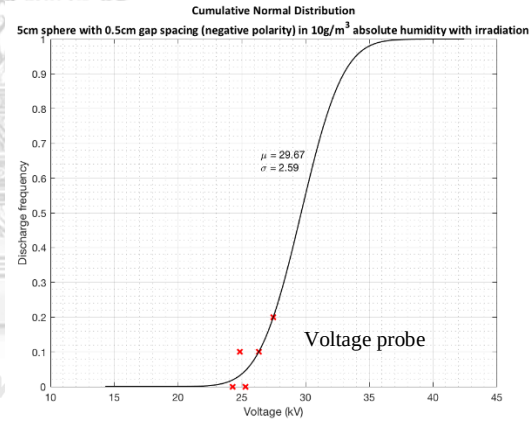

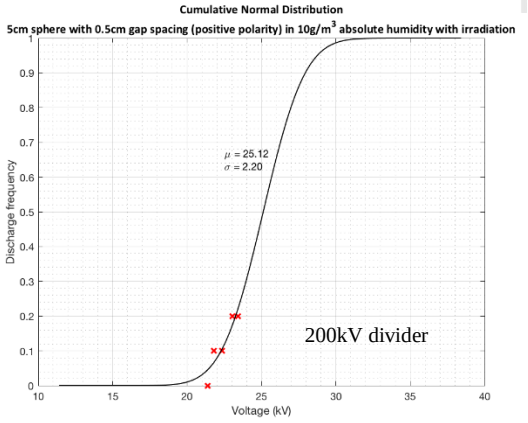

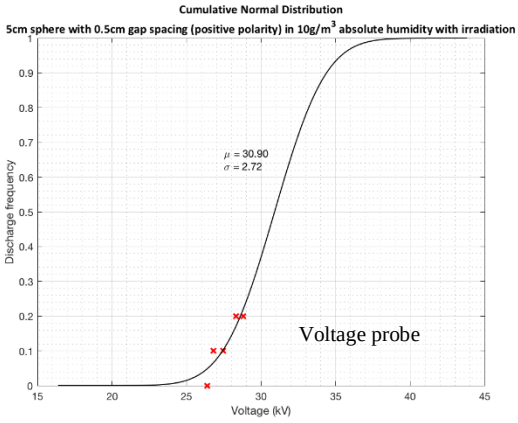

- S=1.0cm (negative and positive polarity)

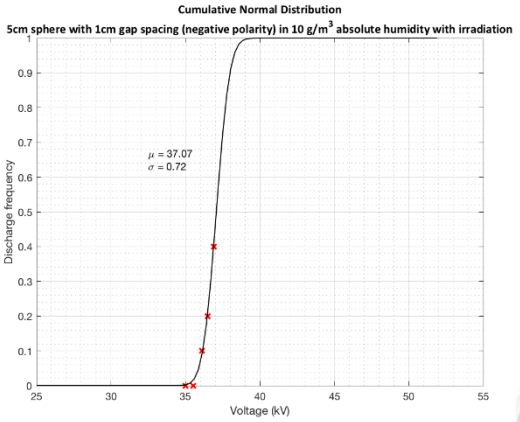

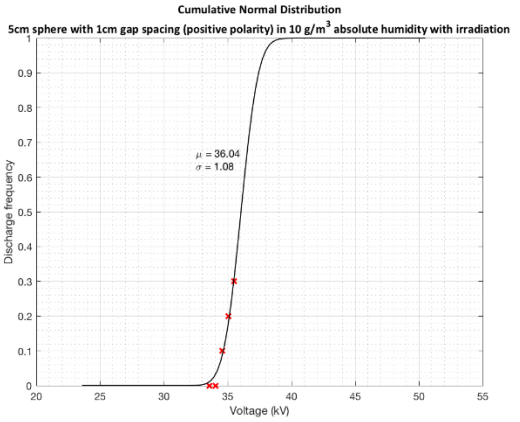

- S=1.5cm (negative and positive polarity)

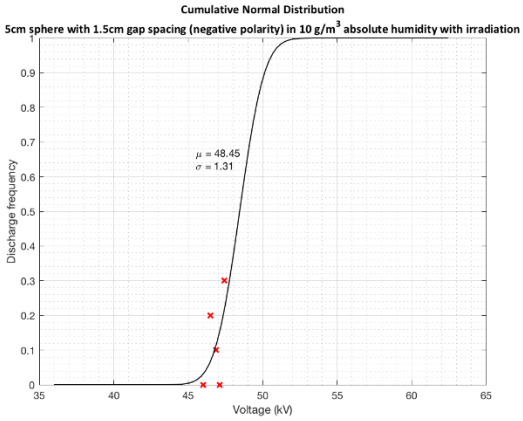

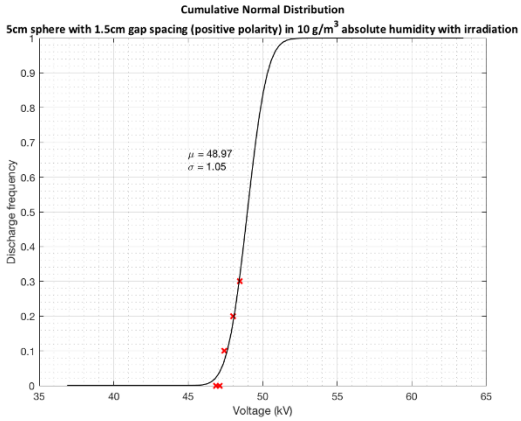

- S=2.0cm (negative and positive polarity)

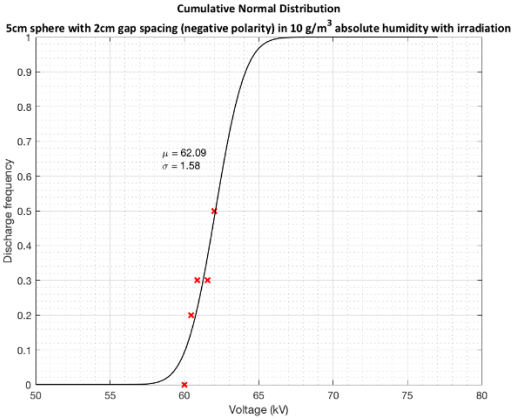

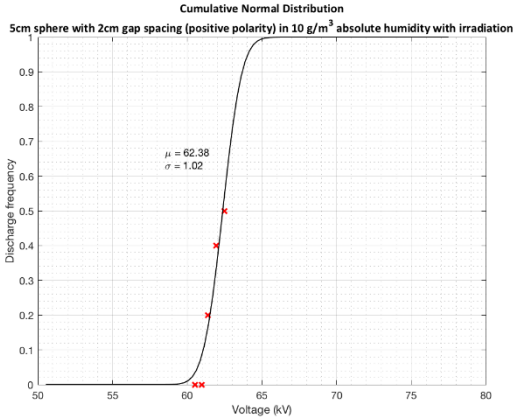

➢ S=2.4cm (negative and positive polarity)

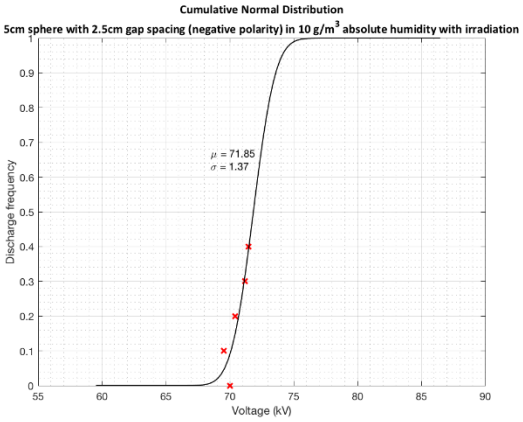

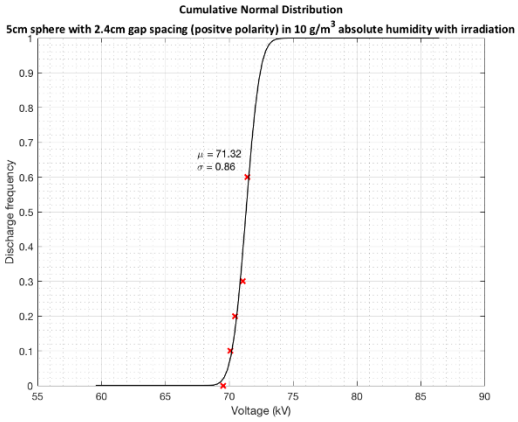

3) Absolute humidity of 18g/m^3

a) Without irradiation

➢ S=0.5cm (negative and positive polarity)

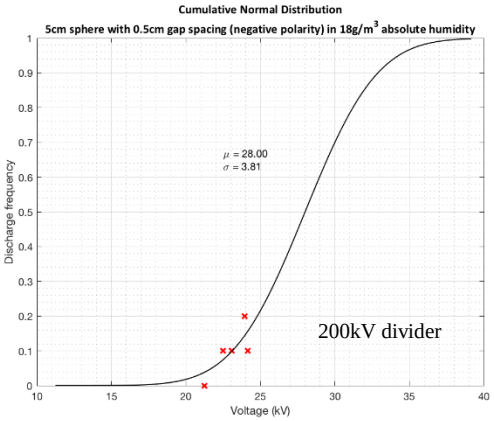

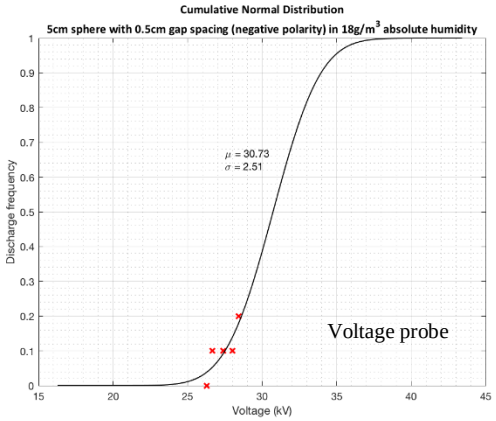

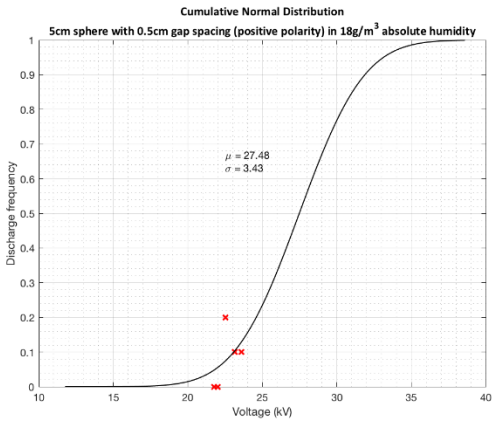

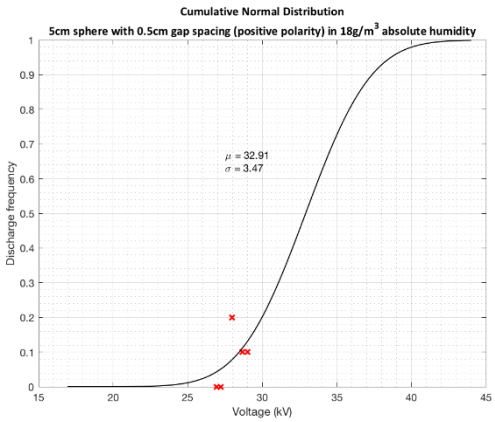

- S=1.0cm (negative and positive polarity)

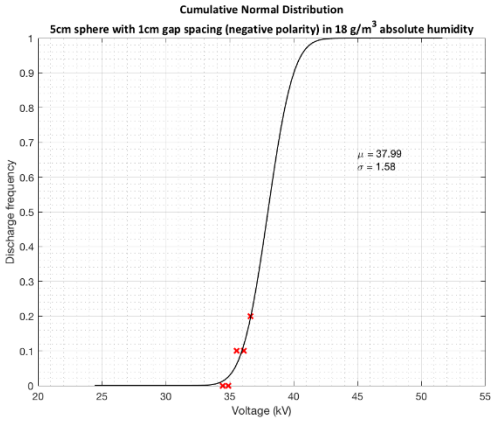

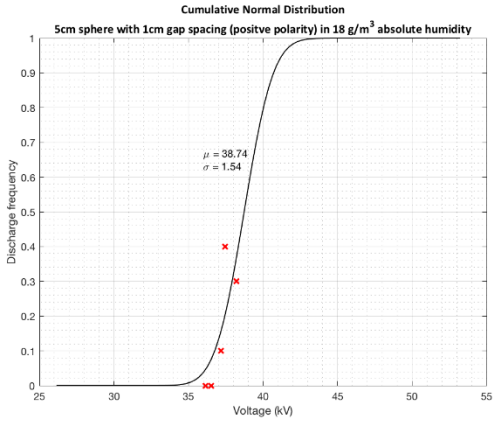

- S=1.5cm (negative and positive polarity)

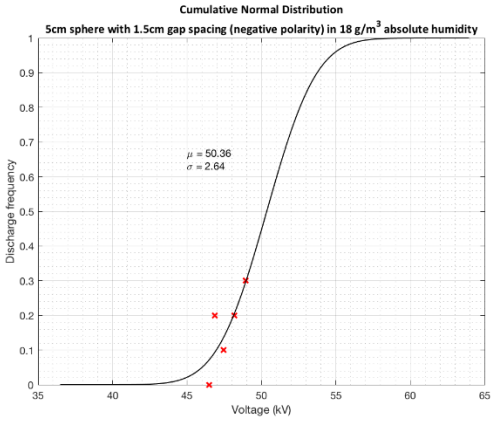

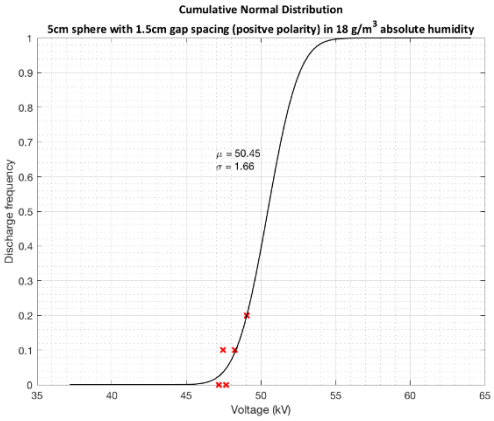

- S=2.0cm (negative and positive polarity)

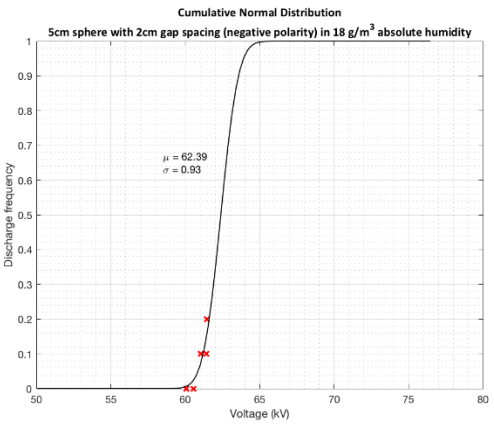

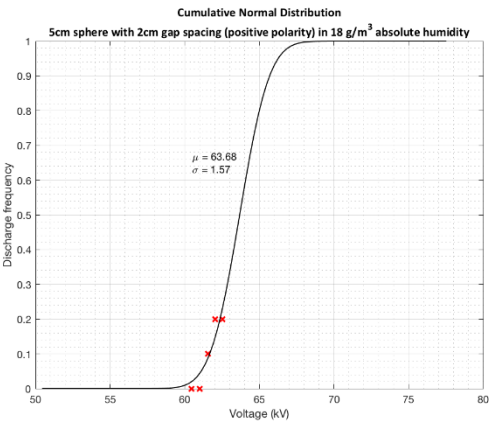

- S=2.4cm (negative and positive polarity)

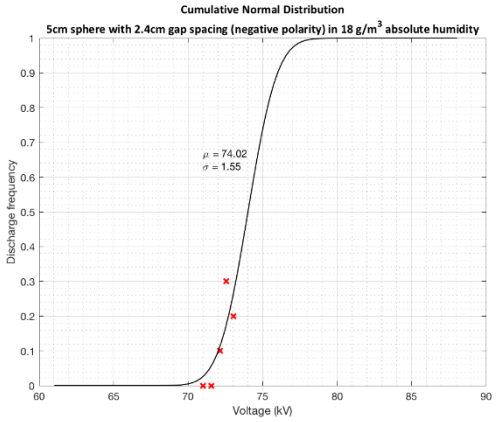

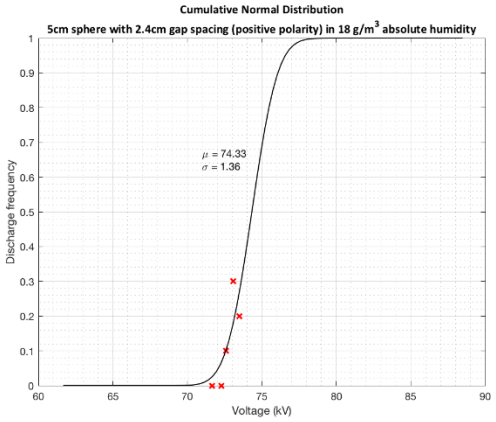

b) With irradiation

- S=0.5cm (negative and positive polarity)

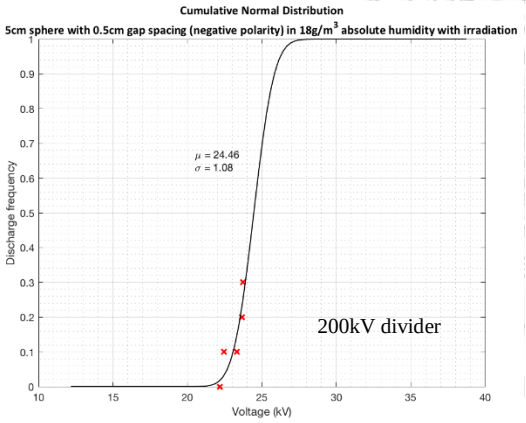

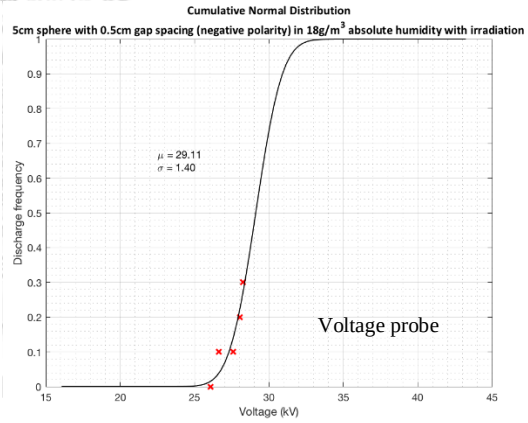

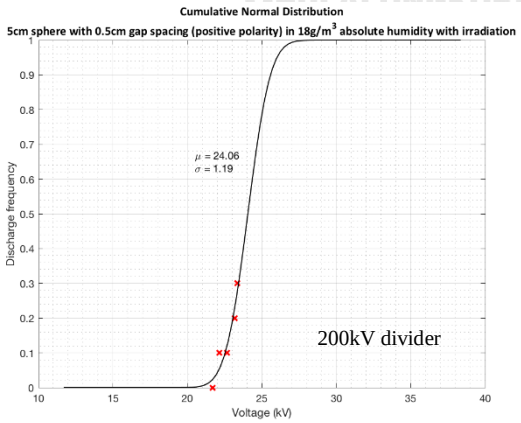

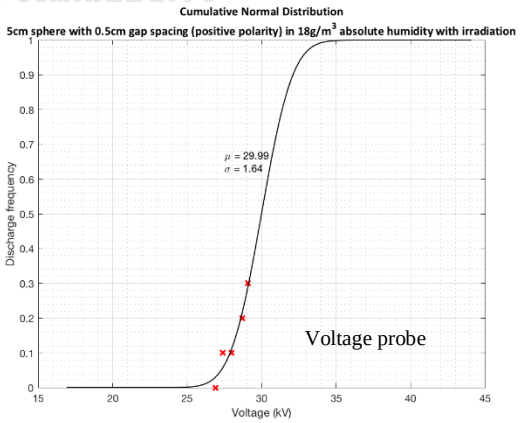

- S=1.0cm (negative and positive polarity)

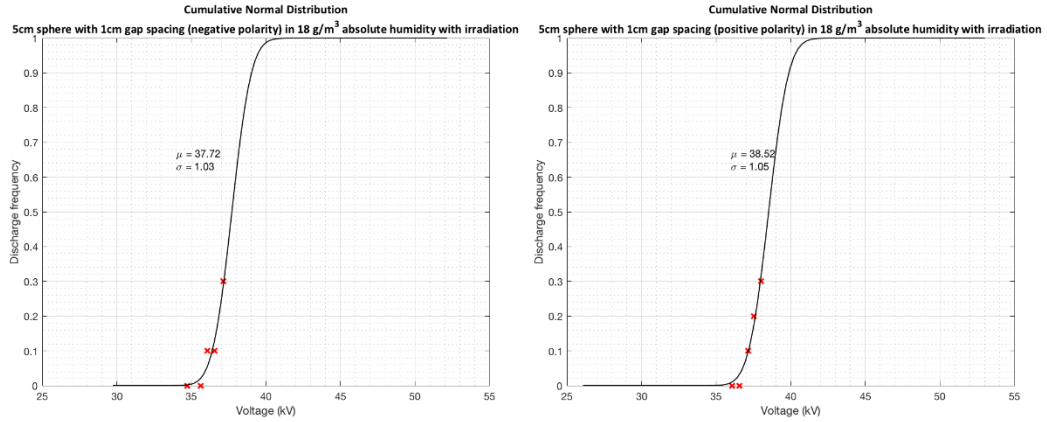

- S=1.5cm (negative and positive polarity)

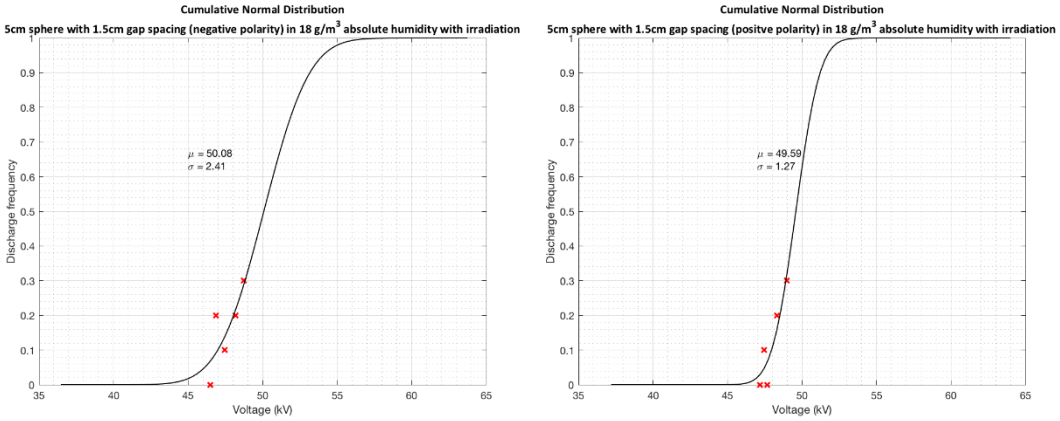

- S=2.0cm (negative and positive polarity)

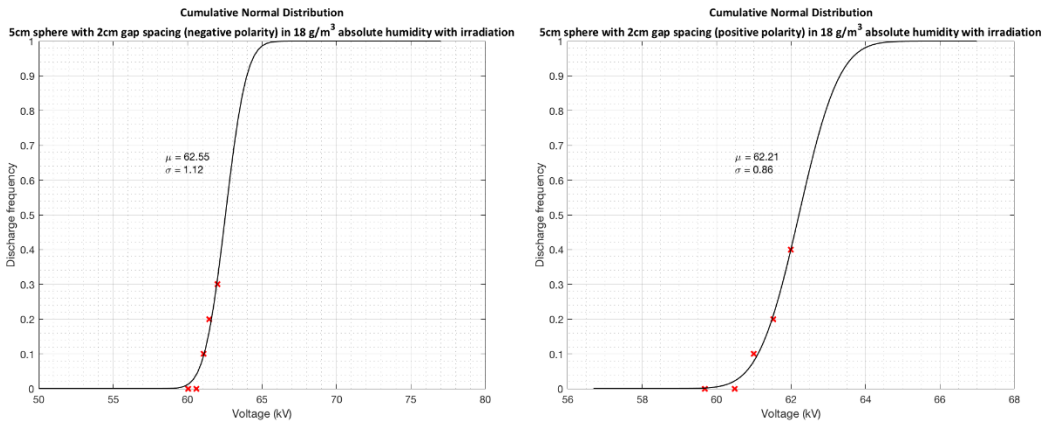

- S=2.4cm (negative and positive polarity)

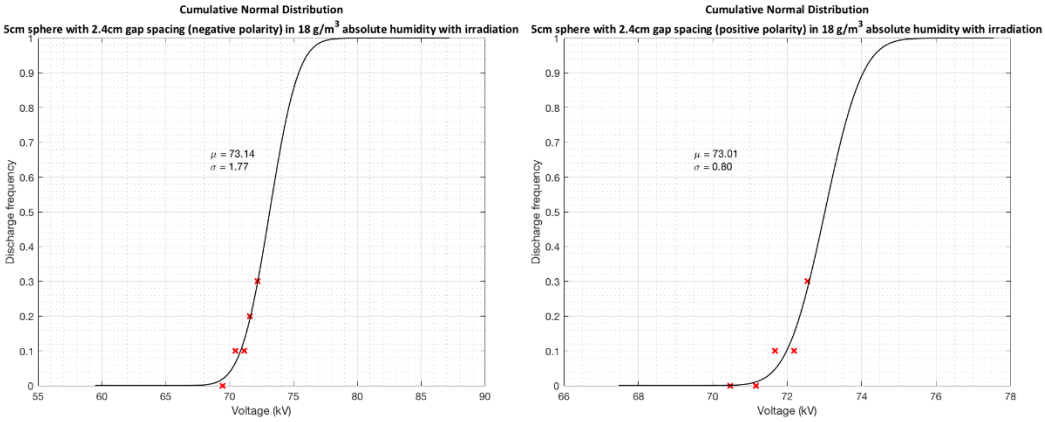

II. The breakdown probability curve of 10cm sphere for negative and positive polarity under various range of humidity:

1) Dry air

a) Without irradiation

- S=0.5cm (negative and positive polarity)

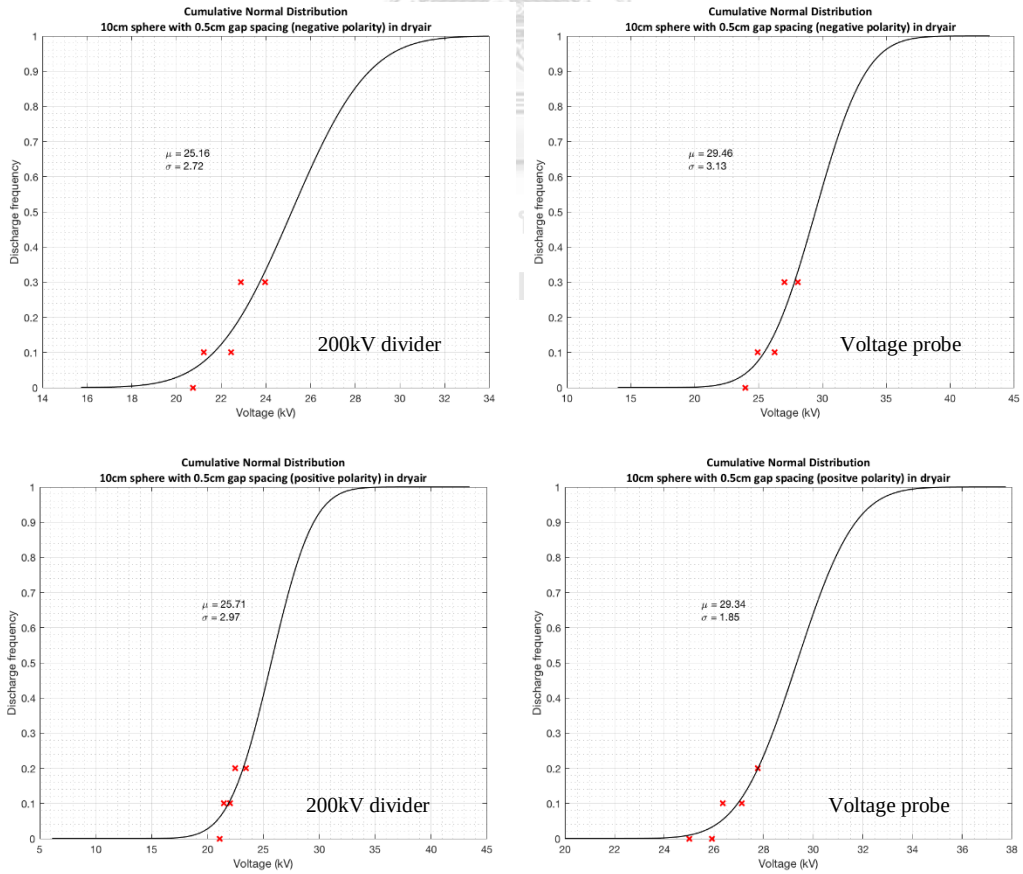

- S=1.0cm (negative and positive polarity)

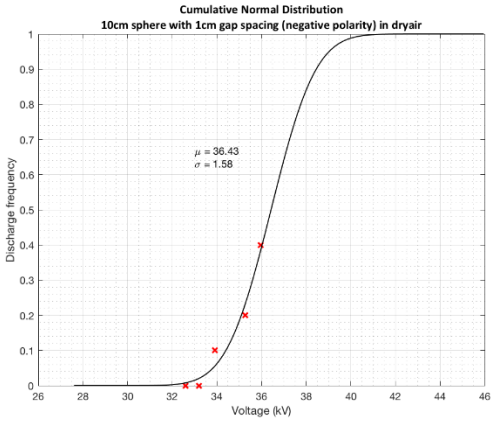

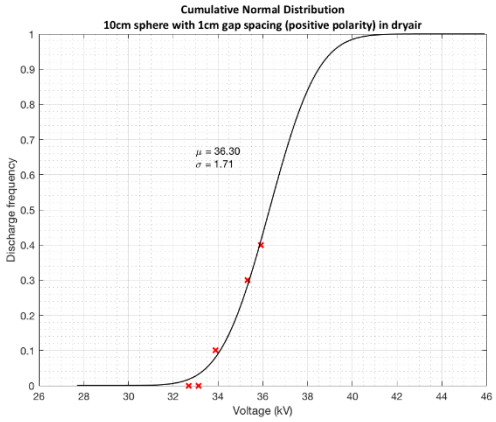

- S=1.5cm (negative and positive polarity)

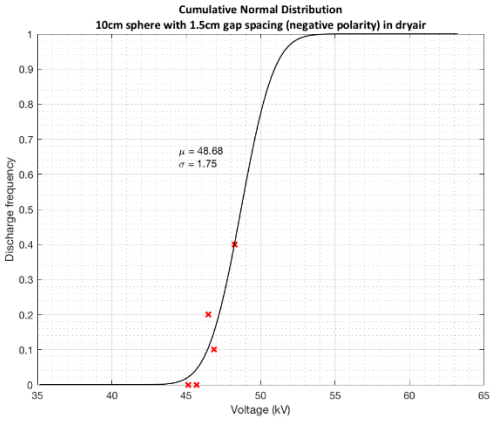

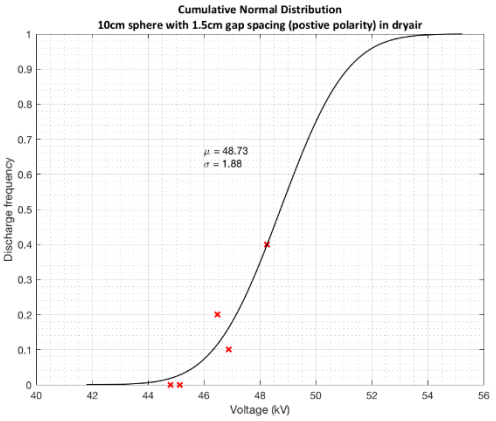

- S=2.0cm (negative and positive polarity)

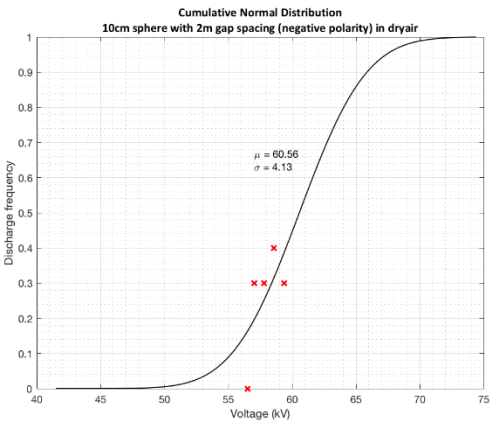

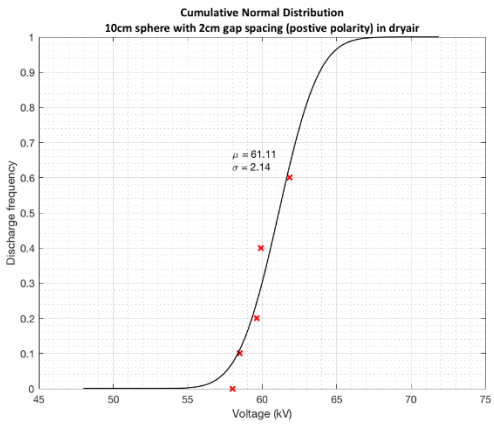

- S=2.4cm (negative and positive polarity)

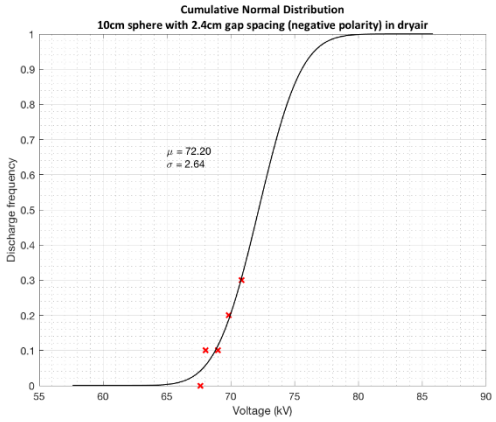

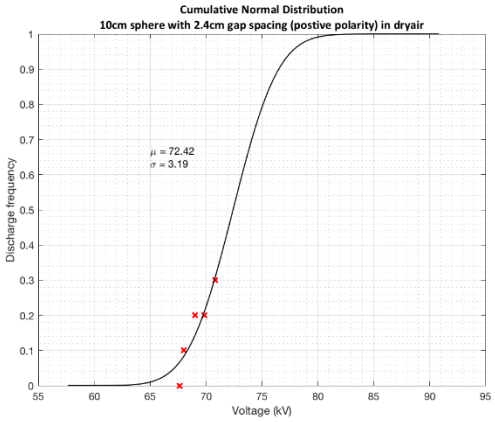

b) With irradiation

- S=0.5cm (negative and positive polarity)

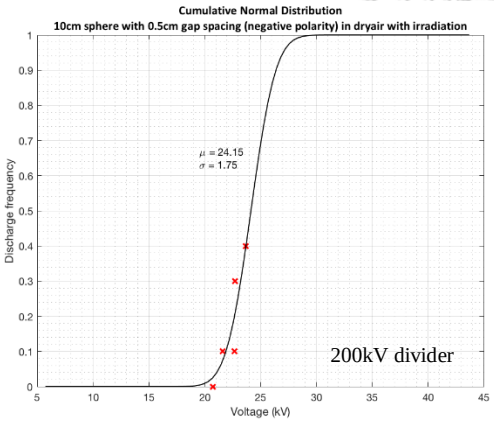

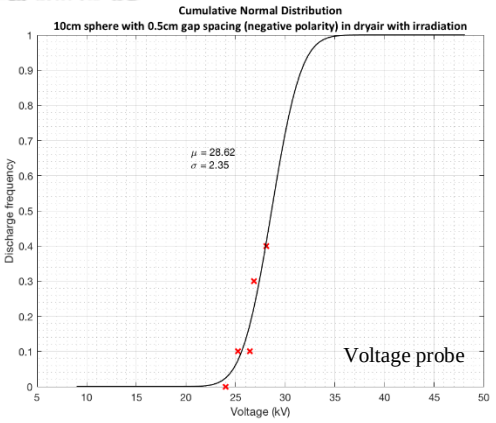

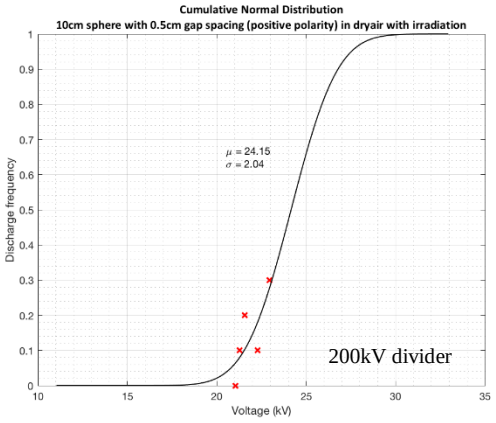

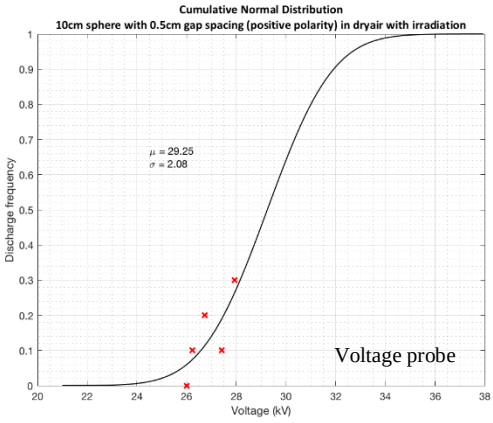

- S=1.0cm (negative and positive polarity)

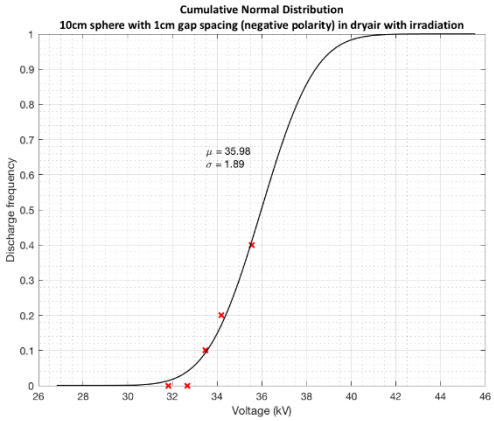

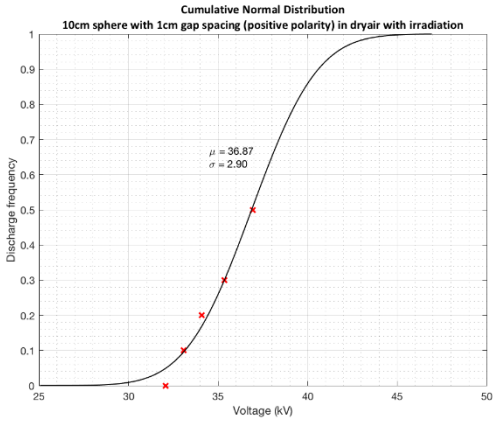

- S=1.5cm (negative and positive polarity)

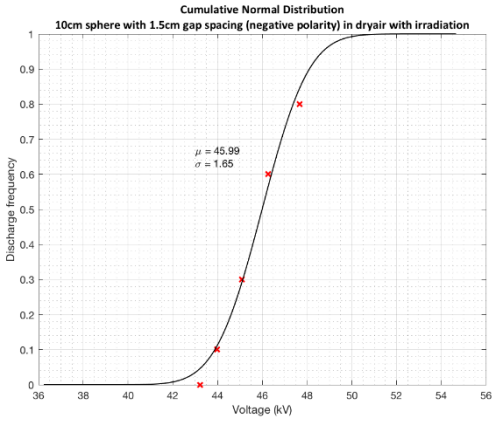

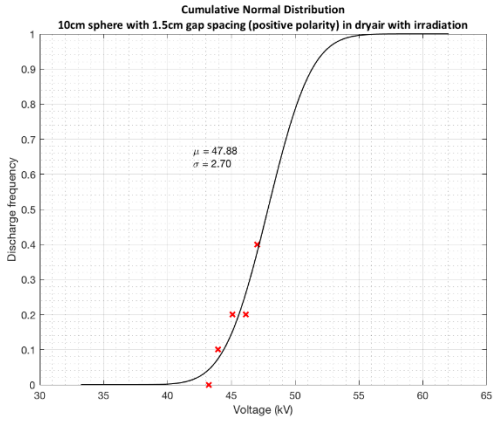

- S=2.0cm (negative and positive polarity)

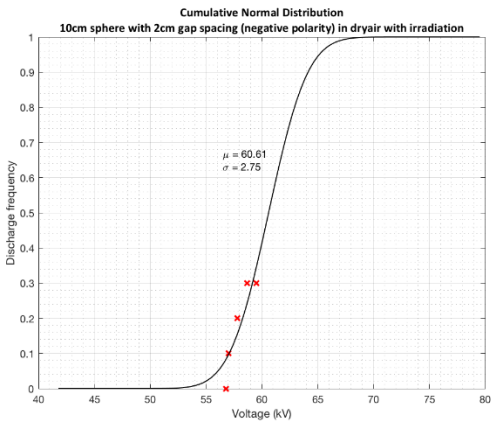

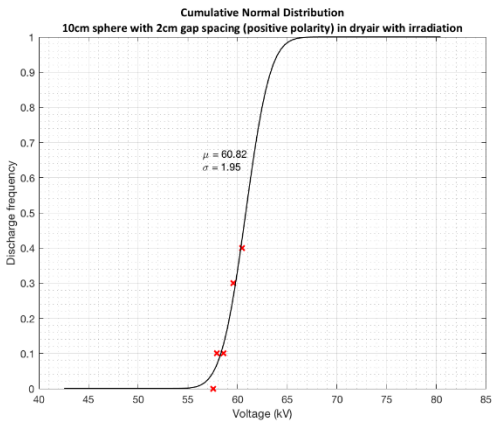

- S=2.4cm (negative and positive polarity)

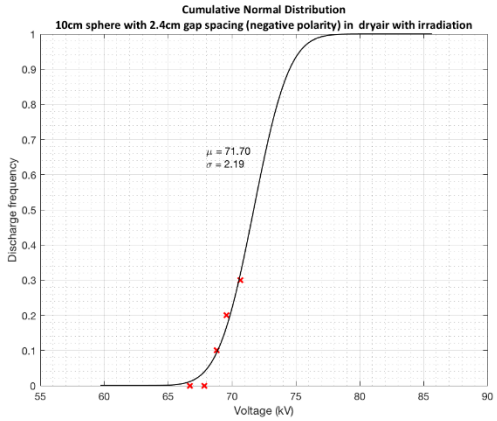

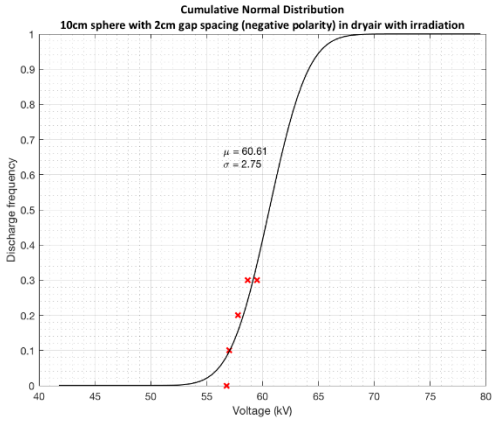

2) Absolute humidity of 10g/m^3

   a) Without irradiation

- S=0.5cm (negative and positive polarity)

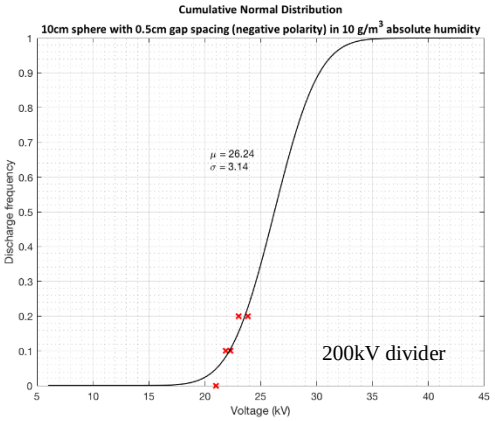

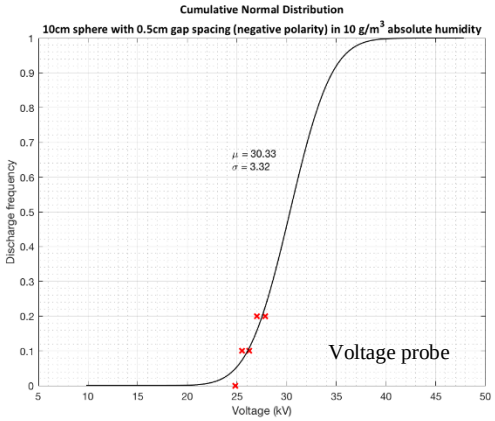

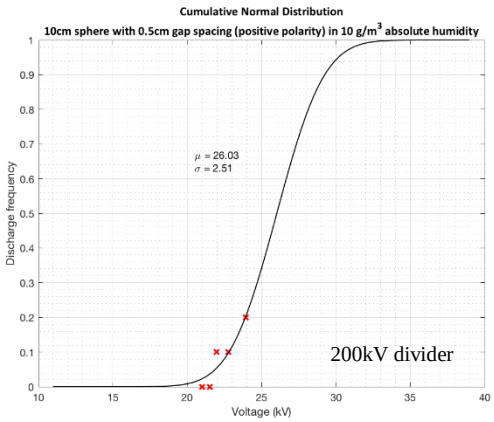

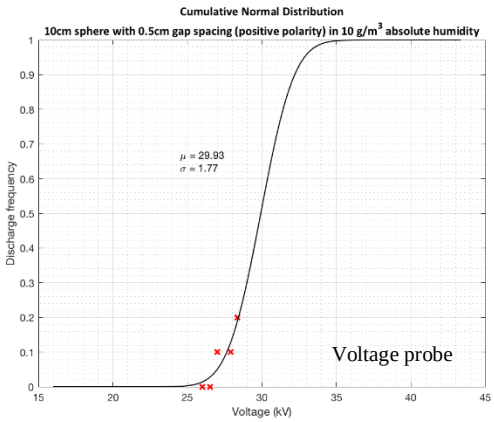

- S=1.0cm (negative and positive polarity)

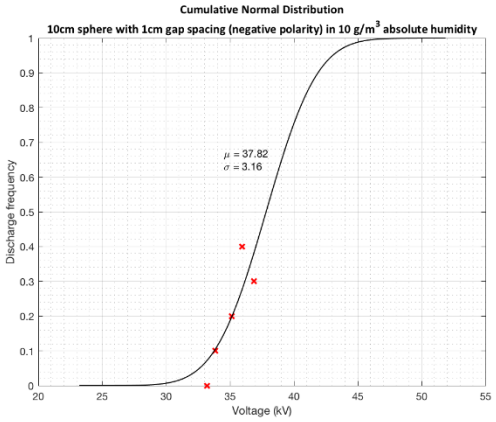

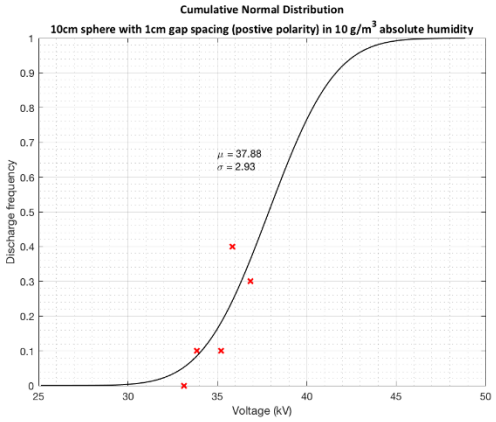

- S=1.5cm (negative and positive polarity)

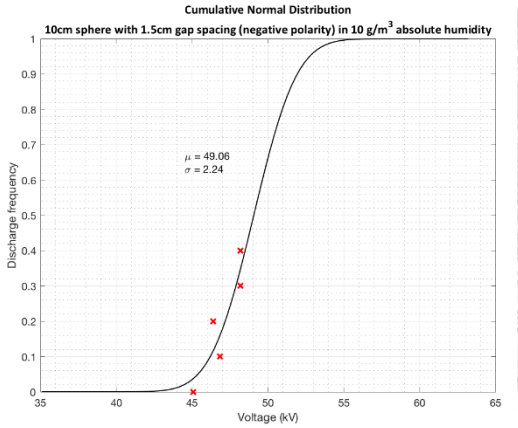

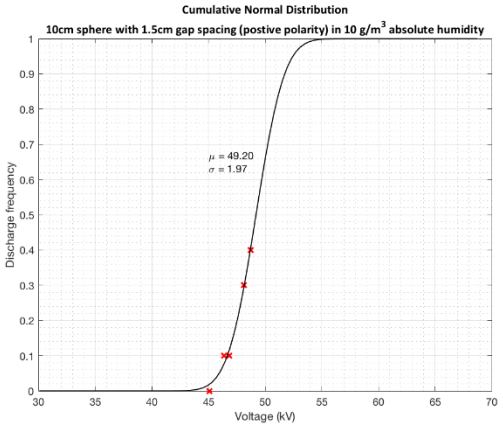

- S=2.0cm (negative and positive polarity)

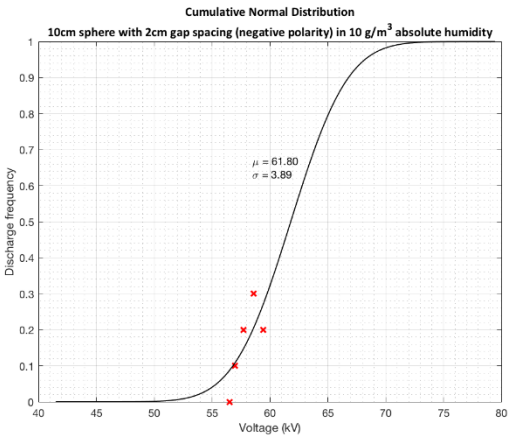

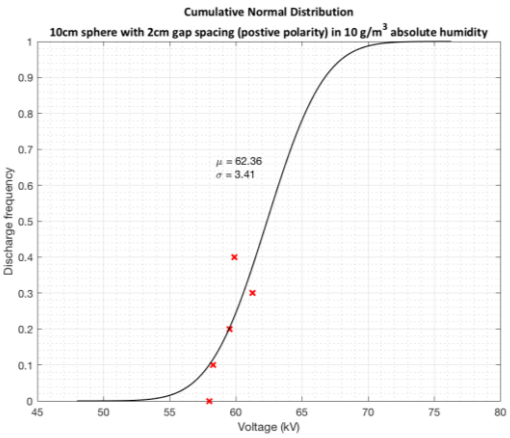

- S=2.4cm (negative and positive polarity)

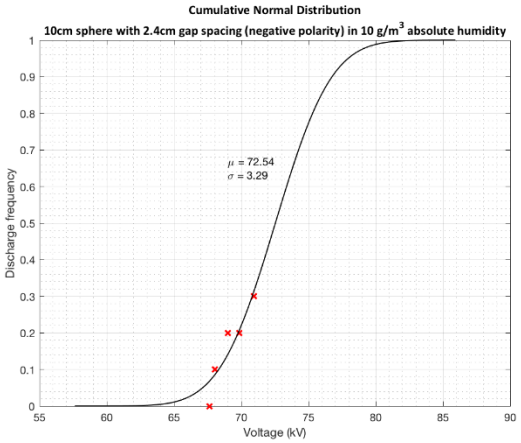

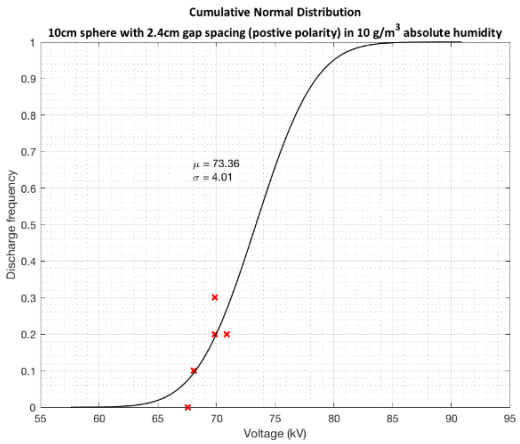

b) With irradiation

- S=0.5cm (negative and positive polarity)

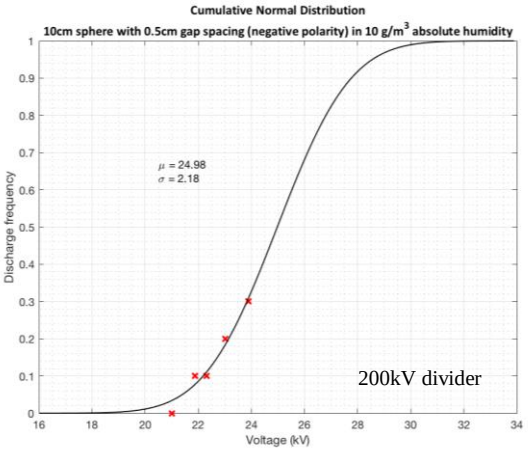

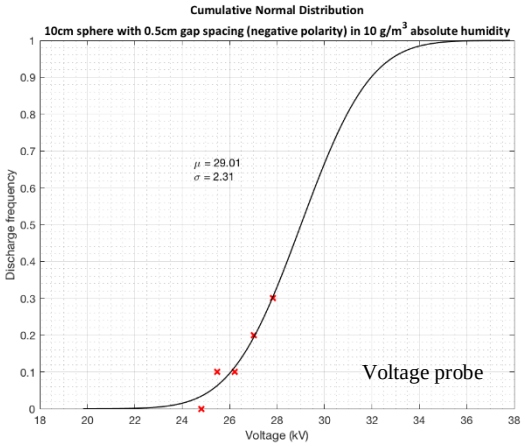

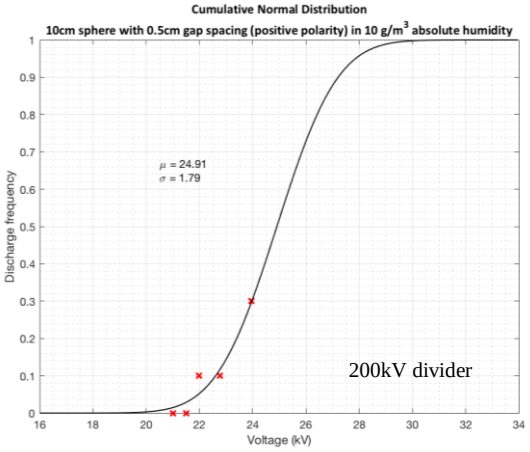

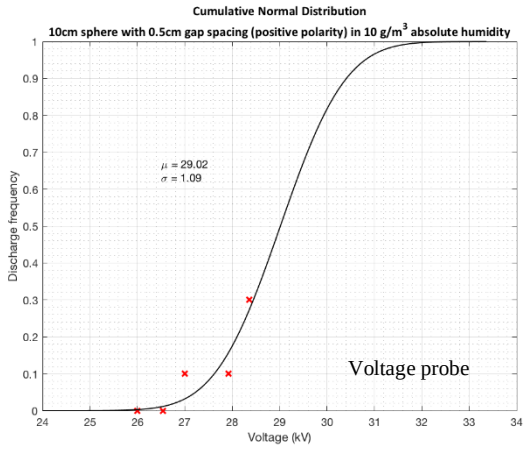

- S=1.0cm (negative and positive polarity)

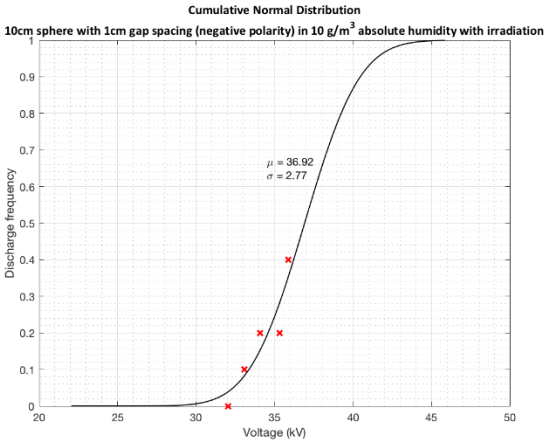

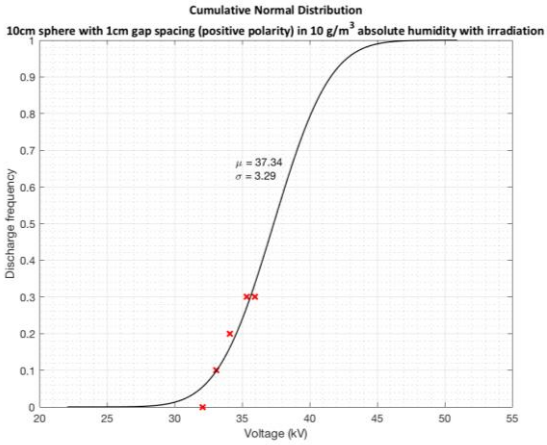

- S=1.5cm (negative and positive polarity)

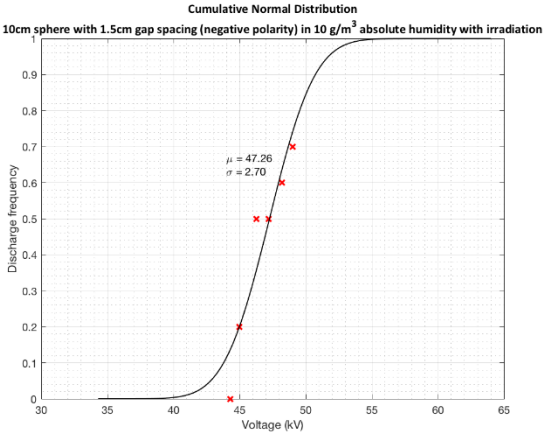

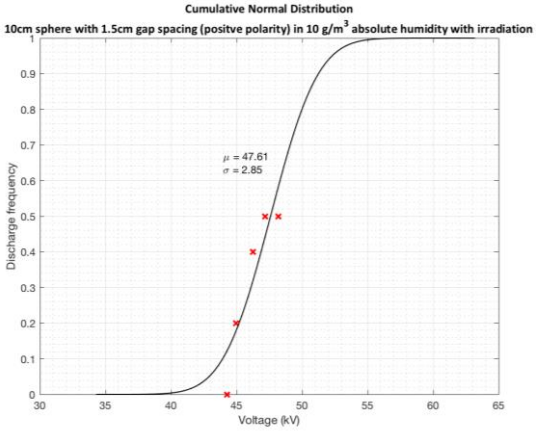

- S=2.0cm (negative and positive polarity)

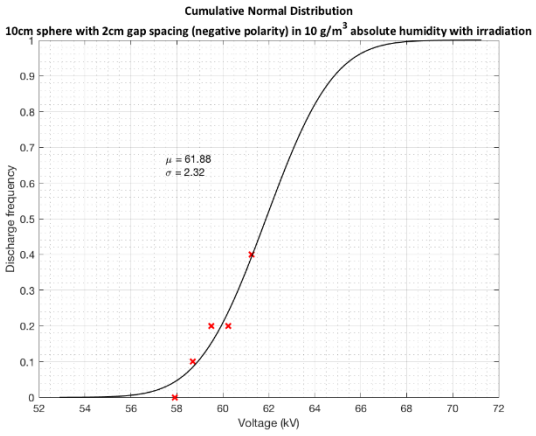

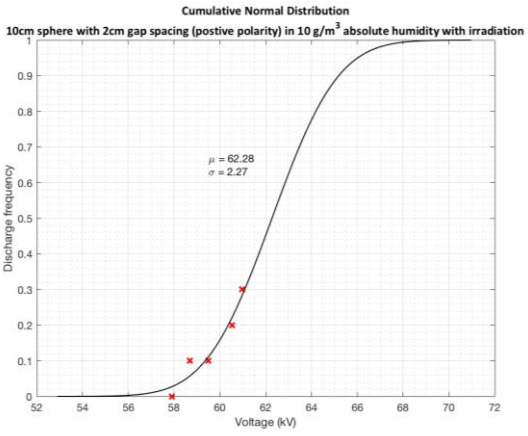

- S=2.4cm (negative and positive polarity)

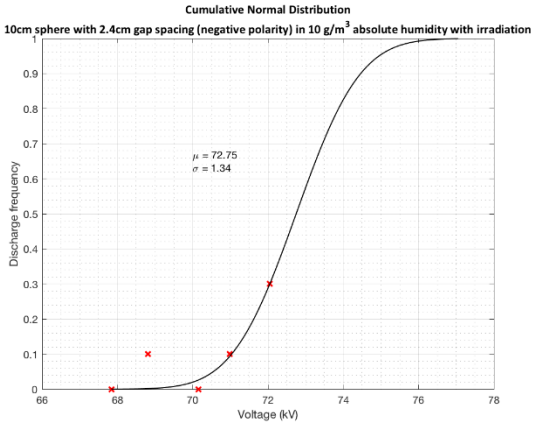

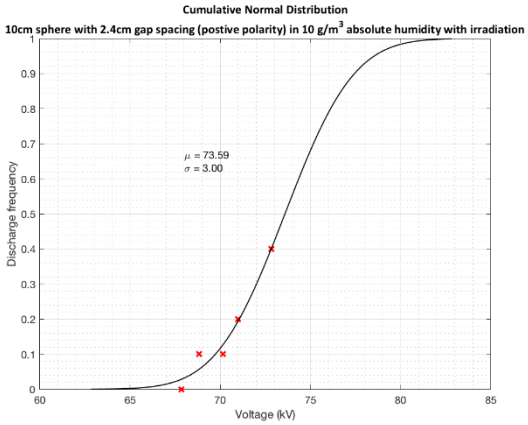

3) Absolute humidity of 18g/m^3

a) Without irradiation

- S=0.5cm (negative and positive polarity)

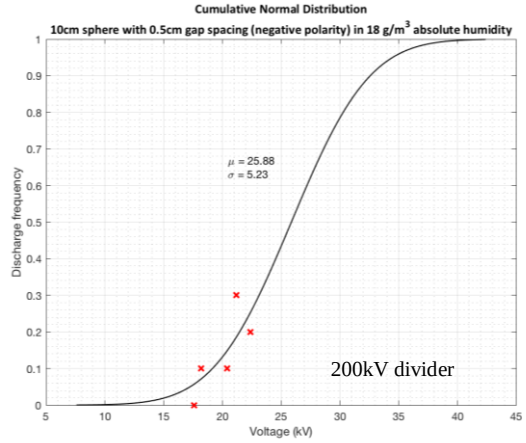

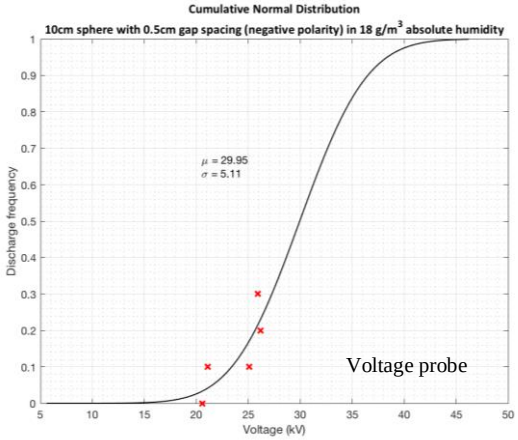

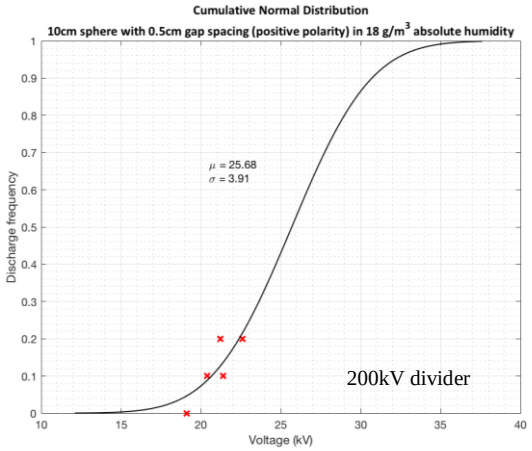

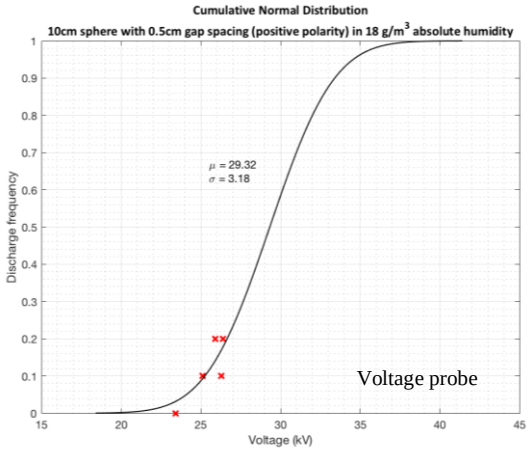

- S=1.0cm (negative and positive polarity)

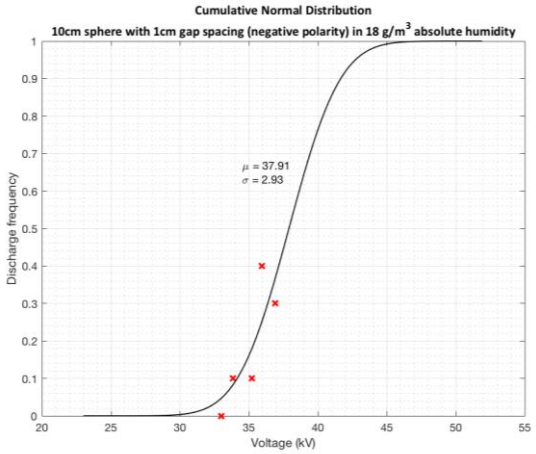

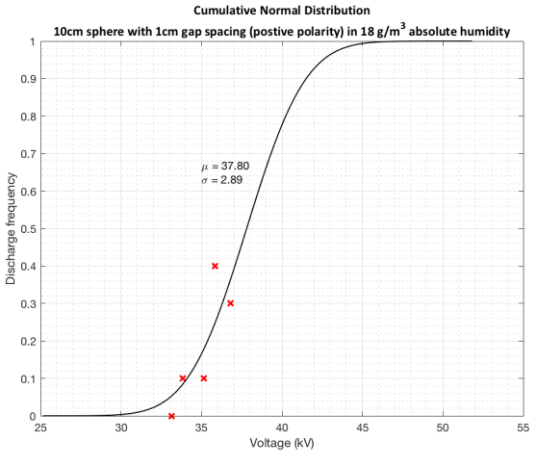

- S=1.5cm (negative and positive polarity)

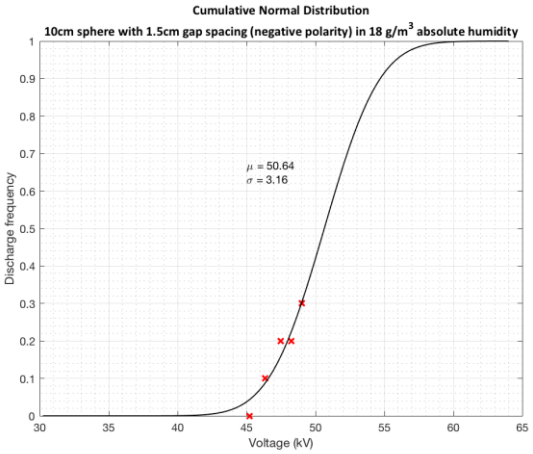

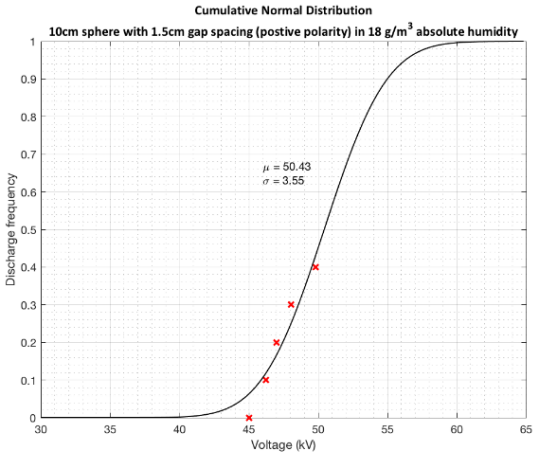

- S=2.0cm (negative and positive polarity)

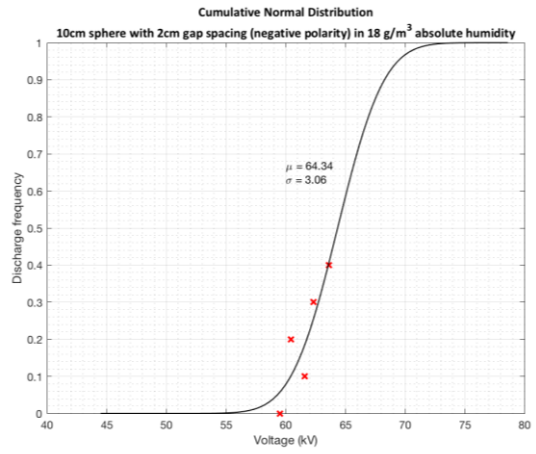

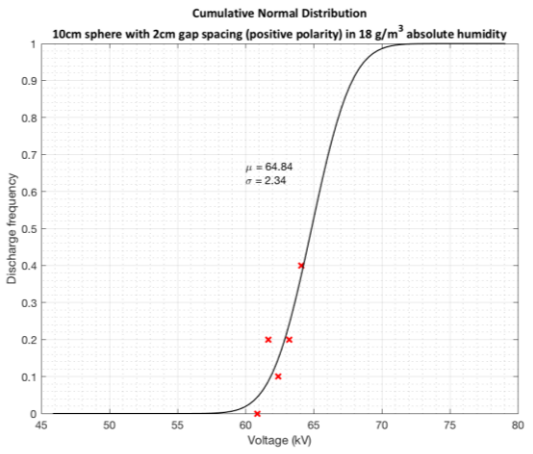

- S=2.4cm (negative and positive polarity)

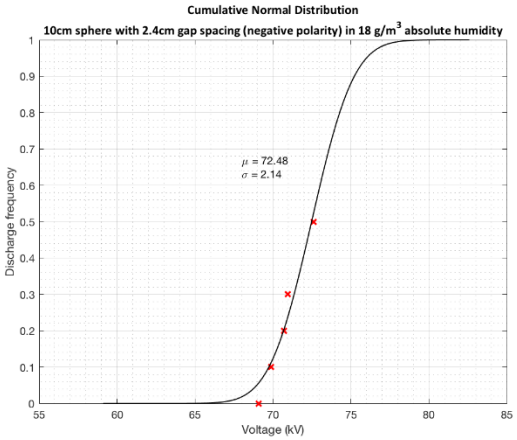

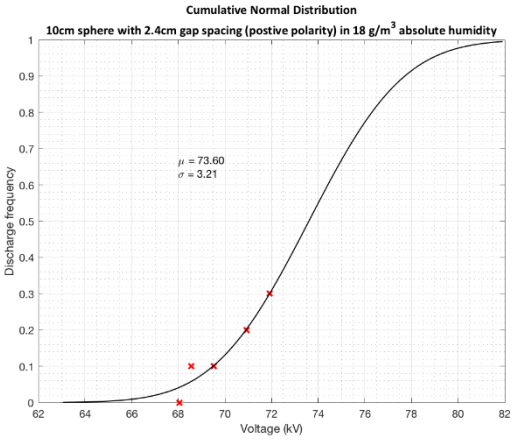

b) With irradiation

- S=0.5cm (negative and positive polarity)

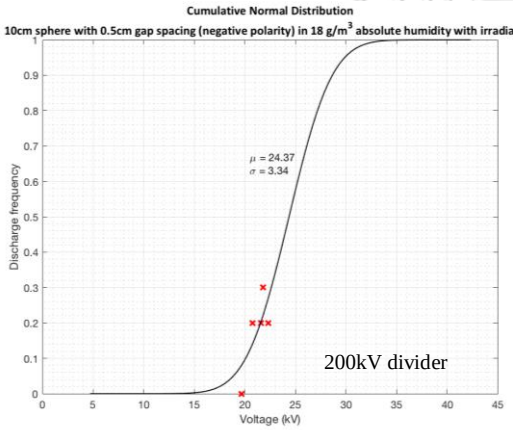

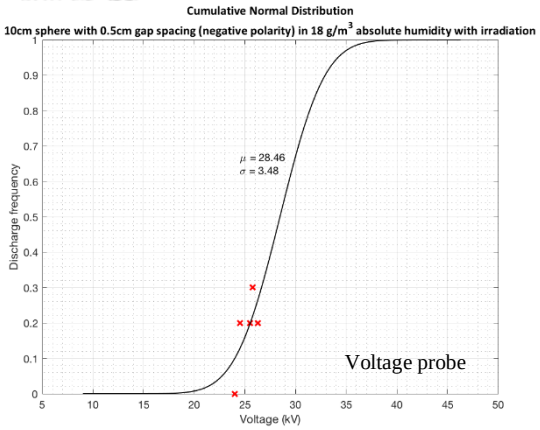

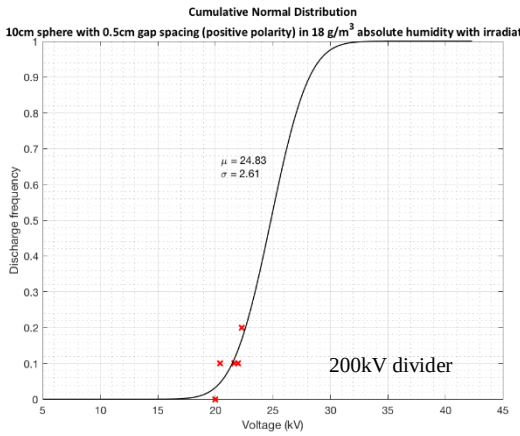

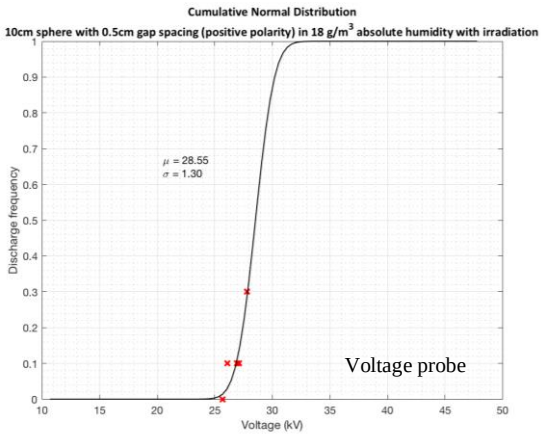

- S=1.0cm (negative and positive polarity)

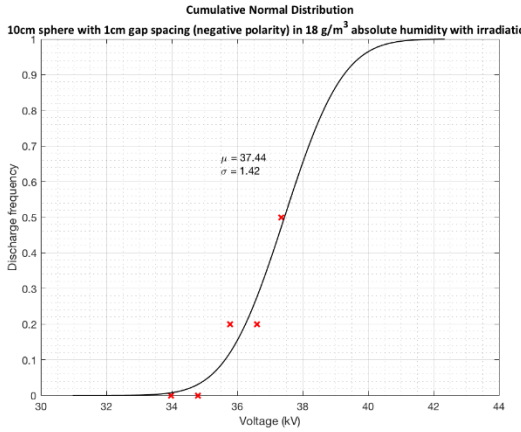

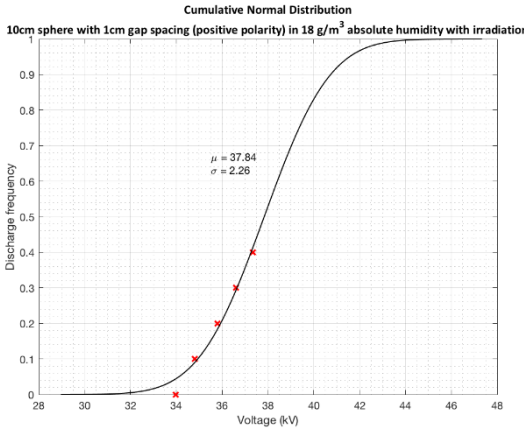

- S=1.5cm (negative and positive polarity)

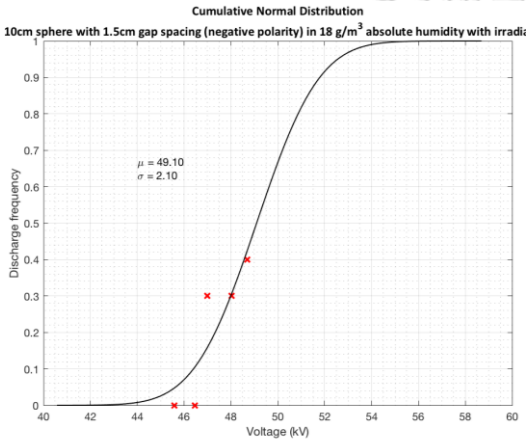

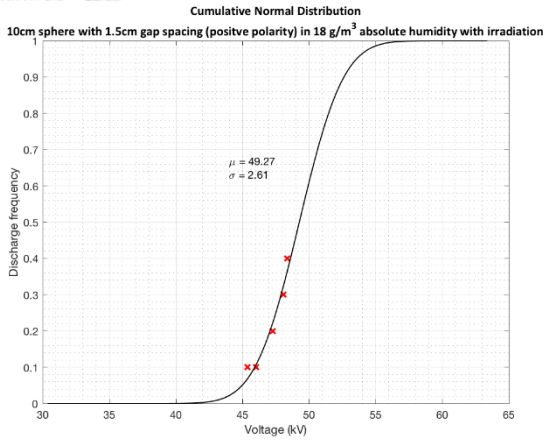

- S=2.0cm (negative and positive polarity)

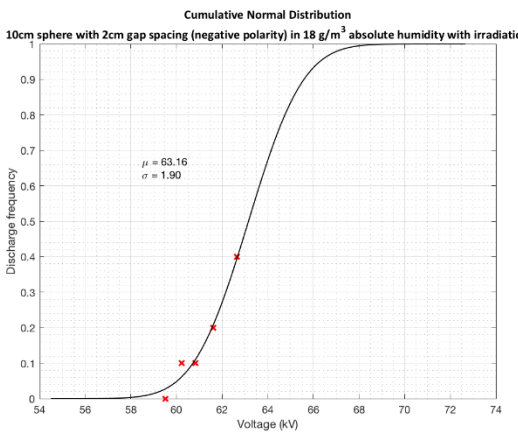

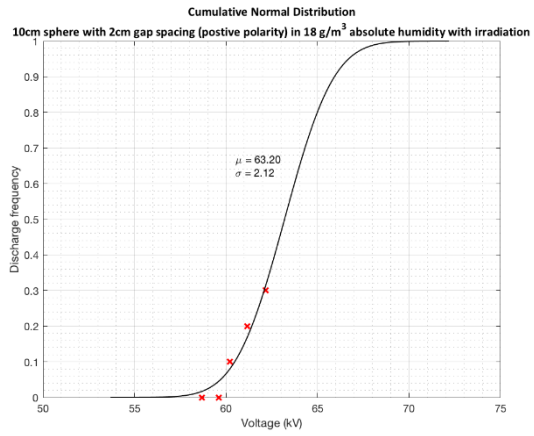

- S=2.4cm (negative and positive polarity)

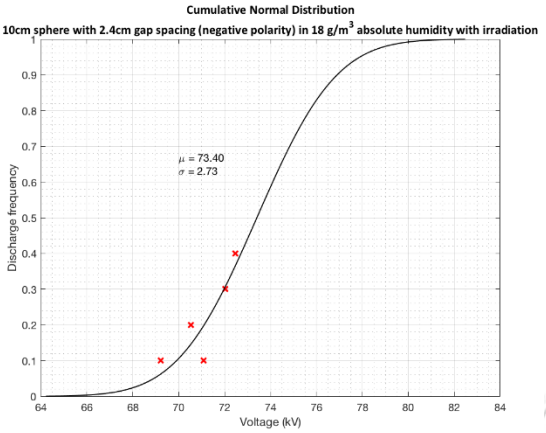

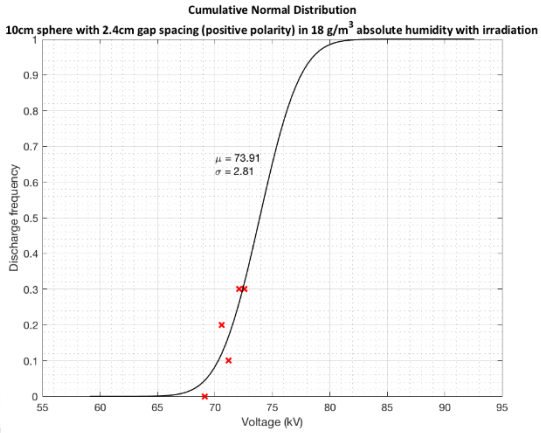

VITA

1999-2011: Primary and high school education in Kandal, Cambodia. 2011-2016: Undergraduate education in electrical engineering at Institute of Technology of Cambodia, Phnom Penh, Cambodia. Graduated with a Bachelor of Engineering degree in 2016. 2016-2018: Graduate study in master degree of electrical engineering at Chulalongkorn University, Bangkok, Thailand. Thesis title: A revisit to impulse breakdownvoltage of standard air gaps.